New Paleontological Records Provide Insights Into the Early Evolution and Biogeography of Gavialoids

by

Kevin I. Vélez

A dissertation submitted in partial fulfillment
of the requirements for the degree of
Doctor of Philosophy
(Earth and Environmental Sciences)
in the University of Michigan
2024

Doctoral Committee:

Professor Jeffrey A. Wilson Mantilla, Chair
Professor Catherine Badgley
Professor Matt Friedman
Associate Research Scientist Miriam Zelditch

Kevin I. Vélez Rosado

kvelez@umich.edu

ORCID iD: 0000-0002-8648-0222

DEDICATION

This dissertation is dedicated to my beloved wife Paola and son Jasper.

ACKNOWLEDGEMENTS

I want to give thanks to my advisor, Jeffrey A. Wilson Mantilla, for giving me constructive criticism in the development of my research ideas, for pushing me to think critically, and encouragement to hone my scientific skills. I also thank my committee members, Catherine Badgley, Matt Friedman, and Miriam Zelditch for providing support throughout my doctoral degree. Special thanks go to Tariq Kareem and Kierstin Rosenbach for providing support in the early stages of Chapters 3 and 4. I want to give special thanks to William Sanders for providing valuable training in molding and casting, mechanical preparation, and for helping me with other projects. I want to thank my parents, Roberto and Omayra, for supporting me in my decision to pursue a degree in paleontology. Another special thanks to my friends Alexis, Angel, Christian, Julio, and Luis, who have supported me from afar. This dissertation was funded by the Rackham Graduate Fellowship, the Department of Earth and Environmental Sciences Scott Turner Student Research Grant Award, the Latin American and Caribbean Studies Tinker Field Research, and the Rackham Graduate Student Research Grant. This work could not have been done without the natural history collections at the University of Michigan Museum of Paleontology, Museo Nacional de Historia Natural de Santo Domingo, Republica Dominicana, and the Florida Museum of Natural History. I want to thank Adam Rountrey for teaching me photogrammetry and Jennifer Bauer for providing access to specimens at UMMP, and Coleman M. Sheehy III for helping me with the herpetology collection at the FMNH. Lastly, I want to give thanks to my colleagues Hernán, Jorge, Juan, and Lázaro for giving insights for future research projects.

TABLE OF CONTENTS

LIST OF TABLES

LIST OF FIGURES

LIST OF APPENDICES

ABSTRACT

Today, crocodylians are separated into three groups, Alligatoridae (*Alligator*, *Caiman*, *Melanosuchus*, *Paleosuchus*), Crocodylidae (*Crocodylus*, *Mecistops*, *Osteolaemus*), and Gavialidae (*Gavialis* and *Tomistoma*). The latter group, Gavialidae, is represented by two species that are restricted to the fluvial habitats of northern India and Nepal, and Indonesia, respectively. However, the gavialid fossil record shows that the group was more diverse and geographically widespread, with specimens occurring on most continents. In this dissertation, I explore the paleontological record of gavialids using new fossil material and test historical biogeographical hypotheses.

In the first part of this dissertation, I explore the evolutionary relationships of the three putative oldest gavialoid groups in a phylogenetic context, all of which are Late Cretaceous in age. These putative early gavialids include *Dolichochampsa minima* from South America, *Ocepesuchus eoafricanus* from Africa, and the 'thoracosaurs' from North America and Europe. Phylogenetic analyses show that *Ocepesuchus* is placed within Alligatoridae, 'thoracosaurs' as basal eusuchians, and *Dolichochampsa* is nested within Gavialidae. The placement of *Dolichochampsa* within Gavialidae suggests a possible South American origin for the clade that can be traced back to the Late Cretaceous.

In the second part of this dissertation, I describe a new fossil gavialid from the Eocene (42 Ma) of Pakistan. The material is represented by cranial, mandibular, and some postcranial (scapula, vertebrae) elements. This new specimen extends the temporal range (42–41 Ma) of

gavialids in Indo-Pakistan, indicating that the group possibly arrived in this region before closure of the Tethys Sea in the Miocene. The results of the morphological analyses demonstrate that the new specimen has strong affinities to Gryposuchinae, a gavialid lineage from the Miocene–Pliocene of South America, suggesting a possible origin for that clade in Asia.

In the third part, I integrate the new paleontological record to reconstruct the historical biogeography of Gavialidae under a model that incorporates geographic and phylogenetic data. I then test the proposed biogeographic hypothesis of dispersals from Africa, Asia, and Europe to the Americas during the Paleocene–Oligocene against a model that does not include such dispersals (i.e., vicariance). The results of this study show strong support for a model that includes the dispersals from Africa, Asia, and Europe to the Americas. Moreover, the best-fitting model shows multiple dispersal events: from Asia to the Americas during the Eocene; from Africa to the Caribbean during the Eocene; and from the Caribbean to South America in the Oligocene. This study highlights the importance of incorporating fossils in biogeographic models to understand the complex history of groups that are represented today by a few taxa.

This dissertation offers valuable evidence for the early history, divergence time, and paleobiogeography of gavialids, and demonstrates the use of Gavialidae as a case study to understand complex evolutionary and biogeographic hypotheses when using the fossil record.

CHAPTER 1

Introduction

Living crocodylians are one of the archosaur groups with a long evolutionary lineage and complex paleobiogeographic history. The clade spans millions of years and can be traced back to the Barremian (130–122 Ma) of the Isle of Wight, with the occurrence of †*Hylaeochampsa vectiana* considered the basalmost member of the group (Clark & Norell, 1992). All crocodylians belong to a larger group called Crocodylia (Fig. 1.1), a clade within the suborder Eusuchia that split over 100 million years ago (Grigg & Kirshner, 2015; Iordansky, 1973). Within Crocodylia there are 27 accepted living species distributed among three families: Alligatoridae (*Alligator*, *Caiman*, *Melanosuchus*, and *Paleosuchus*), Crocodylidae (*Crocodylus*, *Mecistops*, and *Osteolaemus*), and Gavialidae (*Gavialis*) (Grigg & Kirshner, 2015; Salas-Gismondi et al., 2019). Our understanding of the evolutionary relationships of extant forms and their closest fossil relatives has improved during the last three decades owing to innovations in cladistic analyses and the growth in the paleontological record (Clark, 1986; Clark & Norell, 1992; Brochu, 1999; Brochu, 2003; Vélez-Juarbe et al., 2007; Salas-Gismondi et al., 2016; 2019; 2022). Despite such efforts by many paleobiologists, the evolutionary relationships and biogeographic history of some of the earliest members within Gavialidae are still unresolved.

Gavialid crocodylians represent a unique case study because although today they are represented by a single species (*Gavialis gangeticus*) that is geographically restricted to fluvial habitats of India and Nepal, the paleontological record shows that the group was more diverse and geographically widespread (Grigg & Kirshner, 2015; Salas-Gismondi et al., 2016; 2019;

2022; Hua & Jouve, 2004; Jouve et al., 2006). Moreover, early forms and some specimens from the Cenozoic have been recovered from strata that were deposited in coastal marine settings, indicating that gavialids probably had a marine phase and restriction to freshwater occurred relatively recently (Brochu, 2004; Buffetaut, 1987; Carpenter, 1983; Gasparini & Buffetaut, 1980; Hua & Jouve, 2004; Jouve et al., 2006). The spatiotemporal distribution of Miocene–Pliocene gavialids in the Americas and their close affinities to the extant *Gavialis* have also suggested that the group may have dispersed across the Atlantic Ocean during the Paleogene–Neogene (Brochu & Rincón, 2004, Salas-Gismondi et al., 2016; 2019; 2022; Vélez-Juarbe et al., 2007). However, with the incorporation of new biogeographical models of evolution and the discovery of new paleontological data (see Chapters 2 and 3), these hypotheses can be tested to unravel the complex history of gavialids through space and time (Matzke, 2013).

1.1 Early gavialoid evolution

An emerging interest in the evolution of gavialoids is when the clade first appeared in the fossil record and when they acquired such a long snout. All gavialoids are longirostrine (long-snout) and possess a set of characteristics associated with such condition, which include teeth of similar size (homodonty), dentary teeth arranged linearly, and contribution of the splenial bone in the long dentary symphysis (Brochu, 2003). Today, the only representatives of the clade include *Gavialis gangeticus* and *Tomistoma schlegelii* (Bezuijen, 2010; Stevenson, 2015).

The oldest records of longirostrine crocodylians include the thoracosaurs from the Cretaceous–Paleogene of North America and *Dolichochampsa minima* from South America. The North American taxa include *Eothoracosaurus mississippiensis* and *Thoracosaurus neocesariensis*, both from the Ripley Formation of Mississippi (Carpenter, 1983; Brochu, 2004).

These large long-snouted crocodylians may have reached ~5 m in total body length and are usually found in association with marginal or shallow marine deposits (Brochu, 2003b). Cope (1871) regarded these taxa as a distinct family and later considered a subfamily within Crocodylia (Fig. 1.2) by Nopcsa (1928). These thoracosaurs were considered tomistomines due to the presence of plesiomorphic (ancestral characters retained in derived species) characters shared by both clades, but cladistic analyses point to a close relationship to crown gavialids (Brochu, 2004; Vélez-Juarbe et al., 2007; Salas-Gismondi et al., 2016; 2018). Although thoracosaurs have long been considered the earliest gavialoids, their phylogenetic position within Gavialoidea was questioned recently (Gatesy et al., 2003; Lee & Yates, 2018; Salas-Gismondi et al., 2022).

One of the studies that stand out is that of Gatesy et al. (2003) in their approach to solving the phylogenetic position of thoracosaurs. In their analysis, DNA sequences (mitochondrial and nuclear genomes) and anatomical data were utilized together from extinct and extant taxa. According to their results, one of the reasons thoracosaurs are placed within Gavialoidea is because of a series of atavisms in gavialines, characters that were reversed to an ancestral state. More recently, Lee & Yates (2018) performed a similar approach to Gatesy et al. (2003) and found that the similarities between thoracosaurs and gavialids were due to a 'perfect storm' of homoplasy of the former and atavisms in the latter. Although the Lee & Yates (2018: Figure 2) phylogeny shows a more basal placement of thoracosaurs, it is important to notice that their tip-dated Bayesian analysis was based on a combined dataset (see above, page 12). When the molecular component was removed from the dataset, the phylogeny supported the 'traditional' relationship with thoracosaurs on the stem of the gavialoid lineage (Lee & Yates, 2018: Figure 1).

In addition to the thoracosaur problem, another putative early gavialoid is the monospecific taxon *Dolichochampsa minima* from South America. The holotype of *Dolichochampsa* comes from the Yacoraite Formation of Argentina, and other specimens have been found in the El Molino Fm. of Bolivia (Gasparini & Buffetaut, 1980; Buffetaut, 1987; Jouve et al., 2021). *Dolichochampsa* was a small-sized (~1m long) long-snouted crocodylian that shows a set of morphological characters unique to modern gharials and probably represents an earlier radiation of the clade. Until recently, the evolutionary relationships of *Dolichochampsa* have never been considered in a phylogenetic context, probably due to the nature of its preservation and incompleteness (Gasparini & Buffetaut, 1980). Nevertheless, its putative position within Gavialidae has paleobiogeographical implications for the clade that must be addressed.

1.2 Challenges in the historical biogeography of gavialoids

One of the remaining questions in the gavialoid paleobiogeography is the occurrences of the Miocene–Pliocene taxa of South America and the Caribbean, the so-called gryposuchines. Gryposuchinae is a subfamily of gavialids erected by Vélez-Juarbe et al. (2007) that included 11 species within 7 genera (Salas-Gismondi et al., 2018) distributed in Africa, South America, and the Caribbean. Today, the subfamily is only restricted to the South American clades (*Gryposuchus*, *Dadagavialis*, *Ikanogavialis*, *Siquisiquesuchus*, and *Piscogavialis*), which excludes the African (*Argochampsa krebsi*) and Caribbean taxa (*Aktiogavialis puertoricensis*) (Salas-Gismondi et al., 2022). Although trans-oceanic events from Africa and Asia have been proposed (Vélez-Juarbe et al., 2007; Salas-Gismondi et al., 2016; 2018) as likely dispersal scenarios to explain the current distribution of gryposuchines in South America, tests of such

hypotheses using biogeographical models have been used relatively recently at some extent. Salas-Gismondi et al. (2022) performed a statistical dispersal-vicariance analysis (S-DIVA) to reconstruct the optimal biogeographic ancestral ranges and recovered the Peri-Tethys, Africa, and South America with equal marginal probability for gryposuchines. Although Salas-Gismondi et al. (2022) delimit the ancestral ranges for gryposuchines, an essential issue in the analysis was not addressed, which has biogeographical consequences. The strict consensus tree used in the S-DIVA analysis has multiple unresolved (polytomies) nodes that may open several phylogenetic scenarios. Thus, any changes in the topology will result in several paleobiogeographical results.

Finally, the last remaining puzzle is the current geographic distribution of the living taxon, *Gavialis gangeticus*. When and how did this taxon become geographically restricted to these particular areas of the world that today only occur in northern India and Nepal? The oldest gavialids from Greater India include the Miocene *Rhamphosuchus crassidens* and fossils of *Gavialis gangeticus* (Martin, 2019). The phylogenetically closest to these Miocene taxa is *Argochampsa krebsi* from the Paleocene of Morocco (Hua and Jouve, 2004). Thus, a significant gap remains in the evolutionary history of gavialids from Greater India between the Paleocene–Miocene (Brochu, 2004). Fossils found during this time period will be essential to understand what happened with the clade, especially during the collision of Greater India with Eurassia in the Eocene (52–44 Ma).

In this dissertation, I continue the study of the natural history of crocodylians, with an emphasis on gavialids. Chapter 2 investigates the early history and possible geographic origin of gavialids in a parsimony-based context. To determine the early divergence, the three putative oldest groups, *Dolichochampsa*, *Ocepesuchus*, and 'thoracosaurs,' were included in a phylogenetic context. This is the first study to include the three groups under the same

phylogenetic context. Results of phylogenetic analyses show that gharials are a group that may have originated in the Cretaceous of South America.

Chapter 3 examines a new fossil gavialid from the Eocene Domanda Formation of Pakistan to determine its relationships with Crocodylia. Description and parsimony-based analyses demonstrate strong affinities of the Pakistani specimen to the South American gharials, Gryposuchinae. Analysis of the geology and tectonics of the region show that the individual could have been well adapted to occupy marine environments, as has been proposed by early authors. Strong morphological affinities of the new specimen to gryposuchines show more evidence of a Paleocene–Eocene dispersal from Asia origin to the Americas.

In Chapter 4 I first evaluate the evolutionary relationships of the three putative gavialids ('thoracosaurs,' *Dolichochampsa*, and *Ocepesuchus*) and the new Pakistani gharial in a Bayesian framework. A Bayesian analysis was employed to demonstrate that regardless of methodology (i.e., Bayesian, parsimony), this study will support a similar evolutionary relationship for gavialids as in Chapters 2 and 3. Second, I test the biogeographical hypothesis of a Paleocene–Eocene dispersal from Africa+Asia+Europe to the Americas proposed by Brochu & Rincón (2004), Salas-Gismondi et al. (2019), and Vélez-Juarbe et al. (2007). To test this hypothesis, two biogeographic models were tested against each other, and Akaike Information Criterion was used to identify the best-fitting model. The results of the biogeographic analyses indicate that the model with the dispersals from Africa+Asia+Europe is the best-fitting model that explains the distribution of fossil gavialids in the Americas. The results of this study show the importance of using biogeographical models to elucidate the complex history of groups, especially those extant groups that are geographically restricted today.

Chapter 5 is a summary of the research performed in this dissertation. In this chapter, I make emphasis on key parts of the research conducted and the main conclusions. I begin by outlining the research methodologies and highlighting the techniques and approaches utilized throughout the study. The chapter then transitions to a detailed analysis of the findings, examining the data collected and its implications. Finally, I synthesize the main conclusions, discussing their significance and potential impact on the field.

References

Bezuijen, M. R., Shwedick, B. M., Sommerlad, R., Stevenson, C. & Steubing, R. B. (2010). Tomistoma *Tomistoma schlegelii*. In S. C. Manolis, & C. Stevenson (Eds.), *Crocodiles: Status Survey and Conservation Action Plan* (pp. 133–138). Crocodile Specialist Group: Darwin.

Brochu, C. A. (1999). Phylogenetics, taxonomy, and historical biogeography of Alligatoroidea. *Journal of Vertebrate Paleontology*, *19*(2), 9–100. https://doi.org/10.1080/02724634.1999.10011201

Brochu, C. A. (2003). Phylogenetic approaches toward crocodylian history. *Annual Review of Earth and Planetary Sciences, 31*(1), 357–397. https://doi.org/10.1146/annurev.earth.31.100901.141308

Brochu, C. A. (2004). A new Late Cretaceous gavialoid crocodylian from eastern North America and the phylogenetic relationships of thoracosaurs. *Journal of Vertebrate Paleontology, 24*(3), 610–633. https://doi.org/10.1671/0272-4634(2004)024[0610:ANLCGC]2.0.CO;2

Brochu, C. A., & Rincón, A. D. (2004). A gavialoid crocodylian from the lower Miocene of Venezuela. *The Palaeontological Association, 71*, 61–79.

Buffetaut, E. (1987). Occurrence of the crocodylian *Dolichochampsa minima* (Eusuchia, Dolichochampsidae) in the El Molino Formation of Bolivia. *Bulletin de la Société Belge de Géologie, 96*, 195–199.

Carpenter, K. (1983). *Thoracosaurus neocesariensis* (De Kay, 1842) (Crocodylia: Crocodylidae) from the Late Cretaceous Ripley Formation of Mississippi. *Mississippi Geology, 4*(1), 1–10.

Clark, J. M. 1986. *Phylogenetic relationships of the crocodylomorph archosaurs* [Doctoral dissertation, University of Chicago].

Clark, J. M., & Norell, M. A. (1992). The early Cretaceous crocodylomorph *Hylaeochampsa vectiana* from the Wealden of the Isle of Wight. *American Museum Novitates 3032,* 1–19.

Gasparini, Z. B. de, & Buffetaut, E. (1980). *Dolichochampsa minima*, n. g. n. sp., a representative of a new family of eusuchian crocodiles from the Late Cretaceous of northern Argentina. *Neues Jahrbuch Für Geologie Und Paläontologie - Monatshefte*, *1980*(5), 257–271. https://doi.org/10.1127/njgpm/1980/1980/257

Gatesy, J., Amato, G., Norell, M., Desalle, R., & Hayashi, C. (2003). Combined support for wholesale taxic atavism in gavialine crocodylians. *Systematic Biology, 52*(3), 403–422.

Grigg, G. C., & Kirshner, D. (2015). Biology and evolution of crocodylians. *Comstock Publishing Associates a division of Cornell University Press, Ithaca* (pp. 649 pp).

Hua, S., & Jouve, S. (2004). A primitive marine gavialoid from the Paleocene of Morocco. *Journal of Vertebrate Paleontology, 24*(2), 341–350. https://doi.org/doi: 10.1671/1104

Iordansky, N. N. (1973). The skull of the Crocodylia. In C. Gans (Eds.), *Biology of the Reptilia* (pp. 201–262). Academy Press.

Lee, M. S. Y., & Yates, A. M. (2018). Tip-dating and homoplasy: reconciling the shallow molecular divergences of modern gharials with their long fossil record. *Proceedings of the Royal Society B: Biological Sciences, 285*, 20181071.

Martin, J. E. (2019). The taxonomic content of the genus *Gavialis* from the Siwalik Hills of India and Pakistan. *Special Papers in Palaeontology, 5*, 483-497.

Matzke, N. J. (2013). *BioGeoBEARS: BioGeography with Bayesian (and likelihood) Evolutionary Analysis in R Scripts* [Rstudio].

Nopcsa, F. (1923). Die Familien der Reptilien. *Fortschritte der Geologie und Palaentologie, 2*, 1–210.

Jouve, S., Iarochene, M., Bouya, B., & Amaghzaz, M. (2006). New material of *Argochampsa krebsi* (Crocodylia: Gavialoidea) from the Lower Paleocene of the Oulad Abdoun Basin (Morocco): phylogenetic implications. *Geobios, 39*, 817–832.

Jouve, S., de Muizon, C., Cespedes-Paz, R., Sossa-Soruco, V., & Knoll, S. (2021). The longirostrine crocodyliforms from Bolivia and their evolution through the Cretaceous–Palaeogene boundary. *Zoological Journal of the Linnean Society*, *192*(2), 475–509. https://doi.org/10.1093/zoolinnean/zlaa081

Salas-Gismondi, R., Flynn, J. J., Baby, P., Tejada-Lara, J. V., Claude, J., & Antoine, P.-O. (2016). A new 13 million year old gavialoid crocodylian from Proto-Amazonian Mega-Wetlands reveals parallel evolutionary trends in skull shape linked to longirostry. *Plos One*, *11*(4). https://doi.org/10.1371/journal.pone.0152453

Salas-Gismondi, R., Moreno-Bernal, J. W., Scheyer ,T. M., Sánchez, M. R., & Jaramillo, C. (2019). New Miocene Caribbean gavialoids and patterns of longirostry in crocodylians. *Journal of Systematic Palaeontology, 17*(12), 1049–1075. https://doi.org/10.1080/14772019.2018.1495275

Salas-Gismondi, R., Ochoa, D., Jouve, S., Romero, P. E., Cardich, J., Perez, A., DeVries, T., Baby, P., Urbina, M., & Carré, M. (2022). Miocene fossils from the southeastern Pacific shed light on the last radiation of marine crocodylians. *Proceedings of the Royal Society B: Biological Sciences*, *289*(1974), 20220380. https://doi.org/10.1098/rspb.2022.0380

Stevenson, C. J. (2015). Conservation of the Indian gharial *Gavialis gangeticus*: successes and failures. *International Zoo Yearbook, 49*, 150–161.

Vélez-Juarbe, J., Brochu, C. A., & Santos, H. (2007). A gharial from the Oligocene of Puerto Rico: Transoceanic dispersal in the history of a non-marine reptile. *Proceedings of the Royal Society B: Biological Sciences*, *274*(1615), 1245–1254. https://doi.org/10.1098/rspb.2006.0455

Figures

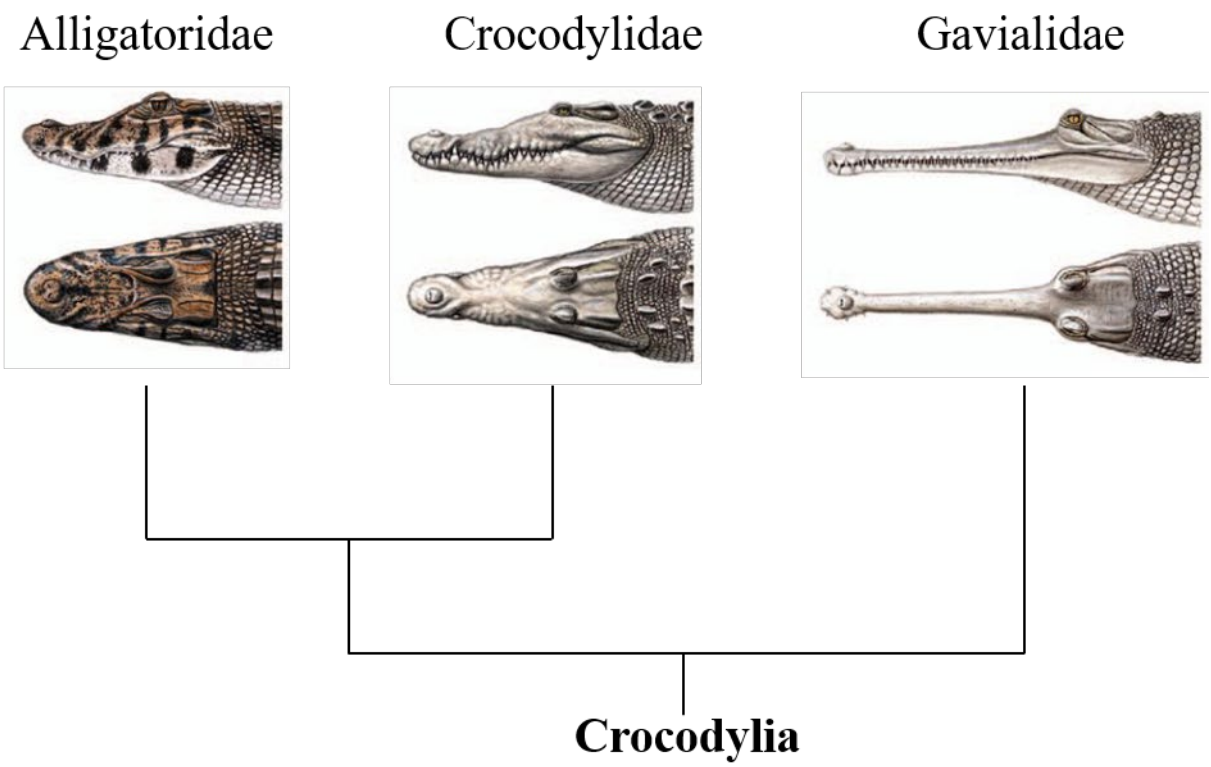

Figure 1.1. Simplified phylogeny of crocodylians showing the relationships of the three main groups: Alligatoridae, Crocodylidae, and Gavialidae.

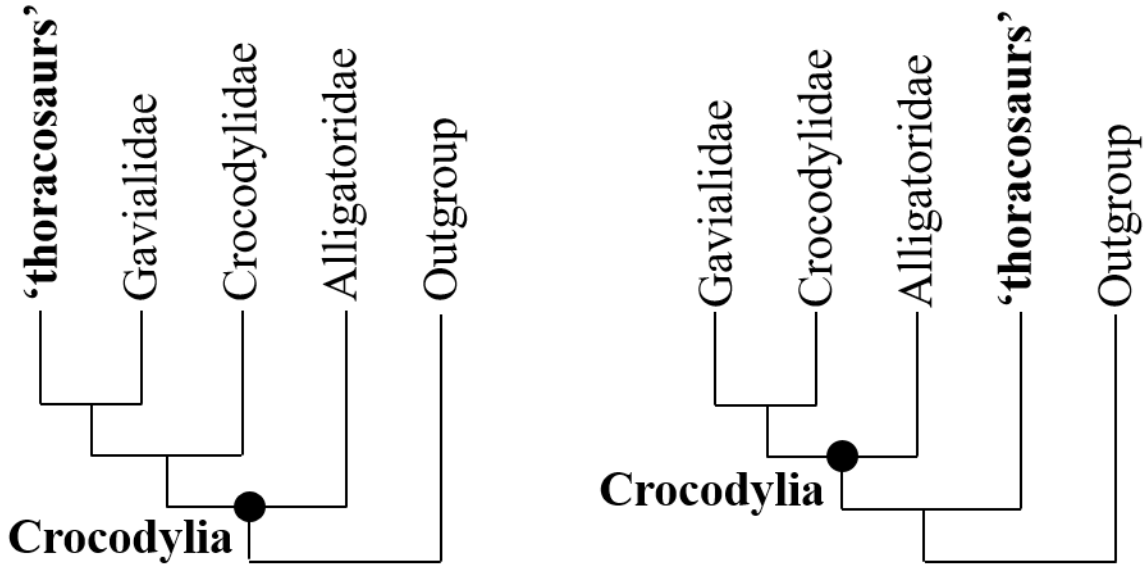

Figure 1.2. Two hypotheses of the evolutionary relationships of 'thoracosaurs.' Phylogeny at the left shows the position of 'thoracosaurs' as the closest group to Gavialidae, and the right shows the position of 'thoracosaurs' recovered outside Crocodylia.

CHAPTER 2

New Material of *Dolichochampsa minima* (Archosauria: Crocodylia) from the Cretaceous–Paleogene El Molino Formation of Bolivia Sheds Light on the Early Evolution of Gavialinae

Abstract

Three Late Cretaceous taxa have been suggested to be among the oldest gavialines: 'thoracosaurs' from North America; *Ocepesuchus eoafricanus* from Africa; and *Dolichochampsa minima* from South America. The evolutionary relationships of these taxa to definitive gavialoids, all of which are Late Cretaceous in age, remain contentious. As a result, the origins of Gavialinae in space (Laurasia vs. Gondwana) and time (Cretaceous vs. Miocene) are unresolved. Here, we report new material of *Dolichochampsa minima* from the Late Cretaceous (73–64 Ma) El Molino Formation of Bolivia. This material provides key anatomical information elucidating the evolutionary relationships of early gavialines. A phylogenetic analysis based on a revised and expanded morphological character dataset recovers *D. minima* nested within Gavialinae. The other putative gavialines, however, were resolved outside of Gavialoidea: *Ocepesuchus* was recovered within alligatorids; and 'thoracosaurs' were recovered outside crown-group Crocodylia. This phylogenetic hypothesis implies that several characters associated with longirostry evolved independently in gavialines and 'thoracosaurs.' The phylogenetic relationships and geographic distribution of early gavialines suggest a plausible center of origination in Gondwana for the group, followed by multiple trans-oceanic dispersals during the

Late Cretaceous to other landmasses and possible dispersals to South America from the peri-Tethys during the late Paleogene.

Introduction

Gavialid crocodylians today are represented by just two species, both of which are restricted to freshwater habitats in Asia (Bezuijen et al., 2009; Stevenson, 2015)—the Indian gharial (*Gavialis gangeticus*) and the Indonesian false gharial (*Tomistoma schlegelii*). The relatively restricted habitat, low diversity, and geographic distribution of living gharial species belie the deeper history of the group, which was more diverse and achieved a nearly global distribution, perhaps due to their dispersal capabilities. Unraveling the history of the earliest gavialids is essential for understanding when and where the group originated, which has important implications for their biogeographic history and paleobiology.

Several Late Cretaceous taxa have been suggested to be among the earliest fossil gavialids: the 'thoracosaurs' from North America and Europe; *Ocepesuchus eoafricanus* from Africa; and *Dolichochampsa minima* from South America (Brochu, 2004; Carpenter, 1983; Gasparini & Buffetaut, 1980; Jouve et al., 2008; Rio & Mannion, 2021). The evolutionary relationships of these three taxa to gavialoids are either ambiguously resolved ('thoracosaurs,' *O. eoafricanus*) or have not been tested in a phylogenetic framework (*D. minima*). 'Thoracosaurs' comprise several North American (*Thoracosaurus* and *Eothoracosaurus*) and European (*Eosuchus*) species, and some reached body lengths of up to 6 m (Brochu, 2004; Carpenter, 1983; Delfino et al., 2005; Rio & Mannion, 2021). They are generally associated with sediments and fauna from coastal to shallow marine environments, an indication that perhaps they were capable of tolerating marine waters (Brochu, 2004; Carpenter, 1983; Delfino et al., 2005;

Erickson, 1998; Gallagher et al., 1986; Schwimmer, 1986; Troxell, 1925). 'Thoracosaurs' share a suite of morphological attributes with crown-group gharials, some of which are associated with longirostry (Brochu, 2004; 2006; Delfino et al., 2005; Rio & Mannion, 2021; Vélez-Juarbe et al., 2007). As a consequence, 'thoracosaurs' have been placed consistently within Gavialoidea in numerical phylogenetic analyses (Brochu, 2004; 2006; Salas-Gismondi et al., 2016; 2019; Vélez-Juarbe et al., 2007). The hypothesis that 'thoracosaurs' are closely related to gharials implies that Gavialoidea originated by the Late Cretaceous, which contrasts with molecular-based hypotheses that suggest a much younger, Miocene origin for the clade (Densmore & Dessauer, 1984; Hass et al., 1992; Janke et al., 2005; Willis et al., 2007).

Total-evidence approaches resolving the apparent disagreement between molecular and morphological data have produced an entirely new hypothesis of relationships for 'thoracosaurs.' Analysis of a dataset combining DNA and morphology recovered 'thoracosaurs' outside of Crocodylia (alligators and caimans, crocodiles, and gharials), on the stem lineage leading to the group (Lee & Yates, 2018). With 'thoracosaurs' resolved outside of Crocodylia, Gavialoidea was hypothesized to originate in the Miocene, consistent with molecular-based analyses (Densmore & Dessauer, 1984; Hass et al., 1992; Janke et al., 2005; Willis et al., 2007). Lee & Yates (2018) offered an explanation for why 'thoracosaurs' and gharials previously had been linked together, referring to a 'perfect storm' of morphological similarities due to shared feeding behavior (i.e., fish-eating) and atavisms (plesiomorphic traits) in gavialids. It is important to state that although the results of their total-evidence approach resolve 'thoracosaurs' outside Crocodylia, analysis of the morphological data alone still supports a sister-clade relationship to crown gharials (Lee & Yates, 2018; Fig. 1), as proposed by other morphology-based studies (Brochu, 1997; 2003; 2004; 2012; Salas-Gismondi et al., 2016; 2019; Vélez-Juarbe et al., 2007).

The two putative gavialoid species from the Late Cretaceous of Gondwana, *Ocepesuchus eoafricanus* and *Dolichochampsa minima*, may have important implications for the geographical origin of the clade. *O. eoafricanus* is from the latest Cretaceous of the Oulad Basin of Morocco and is represented by a partial skull (Jouve et al., 2008). A morphology-based phylogenetic analysis recovered both *O. eoafricanus* and 'thoracosaurs' within crown gharials, a result that seems to corroborate morphology-based studies (Brochu, 1997; 2003; 2004; 2012; Salas-Gismondi-et al., 2016; 2019; Jouve et al., 2008; Vélez-Juarbe et al., 2007). *Dolichochampsa minima*, in turn, is a small (body length ca. 1 m) longirostrine crocodylian from South America (Gasparini & Buffetaut, 1980; Jouve et al., 2021). The holotype of *D. minima* is a partial dentary from the Cretaceous of the Yacoraite Formation of Salta Province in Argentina (Gasparini & Buffetatut, 1980). Referred materials from the same locality and from Bolivia include portions of the skull, axial column, pelvis, and hindlimb. *Dolichochampsa* was proposed to be a gavialid based on features present only in the basally diverging gharials, *Eogavialis africanus* and *Argochampsa krebsi*: (1) a long and flat symphysis; (2) an estimated tooth count of approximately 20 teeth, separated by deep lateral sulci; (3) alveoli of similar size and located lower than the medial margin of the symphysis; and (4) presence of a basioccipital tuber (Buffetatut, 1987; Gasparini and Buffetaut, 1980; Jouve et al., 2021).

The evolutionary relationships of 'thoracosaurs,' *Ocepesuchus eoafricanus*, and *Dolichochampsa minima* have important implications for the temporal (Cretaceous vs. Miocene) and geographical (Laurasia vs. Gondwana) origin of early gavialoids, as well as their past dispersal history. Here, we report new material of a small-sized eusuchian from the Cretaceous–Paleocene El Molino Formation of Bolivia. We present a detailed morphological description of the new specimen, which appears to be referable to *D. minima*, and compare it with

contemporaneous and related crocodylian taxa. We examine the phylogenetic relationships of *D. minima* for the first time and reevaluate the gavialoid affinities of 'thoracosaurs' and *Ocepesuchus eoafricanus* within a parsimony framework using an expanded morphological dataset. We discuss the implications of this phylogenetic hypothesis and the paleobiogeography of Cretaceous gavialines in South America

Institutional abbreviations

FCGV: Universidad Mayor de San Andrés, Facultad de Ciencias Geológicas Vertebrados, La Paz, Bolivia; MLP: Collection of the Division Paleontologia Vertebrados, Museo La Plata; MUSM: Vertebrate Palaeontology Collection of the Natural History Museum of San Marcos University; **UM**: University of Michigan, Ann Arbor, Michigan, U. S. A.

Geological and paleoenvironmental setting

The new specimen of *Dolichochampsa minima* (FCGV-8178) described herein was found in 2019 during a field survey of exposures of the Middle and Upper Members of the El Molino Formation of the Potosí Basin near the village of Maragua, approximately 18 km west of Sucre, Bolivia (Howes, 2023; Fig. 1). The Potosí Basin is a back-arc flexural basin formed in response to the emergence of the Andes. The basin accumulated up to 450 m of sediment from the Cenomanian to middle Paleocene (Lamb et al., 1997; Sempere, 1994; Sempere et al., 1997). The El Molino Formation is exposed throughout Bolivia, particularly in the Eastern Cordillera and on the Altiplano, and it may be penecontemporaneous with the Yacoraite Formation of Argentina,

where the holotype of *D. minima* was collected (Gasparini & Buffetaut, 1980; Marquillas et al., 2011; Sempere & Marshall, 1997).

During the Late Cretaceous, the deepest portion of the basin, the foredeep, was in what is now the Altiplano in western Bolivia. The shallower portion of the basin, potentially the forebulge or backbulge, is preserved in the Eastern Cordillera, which includes Maragua (Sempere, 1994). The latest Cretaceous–Early Paleocene sediments of the Potosí Basin are represented by mudrocks, carbonate strata, sandstones, and minor evaporates. These rocks record a tropical-to-subtropical (23–25°S) lacustrine environment roughly the size of the modern Caspian Sea (370,000 km2; Matthews et al. 2016). This environment experienced fluctuating water levels and occasional marine influence as seen in obliquity-scale periodicity in sedimentation (Rouchy et al., 1993; Gayet et al., 1993; Camoni et al., 1997; Tasistro-Hart et al., 2020).

The cause of fluctuating water levels and the degree to which the basin was connected to the ocean has been a source of debate. Gayet et al. (1993) and Sempere (1994) argued that eustasy was the primary control on water levels in the Potosí Basin, based on a correlation between the transgressions at the base of the Lower, Middle, and Upper Members of the El Molino Formation and the global marine transgressions of the Haq (1987) sea-level curve. However, Rouchy et al. (1993) and Camoin et al. (1997) suggested that fossil (vertebrate, invertebrate, and pollen) assemblages of the El Molino are almost entirely continental and that some previously identified fossils were incorrectly attributed to marine environments. Rouchy et al. (1993) and Camoin et al. (1997) also argued that sulfur isotopes from evaporitic gypsum from the Chaunaca and Santa Lucia Formations are lighter than would be expected from evaporating

marine waters, and therefore it is most likely that the El Molino also is predominantly continental.

A recent cyclostratigraphic study of the El Molino Formation seems to reconcile both the marine and lacustrine viewpoints by demonstrating that regional hydrology and global sea level were both primary drivers of lake levels and sediment composition, but at different times (Tasistro-Hart et al., 2020). The sediments at the bottom of the Lower El Molino preserve periodicities consistent with semi-precession, precession, and eccentricity (which modulates precession), potentially reflecting the orbitally driven changes in the position of the intertropical convergence zone (ITCZ). The sensitivity to the position of the ITCZ implies that regional hydrology was the driver of lake levels and sediment flux during the deposition of the lower portion of the Lower Member of the El Molino Formation. In the upper portion of the Lower Member of the El Molino Formation, the precession signal disappears, and an obliquity signal becomes statistically significant, which Tasistro-Hart et al. (2020) attributed to a strengthened connection with the ocean. It appears that at that time, the ocean was experiencing obliquity-driven glacioeustasy (according to the sea-level curve from Miller et al., 2005), which is recorded by the El Molino Formation.

In addition to clarifying the depositional history of the El Molino, the cyclostratigraphic study of the Potosí Basin provided new age estimates for the El Molino Formation. Previous paleontological work had determined that the Maastrichtian-Danian boundary is within the El Molino Formation, but had not precisely located the position of the K-Pg boundary. The U-Pb ages and astrochronology from Tasistro-Hart et al. (2020) determined that the K-Pg boundary is near the contact between the Middle and Upper Members of the El Molino Formation at Maragua. The sample in this study was collected in the uppermost portion of the Middle Member

of the El Molino Formation, and so our best estimate of the age places the sample in the late Maastrichtian (73 Ma), but uncertainty in the U-Pb ages and astrochronology do not preclude an early Danian (64 Ma) age for this sample.

Phylogenetic methods

The new Bolivian crocodylian specimen (FCGV-8178) possesses features that place it within Neosuchia (e.g., choana within pterygoids, procoelous vertebral centra). We incorporated FCGV-8178 into a dataset of a subset of Neosuchia that includes Crocodylia (crown-group crocodylomorphs, uniting Alligatoridae, Crocodylidae, and Gavialidae), its immediate relatives (e.g., *Hylaeochampsa*), and three putative gavialoid taxa (i.e., 'thoracosaurs', *Ocepesuchus eoafricanus*, *Dolichochampsa minima*). Below, we outline the methods that we implemented for the parsimony analysis.

Character-Taxon Matrix

The taxonomic scope of our analysis (Crocodylia and immediate relatives) is similar to that of many previous phylogenetic studies. We chose the Salas-Gismondi et al. (2022) dataset as a starting point because it is the most recent iteration of a character list that has been in development for more than two decades (Brochu, 1997; Brochu, 2003; 2004; Salas-Gismondi et al., 2016; 2019; Vélez-Juarbe et al., 2007), and because it includes a large number of gavialoid operational taxonomic units (OTUs). The Salas-Gismondi et al. (2022) dataset contained 233 discrete morphological characters that include 185 cranial (79%), 22 axial (9%), 14 appendicular (6%), 8 osteodermal/shield (3%), and 4 soft-tissue (2%) features.

We reevaluated the character list of Salas-Gismondi et al. (2022) and modified the states of 24 characters to reflect better the morphological variation in the OTUs included in this analysis (see Appendix S2.1 and 2.2). In addition, we incorporated 26 characters from the Ristevski et al. (2018) dataset. We removed 17 characters from the Salas-Gismondi et al. (2022) dataset, fifteen of which were uninformative (ch. 15, 20, 21, 30, 80, 83, 98, 99, 107, 110, 136, 170, 193, 199, and 214), and 2 of which (ch. 191, 209) were redundant with characters incorporated from Ristevski et al. (2018) that included additional character states. To this revised dataset, we added 6 new discrete characters. The resultant matrix includes 248 osteological characters listed and described in Supplemental Material (Appendix S2.1).

The original matrix of Salas-Gismondi et al. (2022) included 69 OTUs, but we pruned three taxa by safe taxonomic reduction (Wilkinson, 1995): *Charactosuchus fieldsi*, *Crocodylus falconensis*, and *Gavialosuchus eggenburgensis*. We also removed the Siwalik *Gavialis* from the analysis because it requires further taxonomic revision (Martin, 2019), as well as an undescribed taxon (MUSM 1513) for which we were not able to verify scorings. We added *Isisfordia duncani* and *Ocepesuchus eoafricanus* to the dataset for a total of 67 OTUs. Specimen FCGV-8178 is a single individual that we refer to *Dolichochampsa minima*, based on its morphological similarities to the holotype and other individuals associated with the same taxon, as discussed below (Gasparini & Buffetaut, 1980; Buffetaut, 1987; Jouve et al., 2021). We scored *D. minima* based on first-hand observations from FCGV-8178, photographs and descriptions of the holotype and referred material from Bolivia available in the published literature (Buffetaut, 1987; Gasparini & Buffetaut, 1980; Jouve et al., 2021). We were able to score *D. minima* for 35 of the 248 characters (86% missing), including 24 cranial, 10 mandibular, and 1 girdle features.

Parsimony analysis

We performed a maximum parsimony analysis in TNT 1.6 (Goloboff & Catalano, 2016). Characters were equally weighted, unordered, and non-additive. *Bernissartia fagesii* was designated as the outgroup taxon. The settings were changed to hold a maximum of 99,999 trees. A traditional heuristic tree search was executed using 1,000 Wagner replicates and random addition sequences, and a tree bisection-reconnection (TBR) algorithm was implemented. Nodal support values were calculated using the *BREMER.RUN* script included in the TNT package and standard bootstrap and jackknife analyses were performed under a traditional search using 1,000 replicates with absolute frequencies activated. Unstable taxa were identified post-analysis by the iterative PCR protocol (Pol & Escapa, 2009) as implemented in TNT 1.6.

Systematic palaeontology

Eusuchia Huxley, 1875

Crocodylia Gmelin, 1789

Gavialoidea Hay, 1930 (sensu Brochu, 1999)

Gavialidae Adams, 1854 (sensu Brochu, 2003)

Gavialinae Nopcsa, 1923 (sensu Brochu, 2003)

Dolichochampsa minima (Gasparini & Buffetaut, 1980)

(Fig. 2)

Diagnosis (emended from Gasparini & Buffetaut, 1980; Jouve et al., 2021). *Dolichochampsa minima* is a small-sized gavialid crocodylian diagnosed by the following unique combination of

character states: the posterior margin of the choana is not defined, being flush within the pterygoids; the "secondary wings" of the pterygoid are large and contribute to the posterior floor of the choana; the interchoanal septum is a narrow bony sheet that does not fully divide the opening. We identified a new autapomorphy based on the skull of FCGV-8178, a flat pterygoid wing. The pterygoid wing is a triangular-shaped plate that expands laterally and ventrally from each pterygoid bone in crocodylians. It serves as the attachment site for the tendons of the pterygoidal muscles (e.g., anterior pterygoidal muscle) associated with the jaw closure (Iordansky, 1999). In crown gharials, the pterygoid wing is relatively small and weakly inclined (less than 30 degrees) in occipital view compared to the condition in other taxa (e.g., *Crocodylus*, *Tomistoma*) within Crocodylia that possess a very inclined (more than 45 degrees) and large pterygoid wing. *Dolichochampsa* differs from all other gavialoids by having a septum that remains recessed within the choana (ch. 125 [1]), which is the primitive condition in basal eusuchians such as *Isisfordia duncani* (Salisbury et al., 2006; Fig. 4).

Referred material. The new material of *Dolichochampsa minima* (FCGV-8178) includes both cranial and postcranial remains. The skull includes part of the braincase, palate (pterygoid, palatine), and rostrum (maxilla). Postcranial elements include the right scapula, a dorsal vertebra, the right ischium, the right femur, a right tibia, and a metatarsal.

Locality, horizon, and age. The new specimen was retrieved near Maragua, Oropeza Province, Bolivia, some 18 km W of Sucre. It was preserved in a brown-to-reddish mudstone unit from the upper portion of the Middle El Molino Formation, which has been dated (U-Pb dating) at ca. 73–64 Ma (Tasistro-Hart et al., 2020: table 3).

Comments. We refer FCGV-8178 to *Dolichochampsa minima* based on morphological similarities shared with the holotype from Argentina and referred specimens from Bolivia. These include a tubular snout with well-defined notches that form an interdigitating jaw closure, procoelous dorsal vertebrae with a well-developed condyle, and the overall resemblance of the femur with specimen MLP 73-II-28-1 from Argentina (Gasparini & Buffetaut, 1980; Fig. 4). The new material described here is stratigraphically older than previously referred material of *D. minima* from the Upper El Molino Fm. of Bolivia (Buffetaut, 1987; Jouve et al., 2021). The body size of the new specimen of *Dolichochampsa minima* is ~1m in total body length, which is similar to the holotype from Argentina (Gasparini and Buffetaut, 1980).

Preservation. Specimen FCGV-8178 consists of a skull and postcranial elements found in tight association in a block measuring 15 x 7 x 3 cm (Fig. 2.2). The skull is exposed in ventral view and lacks most of the rostrum and elements of the skull table. The occipital region is also damaged, impeding a detailed anatomical description of that region. Portions of the ventral surface of the palate are missing, exposing the tubular nasopharyngeal duct. The left pterygoid flange is damaged, and the anteriormost margins of the suborbital fenestrae are incomplete. All hindlimb elements pertain to the right side; the side of the metatarsal is uncertain. Most postcranial bones are complete, except for the ischium, which lacks the shaft and the proximal region; the femur, which lacks its distal end; and the dorsal vertebra, which lacks most of its neural arch processes.

Description. An elongate element preserved along one side of the block probably represents the maxilla, based on its tight association with the skull and absence of features associated with the mandible, such as a symphysis, external mandibular fenestra, sutures, articular facets, and retroarticular process. The maxilla is preserved as a thin slice that approximates a sagittal section along the tooth row. The maxilla has been completely detached from the skull, but it remains in relative proximity to it and may be in its natural position. It is exposed in medial view, showing the inside of some maxillary alveoli. All maxillary sutures (e.g., premaxilla-maxilla) are indistinguishable due to preservation. The maxilla is anteroposteriorly straight and is 68.9 mm long as preserved. Although not complete, it lacks lateral or dorsoventral expansions (festooning), which gives the impression of a tubular snout (also known as the longirostrine condition). The tooth row is located at the lateral margin of the maxilla, and the alveoli are equally spaced. Although we cannot distinguish the alveolar size and shape, occlusal notches to accommodate the dentary teeth are well-developed across the maxilla. Based on the similar space between the alveoli and the length of the notches, we estimate the maxillary tooth count was 15–18 teeth. There is a short portion at the anterior part of the maxilla that has been slightly bent ventrally and does not follow the straight profile of the rest of the rostrum. We suggest that this bend is taphonomic (e.g., from compaction) and does not represent the actual morphology of the specimen. Longirotrine crocodylians (e.g., *Gavialis*) tend to have an anteroposteriorly straight maxillary palate that extends from the tip of the rostrum to the back of the last alveolus.

The palatine is exposed in ventral view, revealing the tubular nasopharyngeal duct. It is more distinguished along the medial margins of the suborbital fenestra and posteriorly at the pterygoid-palatine suture. The palatine meets its opposite at the ventral midline of the skull, where it forms the floor and lateral walls of the nasopharyngeal duct. FCGV-8178 lacks palatine

bullae, although we cannot rule out their loss during burial and diagenesis. The posteriormost part of the palatine meets the pterygoid along a transverse suture at the same level as the posterior edge of the suborbital fenestra. Anterior to this contact, the palate continues, contributing to the medial margin of the suborbital fenestra. The incompleteness of the anterior portion of the palate makes it difficult to distinguish the extent of contribution to the suborbital fenestra and its sutural relationship with the posterior process of the maxilla.

FCGV-8178 preserves both pterygoids, with the left side missing a considerable portion of the pterygoid process (flange). Both pterygoids lack the posterolateral contact with the ectopterygoids. The pterygoid is located in the posteriormost region of the skull, where it encloses the secondary palate. It meets its opposite at the midline anterior to the choana, along an anteroposteriorly oriented suture. Most of its ventral surface is flat and smooth. Posterolaterally, the pterygoid expands to form the well-developed transverse process (pterygoid wing) that is inclined at a low angle in occipital view. Extending posterior to the skull are two triangular-shaped and robust processes that contribute to the roof of the choana. These are relatively closely placed processes that meet at the midline of the choana, where the septum is visible. We refer to these processes as “secondary wings” to differentiate them from the transverse processes of the pterygoids. The pterygoid contributes to the posterior and lateral margins of the suborbital fenestra, although its lateral extent is uncertain due to preservation. Its anteromedial extension terminates where it meets the posterior margin of the palatine along a transverse suture. The choana pierces the pterygoid at its posteriormost border, as in eusuchians. The choanal opening is wider than long (10 mm wide and 5.2 mm long) and posteroventrally oriented. The anterior and lateral margins of the choana are well-defined, but the posterior portion lacks a dividing margin and is continuous within the secondary wings of the pterygoids. An interchoanal septum

projects from the dorsal surface of the choana (Appendix S3), as in *Isisfordia duncani* (Salisbury et al., 2006; Fig. 4).

A centrum and neural spine of a dorsal vertebra are preserved. The elements are not coalesced, but we consider them to belong together because of the matching size of the partially preserved neural spine and centrum. The serial position of the vertebra within the dorsal series is uncertain. The centrum is ca. 21 mm long and procoelous, with a well-developed convex condyle protruding 3 mm from the main body. The condyle is circumferentially inset on the centrum, leaving a small, flattened band around the perimeter of the articular surface. The left transverse process projects laterally from the neural arch and is 6 mm wide. The associated neural spine is exposed in a right-lateral view and is ca. 29 mm long as preserved. Although the maxilla covers the anterior edge of the neural spine, its posterior edge indicates that its border was straight from the apex to the mid-section, gradually expanding at its base before meeting the postzygapophysis. The neurocentral suture is entirely fused in the specimen FCGV-8178, indicating that the individual was at least close to its final stages of maturity. The procoelous condition of the specimen of FCGV-8178 is similar to the dorsal vertebra of the referred specimens of *Dolichochampsa minima* from Gasparini & Buffetaut (1980; Fig. 3H) and Jouve et al. (2018; Fig. 3). The condyles are well-developed as in modern eusuchians, which is unlike the incipiently developed condyle of basal eusuchians (e.g., *Isisfordia duncani*; Salisbury et al., 2006)

The right scapula is partially preserved. It is exposed in lateral view, and its medial side is currently embedded in matrix. The scapula is dorsoventrally short (28 mm). The dorsal edge of the scapular blade is nearly straight, being slightly concave in lateral view. Both anterior and posterior edges are weakly flared from the mid-shaft, showing concave profiles. These edges

gradually thicken from the shaft to the tip, making the surface of the scapular blade concave. The distal scapular blade is twice as broad anteroposteriorly (12.2 mm) as it is at mid-length (6.2 mm), which is similar to the breadth of the proximal end (12.7 mm). The blade is dorsoventrally straight, lacking any curvature on the anterior and posterior edges. The area of the acromion process, which is the origin site of the deltoideus muscle (m. deltoideus clavicularis), is incompletely preserved.

The distal portion of the right ischial blade and shaft are preserved (Appendix S3). As preserved, the ischial blade is long posteriorly (28.1 mm). The anterior part of the edge of the blade is broken, and its proximal portion seems to be restricted to the anterior end of the blade, giving the impression of an L-shaped bone. A shallow depression at the center of the blade divides the anterior and posterior parts, probably formed by taphonomic processes (e.g., burial compression).

The right femur is mostly complete, missing a section of the distal end of the shaft and a portion of the distal condyle. Detailed description and measurements of the femur are based on μCT scan observations, because the proximal end and shaft are buried in the block, mainly below the tibia. The μCT scan of the specimen of FCGV-8178 is available in the Supporting Information. The femur is long (91 mm) and sigmoid (S-shaped) to a minor degree. It is sub-circular in cross-section at mid-shaft (diameter = 9 mm), becoming mediolaterally compressed at the head (20 mm), which forms a convex surface for articulation with the acetabular area of the ilium. The head bends anteriorly to a minor degree and is twisted relative to the shaft. Additional information is provided by μCT scan imaging of the block containing the fossil. The femur resembles that of *Dolichochampsa minima* in possessing a weekly sigmoidal shaft, which is the condition of eusuchians. It is unclear whether the femoral fourth trochanter of FCGV-8178 is

'less pronounced' than that of modern eusuchians, as was described for a referred specimen of *Dolichochampsa* (Gasparini & Buffetaut, 1980; Fig. 4B).

The right tibia is preserved in near-articulation with the femur. It is exposed in medial view, and the inaccessibility in other views precludes the description of additional aspects of the bone. The tibia is straight with broad proximal and distal ends. It is a long and robust bone (57.8 mm long) that is 64% of the total length of the femur. Observations from the CT scan show that the shaft is circular in cross-section at mid-shaft (diameter = 7 mm) and becomes gradually elliptical at both ends. The proximal head and distal extremity are almost twice as wide (12.7 proximal and 13.2 mm distal) as the minimum shaft width. The distal edges bulge to form well-defined crests with ridges, and they flatten to form a spoon-shaped medial surface of the tibia.

The metatarsal is completely preserved and is visible on surface of the block. A small section of the shaft has been damaged, which is covered by the proximal end of the scapula. The metatarsal is long (40.4 mm), comprising 70% of the length of the tibia. The proximal end is flat and slightly wider transversely (8.4 mm) than both the shaft (5 mm) and the distal end (7.1 mm). The metatarsal shaft is sub-circular in cross-section. The close association of this element with the right hind foot suggests that it might pertain to that side and may represent the first metatarsal.

Phylogenetic and iterPCR results

Phylogenetic analysis of Crocodylia and closely related taxa recovered 987 most parsimonious trees of 479 steps (CI: 0.376, RI: 0.760) after removing uninformative characters (Fig. 3A). Despite the relatively large number of most parsimonious trees, much of the topology is fully resolved, with uncertainty localized within Gavialinae. Crocodylia is recovered as a

monophyletic group, as are crown-group alligatorids (*Alligator*, *Caiman*, *Melanosuchus*, and *Paleosuchus*) and their fossil allies (Fig. 3A). Crocodylids (*Crocodylus*, *Mecistops*, *Voay*, *Osteolaemus*) form a clade that is the sister-taxon to Gavialoidea. The node containing the genus *Crocodylus* is resolved with the exception of *C. moreletii* and *C. intermedius* (see Appendix S4). *Tomistoma* and morphologically similar taxa (e.g., *Kentisuchus*, *Paratomistoma*) form a paraphyletic group at the stem of Gavialoidea; their placement within the clade is weakly supported (see Appendix S4). Gavialinae is resolved as a monophyletic clade with high support values, although the interrelationships of most taxa are unresolved. Our analysis resolves 'thoracosaurs' as a clade outside Crocodylia, as the sister clade to *Borealosuchus formidabilis* (Fig. 3A).

Dadagavialis gunai, *Dolichochampsa minima*, and *Ocepesuchus eoafricanus* were identified as unstable OTUs by the iterPCR analysis. When the uncertainty surrounding their relationships was accounted for, the strict consensus tree was improved (Fig. 3B). The putative gavialid *O. eoafricanus* (Jouve et al., 2008) was recovered deeply nested within Alligatoridae. *D. gunai* is placed within *Aktiogavialis* spp. and in multiple places within the two gryposuchine clades (Fig. 3B). *Dolichochampsa minima* was deeply nested within Gavialinae, but its position within the clade was not resolved; equally parsimonious trees place it close to species of *Aktiogavialis*, *Gavialis*, and *Gryposuchus*.

Discussion

The new specimen of *Dolichochampsa minima* has important implications for the taxonomy, paleobiology, and paleobiogeography of early gavialines. In the following sections, we provide a

revised diagnosis of *D. minima* and discuss the implications of its phylogenetic position, the evolution of longirostry, and the paleobiogeography of South American gavialines.

Phylogenetic placement of 'thoracosaurs' and *Ocepesuchus eoafricanus*

'Thoracosaurs' have long been considered basally diverging gavialids based on morphological characters, which we included in our dataset (Brochu, 2004; Salas-Gismondi et al., 2016; 2019; Vélez-Juarbe et al., 2007). Our analysis resolves 'thoracosaurs' outside Crocodylia, within the Genus *Borealosuchus*, whose two species are rendered paraphyletic (see Appendix S2.1, 2.2, and S5). *Borealosuchus* species range from the Late Cretaceous to the Eocene of North America, a spatiotemporal distribution that coincides with that of 'thoracosaurs.' Although the relationship of 'thoracosaurs' with *Borealosuchus* is only weakly supported (see Appendix S4), their placement outside Crocodylia in our parsimony analysis is consistent with results of previous studies (Lee & Yates, 2018; Rio & Mannion, 2021; Salas-Gismondi et al., 2022).

Ocepesuchus eoafricanus was resolved as an early gavialoid when first included in a phylogenetic context (Jouve et al., 2008). Our parsimony analysis recovered *O. eoafricanus* within crown alligatorids, in one of five different positions (Fig. 3A, B). This result is consistent with the absence of key gavialoid characters in *O. eoafricanus* such as participation of the splenial in mandibular symphysis and telescoped orbits. In contrast, the presence of a homodont maxillary dentition (ch. 93[5]) is shared with crown gharials, underscoring the complex nature of this taxon.

Phylogenetic placement of *Dolichochampsa minima*

Our phylogenetic analysis resolves *Dolichochampsa minima* within Gavialinae (Fig. 3A), consistent with previous morphological studies (Gasparini & Buffetaut, 1980). The placement of *D. minima* within Gavialinae could not be resolved unambiguously, but iterPCR narrows its possible positions to the sister taxon of *Gavialis*, within or immediately outside *Aktiogavialis*, or within *Gryposuchus* (Fig. 3B). Characters from the skull and mandible support inclusion of *D. minima* within Gavialinae. Its uncertain lower-level interrelationships are the result of high levels of missing data in *D. minima* and variation in scorings within Gavialinae. For example, *D. minima* shares character state 23[0] with *Gavialis gangeticus*, but the optimization of that character is ambiguous for other gavialine taxa. *Dolichochampsa* shares character states 51[2], 54[0], 123[0], 127[1], 252[0], and 253[0] with most gavialines that can be scored. *Dolichochampsa* also shares characters 202[0] and 251[0] with *Gavialis* and *Aktiogavialis*, but the scorings within *Gryposuchus* differ. Among Gavialinae, character 247[0] is only shared among *D. minima*, *Gryposuchus,* and *Aktiogavialis*.

Although the exact placement of *D. minima* within Gavialinae remains unknown, its unambiguous placement within the clade is strongly supported (see Appendix S4), which has important implications. The age of *D. minima* pushes back the origin of Gavialinae to the Late Cretaceous (73–64 Ma) and opens the possibility that they originated in South America. The results of our study are consistent with elements of both molecular- and morphology-based analyses. Like molecular-based hypotheses, we recover a sister-clade relationship between morphological tomistomines and Gavialinae (Lee & Yates, 2018; Willis et al., 2007). Like morphology-based studies, our results imply an early, Gondwanan origin for Gavialinae (Brochu, 1997; 2003; 2004; Salas-Gismondi et al., 2016; 2019; Rio & Mannion, 2021; Vélez-Juarbe et al., 2007).

Paleobiogeography of Cretaceous gavialines

The temporal and geographic distributions of numerous gavialine taxa associated with marine environments (i.e., *Dadagavialis*, *Piscogavialis*, *Argochampsa*, *Aktiogavialis*) and their close phylogenetic relationships imply that the group likely underwent multiple trans-oceanic dispersals events between the Gondwanan and Laurasian landmasses (Brochu & Rincón, 2004; Jouve et al., 2006; Salas-Gismondi et al., 2016; 2019; 2022; Vélez-Juarbe et al., 2007). This hypothesis requires that gavialines have the physiological capabilities to tolerate saltwater conditions, which are not present in the modern, freshwater-restricted forms (*Gavialis* and *Tomistoma*) (Salas-Gismondi et al., 2016; 2019; Vélez-Juarbe et al., 2007).

The ancestral range for gavialines has been suggested to be the northern peri-Tethyan coasts (northern Africa + southern Europe), based on statistical dispersal-vicariance analysis (Salas-Gismondi et al., 2022; Fig. 3). In that analysis, the Paleocene taxon *Argochampsa krebsi* from Morocco (Jouve et al., 2006) represented the oldest gavialine, because 'thoracosaurs' were resolved outside Crocodylia. Such statistical analyses are sensitive to changes in topology (Yu et al., 2010), and so recovering *Dolichochampsa minima* deeply nested within gavialines in our analysis may add more complexity to the proposed hypothesis of a peri-Tethyan origin.

The results of our phylogenetic analysis provide equal support for *Dolichochampsa minima* as the sister taxon to *Gavialis*, to *Aktiogavialis*, and to *Gryposuchus*. The latter two genera are predominantly South American (with the exception of *A. puertoricencis* from the Caribbean), implying that these clades diversified from a South American ancestor and do not represent a dispersal from the peri-Tethys. In contrast, if *D. minima* is phylogenetically closer to *Gavialis* than to the other gavialines, then a more complex paleobiogeographic distribution is

implied, with multiple trans-oceanic dispersals between Laurasian and Gondwanan landmasses (Salas-Gismondi et al., 2019; 2022; Vélez-Juarbe et al., 2007). We recognize the current uncertainty in the phylogenetic position of *D. minima* within Gavilinae, but its placement within this lineage provides insights into the dispersal capabilities of the group. The gavialines hypothesized to be closest to *D. minima* are *Argochampsa krebsi* and *Eogavialis africanum*, from the Paleocene and Eocene of Africa, respectively (Hua & Jouve, 2004; Jouve et al., 2006; Salas-Gismondi et al., 2022). Even if the evolutionary relationships of *D. minima* within Gavialinae remain unknown, its age and geographic distribution with respect to the other gavialines suggests a possible transoceanic dispersal during the Cretaceous–Paleogene, lending support that early gavialines were able to tolerate and cross marine waters (Brochu & Rincón, 2004; Vélez-Juarbe et al., 2007).

Conclusions

We describe new material of a small-bodied (~1 m), long-snouted crocodylian collected from the Cretaceous–Paleogene (73–64 Ma) El Molino Formation referable to *Dolichochampsa minima*. We incorporated the new specimen into an expanded and modified osteological data matrix, along with other putative oldest gavialid crocodylians from North America ('thoracosaurs') and Africa (*Ocepesuchus eoafricanus*), to test their evolutionary relationships in a phylogenetic context. Our results reveal that *D. minima* is a gavialine, whereas 'thoracosaurs' are recovered outside of Crocodylia, and *O. eoafricanus* is recovered within alligatorids. The phylogenetic position of 'thoracosaurs' and differences in character states from gavialines imply that longirostry evolved independently in both clades. The age and provenance of *D. minima* has

important implications for gavialine origins and paleobiogeography. Its Late Cretaceous to early Paleogene age pulls the origin of Gavialinae into the Mesozoic (73–64 Ma). Its South American provenance opens the possibility of an origin for Gavialinae on that landmass or elsewhere in Gondwana. Importantly, the occurrence of a Cretaceous–Paleogene gavialine in South America suggests a possible dispersal to Africa and Asia, lending support to the hypothesis that salinity tolerance appeared in early gavialine history, as previously proposed (Brochu & Rincón, 2004; Vélez-Juarbe et al., 2007).

Acknowledgments

We are indebted to Jorge Jora, Ryan Manzuk, Adrian Tasistro-Hart, and Sarah Brown for collecting the fossil material and to the Universidad Mayor de San Andrés, Facultad de Ciencias Geológicas, La Paz, Bolivia, for loaning the FCGV-8178 specimen to the University of Michigan Museum of Paleontology. We thank the Princeton University Department of Geosciences for funding that supported the field work. We are grateful to William Sanders, Chief Preparator at UMMP, for preparing the FCGV-8178 specimen and Matt Friedman for generating the µCT scan data that allowed for a detailed comparison and description. We thank Rodolfo Salas-Gismondi, Lázaro Viñola López, and Jorge Vélez-Juarbe for discussions on the new specimen. We also thank reviewers Y and X for constructive criticism that improved this manuscript.

References

Bezuijen, M. R., Shwedick, B. M., Sommerlad, R., Stevenson, C. & Steubing, R. B. (2010). Tomistoma *Tomistoma schlegelii*. In S. C. Manolis, & C. Stevenson (Eds.), *Crocodiles: Status Survey and Conservation Action Plan* (pp. 133–138). Crocodile Specialist Group: Darwin.

Brochu, C. A. (1997). Morphology, fossils, divergence timing, and the phylogenetic relationships of *Gavialis*. *Systematic Biology, 46*(3), 479–522. https://doi.org/10.1093/sysbio/46.3.479

Brochu, C. A. (1999). Phylogenetics, taxonomy, and historical biogeography of Alligatoroidea. *Journal of Vertebrate Paleontology, 19*(2), 9–100.

Brochu, C. A. (2003). Phylogenetic approaches toward crocodylian history. *Annual Review of Earth and Planetary Sciences, 31*, 357–397.

Brochu, C. A. (2004). A new Late Cretaceous gavialoid crocodylian from eastern North America and the phylogenetic relationships of thoracosaurs. *Journal of Vertebrate Paleontology, 24*(3), 610–633.

Brochu, C. A., & Rincón, A. D. (2004). A gavialoid crocodylian from the lower Miocene of Venezuela. *The Palaeontological Association, 71*, 61–79.

Buffetaut, E. (1982). Radiation évolutive, paléoécologie et biogéographie des crocodiliens mésosuchiens. *Mémoires de la Société Géologique de France, 142*, 1–88.

Buffetaut, E. (1987). Occurrence of the crocodilian *Dolichochampsa minima* (Eusuchia, Dolichochampsidae) in the El Molino Formation of Bolivia. *Bulletin van de Belgische Vereniging voor Geologie, 96*(2), 195–199.

Camoin, G., Casanova, J., Rouchy, J.-M., Blanc-Valleron, M.-M. & Deconinck, J.-F. (1997). Environmental controls on perennial and ephemeral carbonate lakes: the central palaeo-Andean Basin of Bolivia during Late Cretaceous to early Tertiary times. *Sedimentary Geology*, *113*: 1–26.

Carpenter, K. (1983). *Thoracosaurus neocesariensis* (De Kay, 1842) (Crocodylia: Crocodylidae) from the Late Cretaceous Ripley Formation of Mississippi. *Mississippi geology, 4*(1), 1–10.

Costa, E., Garcés, M., Sáez, A., Cabrera, L. & López-Blanco, M. (2011). The age of the "Grande Coupure" mammal turnover: new constraints from the Eocene–Oligocene record of the Eastern Ebro Basin (NE Spain). *Palaeogeography, Palaeoclimatology, Palaeocology, 301*(1–4), 97–107.

Delfino, M., Piras, P., & Smith, T. (2005). Anatomy and phylogeny of the gavialoid crocodylian *Eosuchus lerichei* from the Paleocene of Europe. *Acta Palaeontologica Polonica, 50*(3), 565–580.

Densmore, L. D., & Dessauer, H. C. (1984). Low levels of protein divergence detected between *Gavialis* and *Tomistoma*: evidence for crocodilian monophyly. *Comparative Biochemistry and Physiology Part B: Comparative Biochemistry, 77*(4), 715–720.

Erickson, B. R. (1998). Crocodilians of the Black Mingo Group (Paleocene) of the South Carolina coastal plain. *Transactions of the American Philosophical Society, 88*(4), 196–214.

Gallagher, W. B., Parris, D. C., & Spamer, E. E. (1986). Paleontology, biostratigraphy, and depositional environments of the Cretaceous–Tertiary transition in the New Jersey Coastal Plain. *Mosasaur, 3*, 1–35.

Gasparini, Z. B., & Buffetaut, E. (1980). *Dolichochampsa minima*, n. g. n. sp., a representative of a new family of eusuchian crocodiles from the Late Cretaceous of northern Argentina. *Neues Jahrbuch für Geologie und Paläontologie - Monatshefte, 1980*, 257–271.

Gatesy, J., Amato, G., Norell, M., Desalle, R., & Hayashi, C. (2003). Combined support for wholesale taxic atavism in gavialine crocodylians. *Systematic Biology, 52*(3), 403–422.

Gayet, M., Sempere, T., Cappetta, H., Jaillard, E. & Levy, A. (1993). The occurrence of marine fossils in the latest Cretaceous of the central Andes and its paleogeographic implication. *Palaeogeography, Palaeoclimatology, Palaeoecology*, *102*: 283–319.

Gmelin, J. F. (1789).Caroli a Linné Systema Naturae. G. E. Beer, Leipzig, 1033–1516 pp.

Goloboff, P. A., & Catalano, S. A. (2016). TNT version 1.5, including a full implementation of phylogenetic morphometrics. *Cladistics, 32*, 221–238.

Hass, C. A., Hoffman, M. A., Densmore, L. D., & Maxson, L. R. (1992). Crocodilian evolution: insights from immunological data. *Molecular Phylogenetics and Evolution, 1*(3), 193–201.

Haq, B. U., Hardenbol, J. & Vail, P. R. (1987). Chronology of fluctuating sea levels since the Triassic. *Science*, *235*: 1156–1167.

Hay, W. (2009). Cretaceous oceans and ocean modelling. In X. Hu, C. Wang, R. W. Scott, M. Wagfreich, & L. Jansa (Eds.), *Cretaceous Ocean Redbeds: Stratigraphy, Composition, Origins, and Paleoceanographic and Paleoclimatic Significance* (pp. 243–271). SEPM (Society for Sedimentary Geology) Special Publication.

Howes, B. H. (2023). From Ooids to Extinction: Developing Physical Paleoenvironmental Proxies for Understanding Earth History, Princeton University, Princeton, NJ.

Hua, S., & Jouve, S. (2004). A primitive marine gavialoid from the Paleocene of Morocco. *Journal of Vertebrate Paleontology, 24*(2), 341–350. https://doi.org/doi: 10.1671/1104

Huxley, T. H. (1875). On *Stagonolepis robertsoni*, and on the evolution of the Crocodilia. *Quarterly Journal of the Geological Society, 31*, 423–438.

Iordansky, N. N. (1999). Jaw muscles of the crocodiles: structure, synonymy, and some implications on homology and functions. *Russian Journal of Herpetology, 7*(1), 41–50.

Janke, A., Gullberg, A., Hughes, S., Aggarwal, R. K., & Arnason, U. (2005). Mitogenomic analyses place the gharial (*Gavialis gangeticus*) on the crocodile tree and provide a pre-K/T divergence times for most crocodilians. *Journal of Molecular Evolution, 61*, 620–626.

Jouve, S., Iarochene, M., Bouya, B., & Amaghzaz, M. (2006). New material of *Argochampsa krebsi* (Crocodylia: Gavialoidea) from the Lower Paleocene of the Oulad Abdoun Basin (Morocco): phylogenetic implications. *Geobios, 39*, 817–832.

Jouve, S., Bardet, N., Jalil, N.-E., Suberbiola, X. P., Bouya, B. & Amaghzaz, M. (2008). The oldest African crocodylian: phylogeny, paleobiogeography, and differential survivorship of marine reptiles through the Cretaceous-Tertiary boundary. *Journal of Vertebrate Paleontology, 28*(2), 409–421.Jouve, S., de Muizon, C., Cespedes-Paz, R., Sossa-Soruco, V., & Knoll, S. (2021). The longirostrine crocodyliforms from Bolivia and their evolution through the Cretaceous–Palaeogene boundary. *Zoological Journal of the Linnean Society, 192*, 475–509.

Lamb, S., Hoke, L., Kennan, L., & Dewey, J. (1997). Cenozoic evolution of the Central Andes in Bolivia and northern Chile. *Geological Society, London, Special Publications*, *121*(1), 237–264.

Lee, M. S. Y., & Yates, A. M. (2018). Tip-dating and homoplasy: reconciling the shallow molecular divergences of modern gharials with their long fossil record. *Proceedings of the Royal Society B: Biological Sciences, 285*, 20181071.

Marquillas, R. A., Salfity, J. A., Matthews, S. J., Matteini, M., & Dantas. (2011). U-Pb zircon age of the Yacoraite Formation and its significance to the Cretaceous–Tertiary boundary in the Salta basin, Argentina. *Cenozoic Geology of the Central Andes of Argentina*, 1, 227–246.

Martin, J. E. (2019). The taxonomic content of the genus *Gavialis* from the Siwalik Hills of India and Pakistan. *Special Papers in Palaeontology, 5*, 483-497.

Matthews, K. J., Maloney, K. T., Zahirovic, S., Williams, S. E., Seton, M. & Müller, R. D. (2016). Global plate boundary evolution and kinematics since the late Paleozoic. *Global and Planetary Change*, *146*: 226–250.

Nopcsa, F. (1923). Die Familien der Reptilien. *Fortschritte der Geologie und Palaentologie, 2*, 1–210.

Pol, D., & Escapa, I. H. (2009). Unstable taxa in cladistics analysis: identification and the assessment of relevant characters. *Cladistics, 25*, 515–527.

Pucéat, E., Lecuyer, C., & Reisberg, L. (2005). Neodymium isotope evolution of NW Tethyan upper ocean waters throughout the Cretaceous. *Earth and Planetary Science Letters, 236*, 705–720.

Rio, J. P., & Mannion, P. D. (2021). Phylogenetic analysis of a new morphological dataset elucidates the evolutionary history of Crocodylia and resolves the long-standing gharial problem. *PeerJ, 9*, e12094.

Ristevski, J., Young, M. T., de Andrade, M. B., & Hastings, A. K. (2018). A new species of *Anteophthalmosuchus* (Crocodylomorpha, Goniopholididae) from the Lower Cretaceous of the Isle of Wight, United Kingdom, and a review of the genus. *Cretaceous Research, 84*, 340–383.

Rouchy, J. M., Camoin, G., Casanova, J., & Deconinck, J. F. (1993). The central palaeo-Andean basin of Bolivia (Potosi area) during the late Cretaceous and early Tertiary: reconstruction of ancient saline lakes using sedimentological, paleoecological and stable isotope records. *Palaeogeography, Palaeoclimatology, Palaeoecology, 105*, 179–198.

Salas-Gismondi, R., Flynn, J. J., Baby, P., Tejada-Lara, J. V., Claude, J., & Pierre-Olivier, A. (2016). A new 13 million year old gavialoid crocodylian from proto-Amazonian mega-wetlands reveals parallel evolutionary trends in skull shape linked to longirostry. *PLoS ONE, 11*(4), e0152453.

Salas-Gismondi, R., Moreno-Bernal, J., Scheyerc, T. M., Sánchez-Villagra, M. R., & Jaramillo, C. (2019). New Miocene Caribbean gavialoids and patterns of longirostry in crocodylians. *Journal of Systematic Palaeontology, 17*(12), 1049–1075.

Salas-Gismondi, R., Ochoa, D., Jouve, S., Romero, P. E., Cardich, J., Perez, A., DeVries, T., Baby, P., Urbina, M., & Carré, M. (2022). Miocene fossils from the southeastern Pacific shed light on the last radiation of marine crocodylians. *Proceedings of the Royal Society B: Biological Sciences, 289*, 20220380.

Salisbury, S. W., Molnar, R. E., Frey, E., & Willis, P. M. A. (2006). The origin of modern crocodyliforms: new evidence from the Cretaceous of Australia. *Proceedings of the Royal Society B: Biological Sciences*, *273*, 2439–2448.

Schwimmer, D. R. (1986). Late Cretaceous fossils from the Blufftown Formation (Campanian) in western Georgia. *The Mosasaur, 3*, 109–123.

Sempere, T. (1994). Kimmeridgian? to Paleocene tectonic evolution of Bolivia. Pp. 168–212 in J.A. Salfity (ed) *Cretaceous Tectonics of the Andes*. Vieweg, Braunschweig.

Sempere, T., & Marshall, L. G. (1997). Stratigraphy and chronology of Upper Cretaceous–lower Paleogene strata in Bolivia and northwest Argentina. *Geological Society of America Bulletin, 109*(6), 709–727.

Stevenson, C. J. (2015). Conservation of the Indian gharial *Gavialis gangeticus*: successes and failures. *International Zoo Yearbook, 49*, 150–161.

Tasistro-Hart, A., Maloof, A., Schoene, B., & Eddy, M. P. (2020). Astronomically forced hydrology of the Late Cretaceous sub-tropical Potosí Basin, Bolivia. *GSA Bulletin, 132*(9), 1931–1952.

Troxell, E. L. (1925). *Thoracosaurus*, a Cretaceous crocodile. *American Journal of Science, 57*, 219–233.

Vélez-Juarbe, J., Brochu, C. A., & Santos, H. (2007). A gharial from the Oligocene of Puerto Rico: transoceanic dispersal in the history of a non-marine reptile. *Proceedings of the Royal Society B: Biological Sciences*, 274, 1245–1254.

Vélez-Juarbe, J., Domning, D. P. & Pyenson, N. D. (2012). Iterative evolution of sympatric seacow (Dugongidae, Sirenia) assemblages during the past ~26 million years. *PLoS ONE, 7*(2), 1–8.

Wilkinson, M. (1995). Coping with abundant missing entries in phylogenetic inference using parsimony. *Systematic Biology, 44*(4), 501–514.

Willis, R. E., McAliley, L. R., Neeley, E. D., & Densmore, L. D. 2007. Evidence for placing the false gharial (*Tomistoma schlegelii*) into the family Gavialidae: inferences from nuclear gene sequences. *Molecular Phylogenetics and Evolution, 43*, 787–794.

Yu, Y., Harris, A. J., & He, X. (2010). S-DIVA (Statistical Dispersal-Vicariance Analysis): a tool for inferring biogeographic histories. *Molecular Phylogenetics and Evolution, 56*, 848–850.

Figures

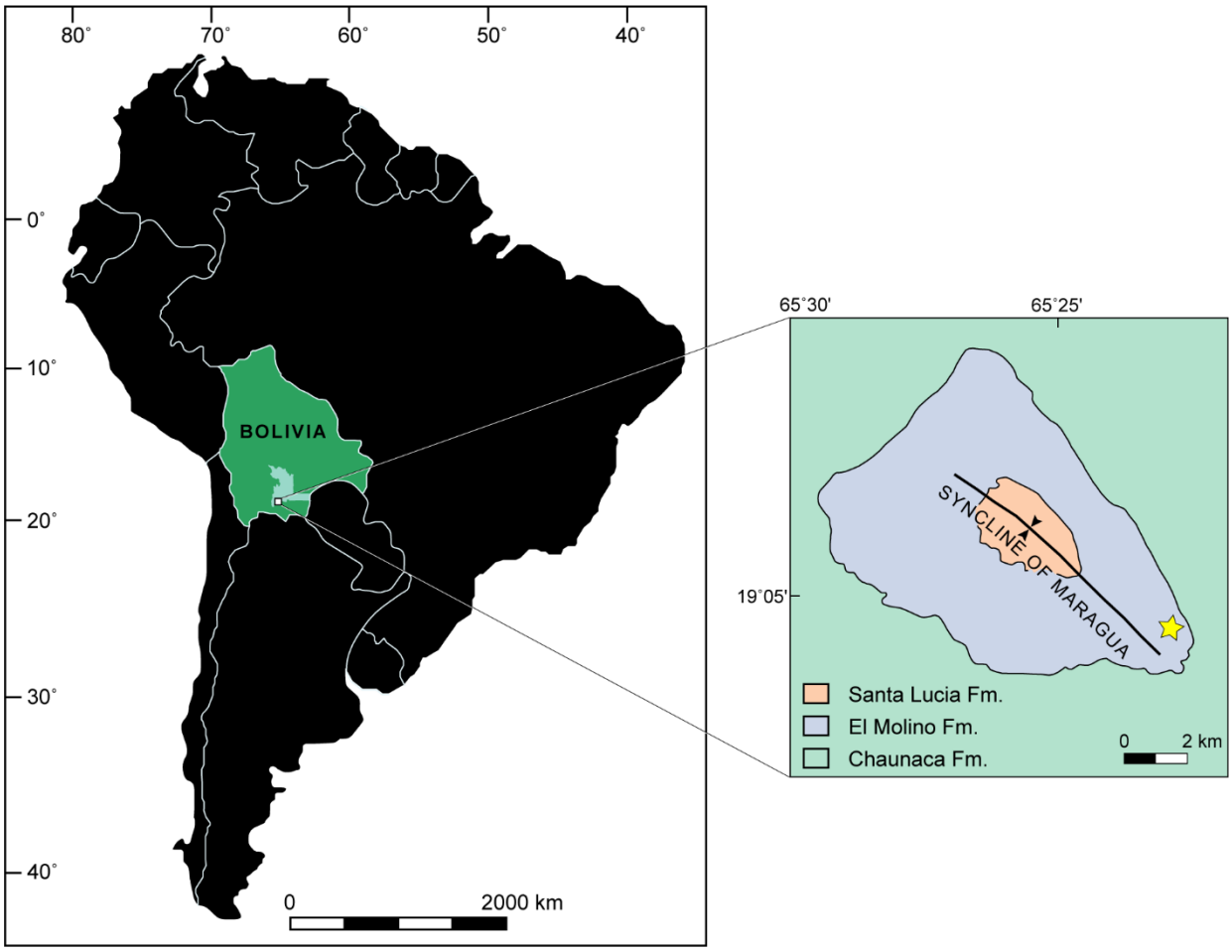

Figure 2.1. Map of South America showing where the new specimen of *Dolichochampsa minima* FCGV-8178 was collected in southern Bolivia. The inset map details the syncline of Maragua and identifies the locality (yellow star) within an exposed section of the Upper El Molino Formation.

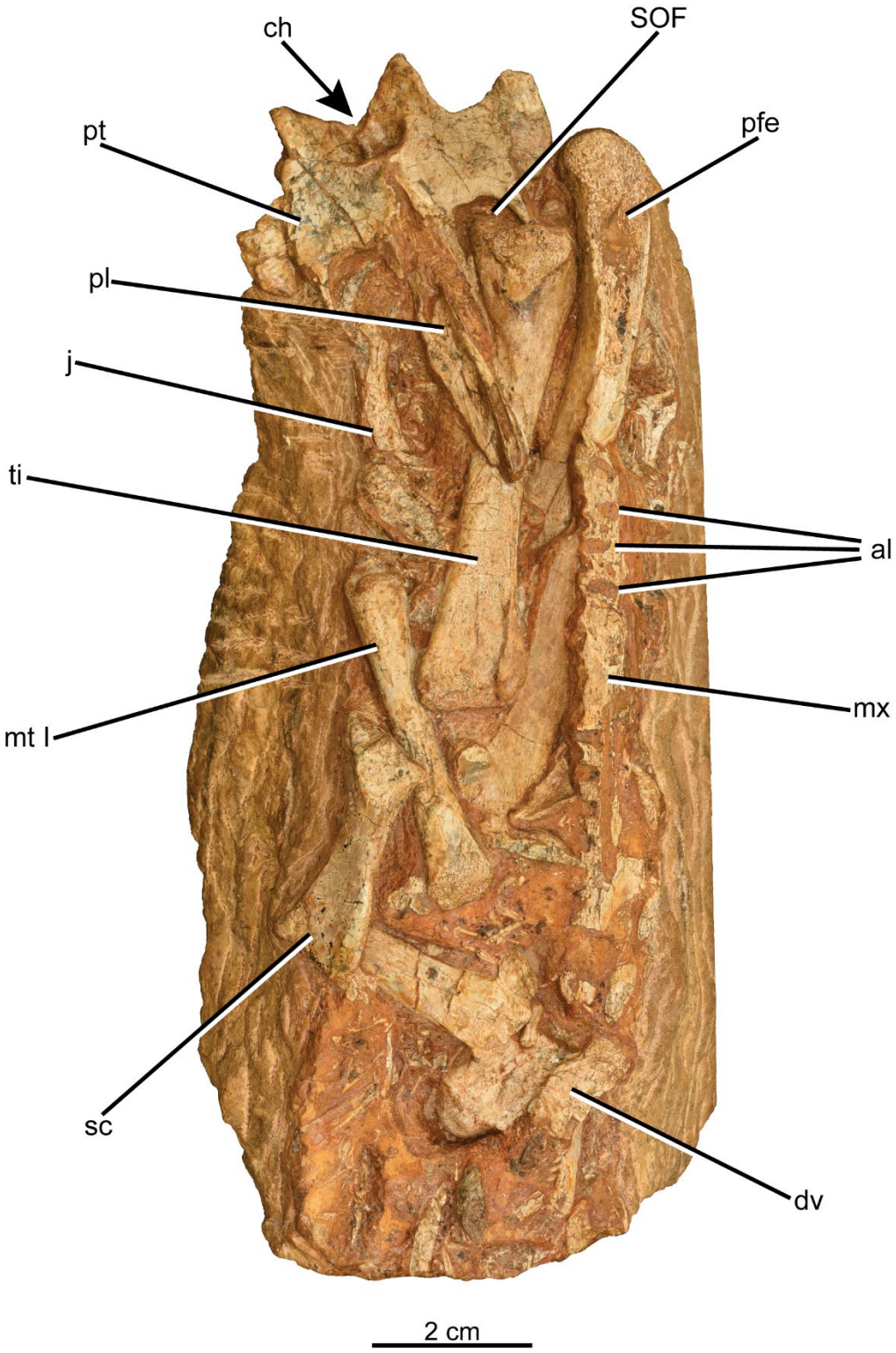

Figure 2.2. Photograph of the block containing all elements of the new specimen of *Dolichochampsa minima* (FCGV-8178). **Abbreviations: al**, alveoli; **ch**, choana; **dv**, dorsal vertebra; **fe**, proximal part of femur; **j**, jugal; **mt I**, metatarsal I; **mx**, maxilla; **ns**, neural spine; **pl**, palatine; **pt**, pterygoid; **sc**, scapula; **SOF**, suborbital fenestra; **ti**, tibia.

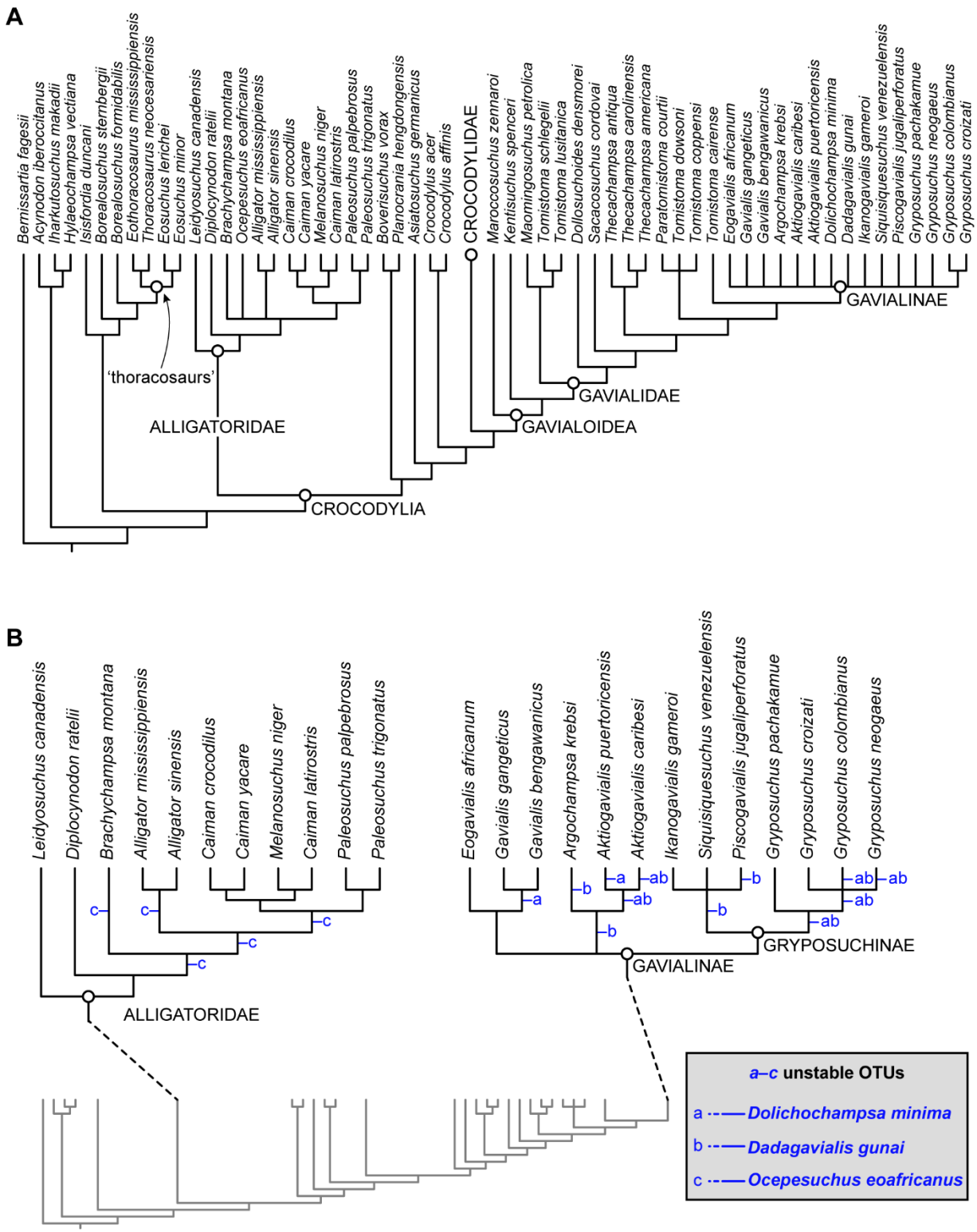

Figure 2.3. Results of parsimony analysis and iterPCR. (**A**) 50% majority-rule consensus of 987 most parsimonious trees. *Dolichochampsa minima* is recovered within Gavialinae, 'thoracosaurs' are placed as the sister clade to *Borealosuchus formidabilis*, and *Ocepesuchus eoafricanus* is nested within Alligatoridae. (**B**) Result of the iterPCR analysis showing the alternative placements of the unstable taxa (*D. minima*, *Dadagavialis gunai*, and *O. eoafricanus*).

CHAPTER 3

A New Basal Gavialine (Crocodylia: Gavialinae) from the Eocene of Pakistan and its Paleobiogeographical Implications

Abstract

The global distribution of fossil gavialines throughout the Cenozoic shows us how diverse the group was and their possible capabilities to cross marine waters. In Greater India, the gavialine record is only represented by the Miocene–Pliocene taxa, *Gavialis* and *Rhamphosuchus*, and fossils that precede this time in South Asia have yet to be found. This apparent gap in the gavialine fossil record in Greater India raises questions on how and when the group arrived in that region, as well as questions on their evolutionary history. Here, we report a new Eocene (43–41 Ma) longirostrine crocodylian, *Pelagosuchus pakistanensis*, from the Upper Domanda Formation of Pakistan. Phylogenetic analysis revealed strong affinities of the new taxon to Gavialinae. Evaluation of character distribution in our strict consensus shows affinities between *Pelagosuchus* and the South American gryposuchines. Assessment of shared characters demonstrates strong homology, suggesting a possible Tethyan origination for gryposuchines. *Pelagosuchus* is the first gavialine associated with open marine settings, lending support to the possibility that early forms were capable of tolerating marine settings. The discovery of an Eocene gavialine in present-day Pakistan suggests that the group possibly arrived in Asia before the final closure of the Tethys Sea, almost 20 million years earlier than previously thought. After the closure of the Tethys Sea and the uplift of the Himalayas, gavialine populations may have

become isolated in the northern parts of Greater India, which explains the current distribution of the extant taxon, *Gavialis gangeticus*, in India.

Introduction

Gavialis gangeticus is a long-snouted crocodylian currently restricted to the fluvial systems of northern India and Nepal, with extinct populations from Bhutan, Myanmar, and Pakistan (Stevenson, 2015). The fossil record, however, shows that gharials (Gavialinae) were a successful lineage that diversified and occupied multiple landmasses in the Cenozoic, including two taxa from Africa, an assemblage from the Americas (Gryposuchinae), and Asia (Brochu & Rincón, 2004; Gürich, 1912; Jouve et al., 2006; Langston & Gasparini, 1997; Martin, 2019; Martin et al., 2012; Salas-Gismondi et al., 2016; 2019; 2022; Vélez-Juarbe et al., 2007). Although fossil gavialines are widely distributed across most of the Cenozoic, apparent gaps in the paleontological record obscure our understanding of their evolutionary and paleobiogeographic histories. Paleobiogeographic scenarios proposed an Eocene–Oligocene dispersal from Africa or Asia to the Americas, but because there is a large hiatus during most of the Eocene (c.a., 56–41 Ma) with no specimens elsewhere, it is difficult to confirm the center of origination and patterns of distribution of more recent clades (Brochu & Rincón, 2004; Vélez-Juarbe et al., 2007). Thus, recovering gavialines from the early stages of the Eocene will be crucial for understanding the distribution of extinct and extant forms.

Reports of fossil longirostrine crocodylians from India and Pakistan date back to the late 1830s, when Captain Proby Thomas Cautley and Dr. Hugh Falconer recovered specimens from the Miocene–Pliocene rocks in the Siwalik Hills and Sindh, respectively (Cautley, 1836; 1840;

Cautley and Falconer, 1840; Martin, 2019). Most of these specimens have been referred to the living taxon *Gavialis gangeticus* (Martin, 2019), although nine species were erected during the mid-nineteenth and early twentieth century primarily based on incomplete material. Recently, Martin (2019) reevaluated the taxonomic status of these Miocene–Pliocene specimens, concluding that one species (*G. hysudricus*) is a junior synonym of *G. gangeticus*, two species (*G. browni* and *G. lewisi*) require further revision, and referred four taxa (*G. leptodus*, *G. pachyrhynchus*, *G. curvirostris*, and *G. breviceps*) are referred to *Rhamphosuchus crassidens*. This revision recognized two species, *G. gangeticus* and *G. bengawanicus*, the latter a recently extinct species from Java and Thailand (Delfino and De Vos, 2010; Martin et al., 2012). Specimens older than these Miocene–Pliocene fossil gharials have not yet been recovered from India. The geographically closest relatives to the Indian fossil gharials are *Eogavialis africanum* from the late Eocene of Egypt (38–33 Ma) and *Argochampsa krebsi* from the Paleocene (66–56 Ma) of Morroco, both of which occurred when the Tethys Sea connected the Atlantic and Indian oceans (Berra & Angiolini, 2014; Clyde et al., 2003; Hay & Jouve, 2004; Jouve et al., 2006; Salas-Gismondi et al., 2022). Even if such a marine connection existed at the time, allowing dispersal from Africa to Asia, there is an apparent gap in the gavialine fossil record in Indo-Pakistan with no occurrences preceding those specimens from the Miocene. As a consequence, this gap in the fossil record raises several questions about when gharials arrived in the northern regions of India and Pakistan prior to the closure of the Tethys Sea and uplift of the Himalayas, how and when the gharials from the Americas (Gryposuchinae) arrived, as well as questions on their evolutionary history.

Here we report new material of a large longirostrine crocodylian from the Eocene Domanda Formation of Pakistan. The fossil specimen is the oldest (43–41 Ma) gavialine from

Greater India, extending the stratigraphic range of the clade in that region to the Eocene. The strong affinities between the new taxon to the Indian and South American gharials give insights into the divergence time and possible origination of the latter clade. The occurrence of the new taxon in marine sediments of the Tethys Sea presents an opportunity for an evaluation of the paleoecology of early gavialines, which holds a central role in understanding the dispersal capabilities of the group.

Locality and Geologic Setting

The new crocodylian specimen (GSP-UM 3332) presented herein was found and collected by William Sanders on November 16, 1999. This new finding was part of a series of field expeditions from 1979 to the late 1990s by a collaboration between the Geological Survey of Pakistan (GSP) and The University of Michigan Museum of Paleontology (UMMP). The holotype and associated remains were collected from the Upper Domanda Formation exposed in the Dabh Nala Monocline (N 30.85453, E 70.22010) on the eastern flank of Balochistan Province, Pakistan (Fig. 1).

During the Eocene, the Sulaiman Basin was located on the northwestern flank of the Indian plate (Gingerich et al., 1995; 2001). The middle section of the Kahan Group, the Domanda Formation, is a 240 to 360 meters-thick sedimentary sequence deposited on the eastern side of the Sulaiman Basin (Gingerich et al., 2001). The Domanda Fm. is divided into three stratigraphic members (Lower, Middle, and Upper) that decrease in thickness from bottom to top, based on the succession of different shale units (Gingerich et al., 1995). Stratigraphically, the Domanda Fm. overlies the Habib Rahi Formation, where sediments progress from green

shales (Lower), gradually transition to red shale units (Middle), and terminate at the top with red shales (Upper), which is overlain by the Pir Koh Formation. Limestone units are minor units along the Lower Member of the Domanda Fm., siltstones are uncommon, and terrestrial (clastic) sediments are virtually absent (Gingerich et al., 1995).

Temporal correlations of chronostratigraphy and Tethyan biostratigraphic zones presented by Gingerich et al. (2001) provide a middle Eocene (Lutetian; 41.0–47.5 Ma) age for the entire Domanda Formation, which shows several periods of high subsidence on a passive continental margin (Gingerich et al., 1995). The stratigraphic sequences of the Domanda Formation record offshore, deep marine depositional environments formed by shallowing-upward cycles of marine regressions that took place during the Eurasian-Indian collision and the closure of the Tethys Sea (Gingerich et al., 1995; 2001; Clyde & Gingerich, 2003; van Hinsbergen et al., 2019).

Materials and Methods

Taxon sampling The new specimen (GSP-UM 3332) was included in a character state matrix of (Vélez-Rosado et al., 2024), which includes 248 discrete morphological characters and 67 operational taxonomic units (OTUs). This dataset is an expansion of previous matrices and includes the majority of eusuchians, especially gavialines (Brochu, 1999; 2011; Buscalioni et al., 1992; Clark, 1994; Norell, 1988; 1989; Norell and Clark, 1990; Poe, 1996; Salas-Gismondi et al., 2016; 2019; 2022; Vélez-Juarbe et al., 2007). We removed *Dadagavialis gunai*, *Dolichochampsa minima*, and *Ocepesuchus eoafricanus* because they have been found to be unstable OTUs, which created a large polytomy within Gavialinae. *Pelagosuchus* was scored for 81 (33%)

characters, which include 64 cranial, 25 mandibular, 1 axial, and 1 girdle elements (Supplementary File 1).

Phylogenetic analysis

We performed a parsimony analysis in TNT v.1.6 (Goloboff & Morales, 2023) under a traditional heuristic search. The maximum number of trees to save was set at 99,999. Wagner trees were performed using a 1,000 number of addition sequences and used the tree bisection and reconnection of the branch swapping algorithm with 10 trees saved per replication. All characters were equally weighted, and multistate characters were unordered. *Bernissatia fagesii* was designated as the outgroup taxon. Nodal support values were performed using the Bremer.run script from TNT, and resampling (bootstrap values) and jacknife were calculated using the traditional heuristic search of 1,000 replicates with absolute frequencies in activated mode. Character distribution and performance (Consistency index) in the strict consensus tree were evaluated in Winclada (Nixon, 2002).

Institutional Abbreviations—GSP-UM, Geological Survey of Pakistan-University of Michigan, Ann Arbor, U.S.A.

Systematic Paleontology

EUSUCHIA Huxley, 1875, sensu Brochu, 1997

CROCODYLIA Gmelin, 1789, sensu Benton & Clark, 1988

GAVIALIDAE Hay, 1930, sensu Brochu, 2003

GAVIALINAE Nopcsa, 1923, sensu Brochu, 2003

PELAGOSUCHUS, gen. nov.

PELAGOSUCHUS PAKISTANENSIS, sp. nov.

(Figs. 2–5)

Holotype—GSP-UM 3332 is a nearly complete skull that includes most of the snout (maxilla, nasal), skull table (frontal, postorbital, parietal, squamosal), braincase elements (supraoccipital, exoccipital), and both mandibular rami (dentary, splenial, angular, surangular, articular).

Etymology— The genus name is the combination of the Greek words for "open ocean" (*pélagos*) and "crocodile" (*suchus*). The species name is the latinized version of Pakistan, where the specimen was found.

Referred Specimens—Additional material includes twenty disarticulated crowns, two thoracic vertebrae found in articulation, and a right scapula.

Differential Diagnosis—*Pelagosuchus pakistanensis* gen. nov. sp. nov. is diagnosed by the following combination of autapomorphies: one pair of enlarged alveoli at mid-rostrum (ch. 93[7]); and a fronto-postorbital suture convergent anteriorly (ch. 151[2]). The holotype also differs from members of Gavialoidea by having a dorsally projected rostrum, and a robust and extremely enlarged quadrate projected posterolaterally—extending 17.5 cm beyond the occipital condyle—from the skull table (Figs. 2, 3E–H).

Locality, Horizon, and Age—The holotype and referred material were collected from Ander Dabh Janubi, Pakistan, from the Upper Member of the Domanda Formation. The Upper

Domanda Fm. is Eocene in age (43–41 Ma; upper Lutetian) based on the Tethyan biostratigraphy and chronostratigraphy of Gingerich et al. (2001: fig. 11).

Preservation

The holotype of *Pelagosuchus pakistanensis* (GSP-UM 3332) was found in the Upper Member of the Domanda Formation, where most of the remaining skeleton resides (W.S. personal communication). Elements of *Pelagosuchus* that were retrieved from the type locality include most of the skull and mandible, and some postcrania. The skull and lower jaw are broken into several pieces that fit together, show the same size, and articulate to form a single individual (Figs. 2, 3). Rostral elements include an almost complete maxilla and nasal, and anterior portion of both jugals. The maxillary toothrows are missing most teeth, and the posteriormost portion of the left side is highly damaged. Elements of the skull table include the frontal, portions of the prefrontals, both postorbitals, the parietal, and the squamosals with their long prongs. Only a section of the left postorbital bar is preserved. Because most portions of the pterygoids are absent, the canal for the olfactory tract of the holotype is readily visible in ventral view. The anterior aspect of the left jugal is present, and the right is almost entirely preserved. Palatal elements include the palatines, the posteriormost parts of both ectopterygoids, and portions of the pterygoid wings. Only the posteriormost portions of both quadratojugals are preserved along the quadratojugal-quadrate contact. Braincase elements include the exoccipital, basioccipital, and both quadrates. The orbits are traceable, though the left side is more complete. Both supratemporal fenestrae are completely visible, and ventrally just the anterior portions of the suborbital fenestrae are appreciable in the holotype. Most cranial and mandibular sutures are

readily visible, except for some dorsal and posterior surfaces of the rostrum and skull table that are slightly damaged by preservation. The rostrum is broken into two large pieces, exposing the morphology of the nasopharyngeal duct. On the dorsal surface of the rostrum, a bite mark is readily visible on the right side of the maxilla.

Elements of the lower jaw include a partial right symphysis that bears six alveoli. The dentaries and splenials are incompletely preserved, and most dentary teeth are missing or broken. Both angular and articular bones are present and show their sutural contact with the other mandibular elements. Muscle scars and aponeuroses are present on the surfaces of the skull (quadrate) and lower jaw (mandibular adductor fossae). Referred material to GSP-UM 3332 includes 20 teeth, most of which are large conical crowns with smooth enamel surfaces. The external mandibular fenestrae are appreciable in the holotype.

Postcranial elements associated with the holotype include a right scapula and dorsal vertebrae. The scapula is broken into two pieces across the deltoid crest with some parts missing, resulting in proximal and distal (scapular blade) parts that do not fit together. The two dorsal vertebrae associated with the holotype are preserved in articulation. These vertebrae have complete centra, with the anterior vertebra having the right parapophyseal and diapophyseal processes. The neural arch includes prezygapophyses and postzygapophyses, and both lack neural spines. Both vertebrae have the hypapophysis, but these are damaged by preservation.

Description

General Description

The following description follows the anatomical and orientational terminology of Romer (1956) and Iordansky (1973; 1999). Description of the holotype specimen, *Pelagosuchus pakistanensis* gen. nov. sp. nov., is based on a nearly complete skull that preserves most of its rostrum, skull table, braincase, and lower jaw (Figs. 2–5). Elements of the mandibular rami include a partial right dentary symphysis, incomplete dentaries and splenials, angulars, surangulars, and articulars. Disarticulated parts treated in the description include twenty crowns, two thoracic vertebrae, and a right scapula. The skull of *Pelagosuchus* is approximately 0.98–1.5 m long, with a body length estimate of 6.5–7 m based on total body length/skull length regressions of Sereno et al. (2001). The skull generally resembles longirostrine crocodylians (ca. 73 % rostral length), such as gharials (e.g., *Gavialis* and gryposuchines) and tomistomines (e.g., *Tomistoma*). The rostrum lacks antorbital fenestrae or fossae and gradually broadens posteriorly to meet the orbits. The orbits are well situated dorsally above the rostrum at the level of the skull platform. The external auditory meatus is triangular, and the associated vertebrae are procoelous, as in crown eusuchians.

Skull

Maxilla—The maxilla is the elongated element of the skull that contributes to the dorsolateral and ventral sides of the rostrum, forming the walls and floor of the secondary palate (Fig. 2A, B). Dorsally the maxilla is separated from its pair by the long nasal. The maxilla-nasal suture is anteroposteriorly straight along the rostrum. The rostrum is dorsoventrally flattened (wider than high) and the lateral sides gradually broaden posteriorly to fit the skull table. Anterior to the largest maxillary alveolus the maxilla arches anterodorsally, which is a condition that has never been documented in crocodylians (Fig. 2). Ventrally the maxilla continues where

it meets its pair along the midline. Although the anterior portion of the maxilla is incomplete, festooning coincides with the largest maxillary alveoli, which is only apparent in dorsal view. The maxillary toothrow is straight, and the anteriormost alveoli are slightly elevated relative to the floor of the maxilla. All alveoli are subcircular in cross-section and well-separated. As preserved, the alveolar size increases in diameter in one wave anteroposteriorly, coincident with the festooning (Fig. 2). Although the maxilla expands laterally along the enlarged alveoli, those from the right toothrow are comparatively larger than the left side (Fig. 2B). Notches are present along the anteriormost margins of the rostrum, and occlusal pits occur irregularly at the lateral and medial sides along the posteriormost part of the maxilla, which gives the impression of a lingual dental occlusion anteriorly and an overbite posteriorly (Fig. 2B). The right maxillary toothrow preserves 15 alveoli and may range from 18 to 22 teeth, more than 22 less likely. At the level of the 8th alveolus (as preserved) on the right side, the maxilla bears a bite mark (puncture/furrow) on its surface that bisects vertically but does not perforate the bone (Fig. 2A) (Drumheller & Brochu, 2016). Ventrally the posteromedial portion of the maxilla is pierced by the palatine, although the maxilla continues posteriorly, contributing to the anteromedial and anterolateral portions of the suborbital fenestra.

The maxilla is broken along two planes, exposing the nasopharyngeal duct. Anteriorly the nasopharyngeal duct is wider than tall (28.4mm dorsoventrally, 36.5mm lateromedially) and becomes taller posteriorly (41.5mm dorsoventrally, 38.5mm lateromedially). The dorsal aspect of the nasopharyngeal duct has a keel at the midline, giving a W-shaped. The keel is less pronounced anteriorly but becomes more prominent posteriorly, where it is visible at the level of the 6th maxillary alveolus (as preserved). The anterior and posterior portions of the maxilla, including the premaxilla-maxilla and maxillo-palatine sutures, are missing due to preservation.

Nasal—*Pelagosuchus pakistanensis* has a nasal that extends anteroposteriorly along the midline of the entire rostrum, contributing to the roof of the secondary palate (Fig. 2). The nasal meets its pair along the midline, and the inter-nasal suture in *Pelagosuchus* is slightly visible externally, which indicates that both elements are not completely fused. The dorsal aspect is smooth without ornamentation and small foramina are present. As preserved, the nasal conserves most of its width along the rostrum, gradually tapering anteriorly. Posteriorly, the nasals bifurcate and terminate at the level of the anterior margin of the orbit (Fig. 2).

Jugal—The jugal is elongated and extends anteroposteriorly along the lateral side of the orbits, although the maxillo-jugal suture on both sides is obscure by preservation (Fig. 2A). The anterior portion seems to form a triangular contact with the maxilla and probably extends beyond the orbit, contributing slightly to the sides of the rostrum. Ornamentation is prominent as subcircular pits and absent on its anteriormost portion. The right jugal is in placed on the posterior side of the quadratojugal, forming a straight jugal-quadratojugal suture.

Lacrimal—The lacrimal is a triangular element that contributes to the anterior margin of the orbit (Fig. 2A). Anteromedially the lacrimal contacts the nasal and posteriorly the prefrontal, excluding it from participation to the maxilla. The lateral margin contacts the maxilla, and its posterolateral border is in tight sutural contact with the jugal.

Prefrontal—The prefrontal is situated lateral to the frontal and forms the anteromedial margin of the orbit (Fig. 3A). Anteriorly the prefrontal is pointed (triangular-shaped)and wedged between the lacrimal and nasal, excluded from the maxilla. Portions of the dorsal surface of the prefrontal are missing, including the prefrontal pillar. The dorsal surface is slightly ornamented with shallow pits.

Frontal—The frontals in *Pelagosuchus pakistanensis* are fused, forming a single plate that contributes significantly to the medial portion of the skull table (Fig. 3A). The dorsal surface is mostly smooth, only bearing ornamentation near the frontal-postorbital suture. Although an anterior portion of the frontal is missing, its process extends beyond the orbit, piercing the nasals medially. At its anterolateral margin, the frontal meets the prefrontal along a straight suture and continues posteriorly to contribute to the medial and posteromedial border of the orbit. The interorbital space is wide (64.9 mm) and concave, displacing the orbits to the lateral sides of the skull. The contribution of the frontal to the orbits terminates where it contacts the postorbital along a straight suture. Posteriorly, the fronto-parietal suture occurs just anterior to the supratemporal fenestra. In the ventral aspect, the canal of the olfactory tract expands anteriorly to house the olfactory bulb and enlarges posteriorly to give space to the anterior portion of the cerebral hemisphere (Fig. 3B).

Postorbital—The postorbital constitutes the anterolateral margin of the skull table and contributes to the temporal bar, margin of the orbit, and supratemporal fenestra (Fig. 3A). In the dorsal aspect, the postorbital contributes to the posteromedial margin of the orbit, and its anterolateral corner is rounded and continuous without a process. The anteromedial side of the postorbital is slightly elevated, and it meets the frontal along a straight suture. Posteriorly the postorbital continues where it contributes to the anterolateral margin of the supratemporal fenestra and terminates along a transverse suture with the squamosal. The lateral margin of the postorbital is oblique, which makes the temporal bar convergent anteriorly in dorsal view. The dorsal surface is highly ornamented with square-shaped and elongated pits. On its lateral side, the postorbital has a shallow sulcus for the attachment of the medial limb of the dense fibrous Y-shaped tissue (the Ypsilon) and the superior ear flap (Shute and Bellairs, 1953; Ziermann et al.,

2019). The Ypsilon also attaches to the M. depressor auriculae inferior, the muscle responsible for the movement of the lower ear flap (Ziermann et al., 2019). A portion of the left postorbital bar is preserved, being ventrolaterally inclined and anteroposteriorly elongated (oval-shaped).

Parietal—In *Pelagosuchus pakistanensis*, the parietals are fused as a single I-shaped element that contributes to the posterior border of the skull table and margins of the supratemporal fenestra (Fig. 3A). The anterior aspect contacts the posterior side of the frontal along a straight suture, preventing the contribution of the frontal to the supratemporal fenestra. Along the fronto-parietal suture, the parietal forms a process that extends to the anterolateral side of the supratemporal fenestra, where it contacts the posteromedial side of the postorbital. It continues posteriorly, sending a short process that contributes to the medial and posteromedial margins of the supratemporal fenestra. Posteriorly the parietal sends a thick process that contributes to the posteromedial side of the supratemporal fossa, also covering the exoccipital in the dorsal view (Fig. 3C). The posterior process terminates along the parietal-squamosal suture medial to the midline of the supratemporal fenestra. Ornamentation is present on the surface as sub-circular pits only in the posterior half. At the foramen lacrum posterior, the parietal elevates to form two domes above the foramina, and they terminate at the midline to develop a shallow depression (Fig. 3D).

Squamosal—The squamosal is a robust element that forms the posterolateral border of the skull table, the margin of the supratemporal fenestra, and the roof of the otoccipital and the external auditory meatus (Fig. 3C). In *Pelagosuchus pakistanensis*, the squamosal sends a long anterodorsal process that forms more than 50% of the temporal bar. Anteriorly the squamosal contributes to the lateral margin of the supratemporal fenestra and terminates where it meets the postorbital along a transversely oriented suture. The squamosal extends medially from the

anterodorsal process, contributing to the posterolateral and most of the posterior border of the supratemporal fenestra. This medial process does not overhang the fenestra, allowing exposure of the anteriormost part of the quadrate in dorsal view. The contribution of the squamosal to the medial surface of the skull table terminates where it meets the parietal as a parasagittally oriented suture. Opposite from the medial margin, the dorsolateral border is somewhat concave in outline, making it the broadest part (290 mm width) of the skull table. The squamosal extends beyond the parietal as a prominent (55 mm long), triangular-shaped, and ventrally projected squamosal prong where it is in tight sutural contact with the paroccipital process. In the occipital view, the medial process of the squamosal rests on the dorsal surface of the exoccipital and the medial side of the quadrate. The dorsal surface of the squamosal is highly ornamented with irregular pits and grooves, although absent along the lateral margin and prong. At the lateral side of the supratemporal fenestra, the squamosal has a shallow depression, which makes the surface of this bone irregular. The lateral aspect bears a deep longitudinal groove (sulcus) that extends forward to the lateral margin of the postorbital and posteriorly terminates before reaching the squamosal prong. The function of this groove is for the attachment of the M. levator auriculae superior and M. depressor auriculae superior, both muscles serve to open and close the upper ear flap (Shute & Bellairs, 1955). The ventral surface of the squamosal is dorsoventrally enlarged, expanding the surface area of the external auditory meatus.

Supraoccipital—The supraoccipital is a triangular-shaped bone situated at the posterior border of the skull table between the foramen lacrum (Fig. 3D). Damage to the dorsal surface of the supraoccipital makes it impossible to assess whether the bone is exposed on the skull table or not. In occlusal view, it is in sutural contact with the exoccipital and terminates ventrally before reaching the basioccipital.

Exoccipital—The exoccipital is a braincase element that forms the posterior and lateral walls of the cerebral cavity and dorsal margin of the foramen magnum (Fig. 3D). In *Pelagosuchus pakistanensis*, the exoccipital is strongly verticalized and expands laterally to form the paroccipital process. On the dorsolateral surface, the exoccipital is sutured with the squamosal and medially with the supraoccipital, the latter excluded from the foramen magnum. The long and robust paroccipital process extends from the lateral sides and lies above the quadrate, overhanging the narrow cranioquadrate passage. In crocodylians, the cranioquadrate passage extends from the paroccipital process to the middle ear, providing a path for the cranial nerve VII (facial), the orbitotemporal cavity, and the cephalic vein (Iordansky, 1973). Cranial nerves and foramina open at the ventrolateral sides of the exoccipital close to the occipital condyle, which includes the cranial nerve XII (hypoglossal foramina), the foramina for cranial nerves IX-XI (glossopharyngeal, vagus, and accessory), and the posterior carotid foramen (Fig. 3D). The foramen magnum in *Pelagosuchus* is oval-shaped.

Basioccipital—The basioccipital lies below the exoccipital and entirely forms the oval-shaped (dorsoventral 49.1 mm and mediolaterally 58.7 mm) occipital condyle, which is the cranial element that articulates with the first cervical vertebra (atlas) (Fig. 3D). The basioccipital is incompletely preserved anteriorly, missing the tuberosities of the basioccipital plate.

Quadrate—The quadrate in *Pelagosuchus pakistanensis* is large and robust, extending posteroventrally (9.5 cm) beyond the occipital condyle (Figs. 3E–H). The anteromedial portion (quadrate head) lies below the squamosal and is exposed through the supratemporal fenestra in dorsal view. Posterior to the quadrate head, the anterolateral side serves as the floor for the triangular-shaped otic aperture (external auditory meatus). It is unclear if the quadrate-squamosal suture extends dorsal to the external auditory meatus or is restricted to the posteroventral corner.

The medial portion is in tight contact with the paroccipital process, which covers the quadrate-exoccipital suture. Posteriorly the articulate condyles form an S-shaped surface, with the medial condyle expanded ventrally. The foramen aëreum is small and lies on the medial surface close to the cranioquadrate passage. In the ventral surface, crests for the tendons and aponeuroses of the M. adductor mandibulae externus medialis and M. adductor mandibulae posterior are well-developed, although damaged on this surface obscures the extent of these crests (Ziermann et al., 2019). Crest A is present as a longitudinal groove along the quadrate-quadratojugal suture, and another crest, probably B', is located at the midline as a shallow knob (Iordansky, 1973).

Quadratojugal—The preserved quadratojugal includes the posterior section that is sutured with the quadrate (Figs. 3E–H). The quadratojugal-quadrate suture extends anteroposteriorly and bends laterally before reaching the quadrate condyle. Although incomplete, the dorsal surface of the quadratojugal seems to be highly ornamented.

Palatine—The palatine is located ventrally posterior to the maxilla, contributing to the medial side of the suborbital fenestra and forming the walls and floor of the nasal passage (Fig. 2B). Anteriorly the palatine sends a long process that extends beyond the suborbital fenestra and reaches the 8th (as preserved) maxillary alveolus. The palatine terminates slightly posterior to the suborbital fenestra, forming a wide U-shaped suture with the pterygoid.

Pterygoid—The remaining portions of the pterygoid include an anterior fragment that sutures with the posterior portion of the palatine and parts of both flanges (wings). Although incomplete, it seems that the anterolateral portion of the pterygoid contributes to the posterior margin of the suborbital fenestra. The pterygoid meets its pair at the midline, and the suture continues posteriorly, where it probably reaches the choana. The choana is not present on the anterior aspect of the pterygoid nor in the palatine, and herein we presumed that its location must

have been on the posteriormost region of the pterygoid as in all eusuchians (Supplementary File 3).

Ectopterygoid—Only the posterior portion of both ectopterygoids are preserved. The ectopterygoid lies below the lateral side of the pterygoid flange (wing), and its posterior extent terminates before reaching the tip of the pterygoid.

Cranial Openings

Orbit—*Pelagosuchus pakistanensis* possess an orbit that is wider than long and is located dorsally at the level of the skull table (Figs. 3A, B). The orbit is smaller than the supratemporal fenestra, lacking the semi-circular crest or rugosities.

Supratemporal Fenestra—The supratemporal fenestra lies on the horizontal plane on the back of the skull plane (Fig. 3A, B). Dermal bones that border the fenestra include the parietal and squamosal, which do not overhang the fossa. Both fenestrae are significantly large and quadrangular in outline (Supplementary File 3). The main axis is oriented anteromedially, which converges anteriorly with the axis of its pair. In dorsal view, the quadrate head and its contact with the laterosphenoid are visible.

Foramen Lacrum Posterior—The foramen lacrum posterior (posttemporal fenestra) is an opening (pneumatic) located below the squamosal-parietal suture that could have been an evolutionary adaptation for an aquatic lifestyle in Crocodylia (Fig. 3D) (Mansharamani, 1965). In *Pelagosuchus pakistanensis*, this opening is medioventrally oriented, significantly enlarged (36.4 mm long and 9.8 mm wide), and separated, which is uncommon for a crocodylian. The surface close to both foramina is broken, making it impossible to assess whether the postoccipital processes (sensu Salas-Gismondi et al., 2022) are open or separated.

Suborbital Fenestra—Although incomplete, the anterior portion of the suborbital fenestra in *Pelagosuchus pakistanensis* is triangular in shape and it might have been proportionally large (Fig. 2B). The anterior limit of the suborbital fenestra extends to the fourth last maxillary alveolus, with an acute anterior end and rounded medially. Although both suborbital fenestrae are incomplete, their anterior margins are bordered by the maxilla and medially by the palatine and probably bounded laterally and posteriorly by the ectopterygoid and pterygoid, respectively.

Mandible

Articular—The articular is the posteriormost element of the mandibular ramus, forming the fossae that articulate with the quadrate of the skull and contributes to the retroarticular process (Figs. 4A–D). It is a complex bone that is sutured with multiple elements of the lower jaw. On the dorsolateral and mediodorsal sides, it is delimited by the surangular and ventrally with the angular. In *Pelagosuchus pakistanensis*, a transverse ridge divides the articular fossae into lateral and medial concavities corresponding to the convexities of the quadrate condyles. The lateral concavity is wider and shallow, whereas the medial side of the fossa is deeper and short, giving space for the expanded medial hemicondyle of the quadrate. Posterior to the fossa, the articular forms a tall wall that differentiates the retroarticular process from the rest of the articular. The retroarticular process is elongated, dorsally oriented, and triangular in outline. A longitudinal ridge divides the retroarticular process into lateral and medial sides, the latter being concave and ventrally expanded. The medial border of this concavity serves to attach one of the jaw-closing muscles, the M. pterygoideus posterior (Iordansky, 1973). The foramen aëreum is situated on the mediodorsal side of the articular fossa. At the surangular-articular suture, the

mandibular adductor fossa—where the M. adductor mandibulae superior attaches—is flushed against the surangular.

Surangular—The surangular in *Pelagosuchus pakistanensis* is an elongated element located at the posterodorsal margin of the lower jaw (Figs. 4A–D). Anterodorsally it is wedged between the dentary on its lateral side and lingually with the splenial, not reaching the last dentary alveoli. Posteriorly, it lies on top of the angular, forming a horizontal suture, and bends ventrally, terminating beyond the articular fossa but without reaching the tip of the retroarticular process. In the lingual aspect, the surangular-angular suture meets at the ventral tip of the articular. A conspicuous dorsally facing fossa is situated at the lateral side of the articular fossa. In *Pelagosuchus*, the fossa is anteroposteriorly elongated and enlarged on both sides (Figs. 4A, B).

Angular—The angular extends from the back of the retroarticular process to the anterior side of the external mandibular fenestra (EMF) (Figs. 4A–D). Laterally, the angular extends anterior to contribute to the posterodorsal and posteroventral margins of the EMF. Medially the angular forms the floor of the mandibular adductor fossa. In the lateral aspect, the angular-surangular suture starts ventral and posterior to the articular fossa and continues dorsally, where it terminates on the posterodorsal side of the EMF. The angular terminates beyond the mandibular fenestra as a V-shaped trough ventrally between the dentary and splenial before reaching the last dentary tooth. In *Pelagosuchus*, the angular is divided by a sculpted surface anteriorly and a smooth surface posteriorly, which serves as the surface area of the lateral portion of the M. pterygoideus posterior (Iordansky, 1973).

Dentary—The description of the dentary bone corresponds to that of the right mandibular ramus, which preserves most of its length, alveoli, and sutures with other lower jaw

elements (Figs. 4A–F). *Pelagosuchus pakistanensis* shows a long symphysis that extends to the 6th dentary alveolus, although its extent is unknown and it could have been as long as in longirostrine forms (i.e., *Gavialis*). In lateral view, the dentary continues below the surangular sending two processes that contribute to the dorsal and posterior margins of the external mandibular fenestra. The ventral process is short, contributing to almost one-third of the anteroventral margin of the EMF. Based on the preserved mandibular rami and relation to the maxilla, the dentary may be missing 7 to 10 alveoli for a total dentary count of 23 to 26. Notches are present anteriorly, with one occlusal pit between the fourth and fifth dentary teeth. As preserved, the alveoli along the symphysis are set in tandem, with the first and fourth slightly medial to the others. Most of these symphyseal alveoli are similar in size, except the fourth, which is larger than the neighboring alveoli and elevated above the dentary surface. Although both dentary toothrows are incomplete, there is an anteroposterior increase in alveolar size. Also coinciding with variation in alveolar size, the interalveolar space seems to decrease anteroposteriorly, and the posterior part of the dentary toothrow shows a sinusoidal pattern that goes from medial (last dentary alveoli) to a more lateral position.

Splenial—The splenial covers the medial aspect of the mandibular ramus, and its extent to the anterior and posterior portions of the mandible is unknown (Figs. 4A–D). Posteriorly the dorsomedial part is sutured with the surangular and ventrally reaches the angular below the foramen intermandibularis caudalis.

Dentition—*Pelagosuchus pakistanensis* has typical eusuchian (thecodont dentition) teeth enclosed in sockets or alveoli (Figs. 4A–D). The premaxilla is missing, though the preserved maxillary and dentary toothrows allow a reasonable estimate of the total number of teeth. The estimated tooth count for *Pelagosuchuss* is 4?(5?)+15–24?/16–26?, which includes 4–5 uncertain

premaxillary teeth, 15 preserved maxillary teeth and may extend to 24, and 16 preserved dentary teeth and may range to 26. Only nine teeth remain in place in the maxilla and four in the dentary. Except for the first dentary tooth that is complete, all other teeth are worn and missing most of the crowns. The first dentary tooth is circular in cross-section, anteromedially oriented, and seems more slender than the posterior teeth. It has a smooth enamel with faintly mesial and distal carinae (Figs. 4E, F). Although the teeth from the posterior part of the toothrows are missing the apical portions, they are bigger than the anterior counterparts. All disarticulated teeth that are associated with *Pelagosuchus* show a similar morphology with conical crowns that increase in thickness from the apex to the base.

Mandibular openings

External mandibular fenestra—The external mandibular fenestra in *Pelagosuchus pakistanensis* is large, which almost reaches the anterior process of the angular (Figs. 4C, D). The fenestra is oval-shaped and inclined, with its anterior end ventral to the posterior end. Although the borders of the fenestra are incomplete, the anterior end seems acute, whereas the posterior end is more rounded. In lateral view, the fenestra is bounded by the surangular, dentary, and angular.

Axial Skeleton

Dorsal Vertebrae—The vertebrae associated with the holotype remain in articulation and possibly are the first two dorsal (D1 and D2) vertebrae (Figs. 5A–C). Both have procoelous centra, having a concave cotyle anteriorly and a convex condyle posteriorly. Anteriorly, D1 has a shallow and circular cotyle with well-defined edges. Although not visible in D1, D2 has a

condyle that protrudes considerably posteriorly (Supplementary File 3). The hypapophyseal processes are present in both centra, although better preserved in D2. The hypapophysis in D2 extends ventrally from the anteroventral surface of the centrum. Posterior to the hypapophysis in D2, the centrum seems to expand ventrally near the condyle, forming a wide U-shaped outline that is visible in lateral view (Figs. 5B, C). This posteroventral expansion of D2 is absent in D1. Projecting from the lateral sides of the centra and neural arches of D1 and D2 are the parapophyseal and diapophyseal processes, respectively. On the left lateral side, D1 shows a sub-circular and shallow capitular facet. D2 has the articular facet of the prezygapophyses projecting dorsally, with a slight ventromedial inclination. Posteriorly, the facet of the postzygapophysis is projecting ventrally (horizontal). Both vertebrae are missing the neural spines. The neurocentral sutures in both vertebrae are mostly closed, only visible in some areas of D2.

Pectoral Girdle

Scapula—The right scapula is broken into two pieces along the shaft (Figs. 5D, E). Both, the anterior and posterior ends of the proximal part of the scapula are similar. The scapula becomes constricted closer to the deltoid crest and the anterior and posterior margins gradually broaden toward the scapular blade. At the dorsal edge, the blade bends slightly. The deltoid crest seems to be broad, however, it is highly damaged by preservation.

Comparisons of *Pelagosuchus pakistanensis*

Key anatomical features associated with the skull and postcrania of the new species presented herein, *Pelagosuchus pakistanensis* gen. nov. sp. nov, opens the discussion for a

comparative analysis with other taxa of similar and distant spatiotemporal distributions. Among these forms of similar temporal and geospatial distribution to *Pelagosuchus* is *Astorgosuchus*, a large crocodylian from the Oligocene of the Bugti Hills, Pakistan (Martin et al., 2019; Pilgrim, 1908; 1912). Comparisons between *Astorgosuchus* and *Pelagosuchus* are based mainly on the overlapping features of the rostrum and lower jaw. *Astorgosuchus* was described as having a highly differentiated maxillary toothrow in which the alveoli decreased in size considerably posterior to the sixth alveolus (Martin et al., 2019:fig. 1). In contrast, the alveoli in *Pelagosuchus* remain of similar size throughout the toothrow (Fig. 2B). In addition, the maxillary toothrow seems to be tight in *Astorgosuchus* compared to the well-separated alveoli of *Pelagosuchus*. A partial dentary associated with *Astorgosuchus* (Martin et al., 2019:fig. 2) preserves a splenial that extends to the sixth dentary alveolus, although not preserved in *Pelagosuchus*, the preserved portion of the dentary symphysis does not show any indication of a splenial that extends to that far anteriorly and is probably located posteriorly as in most gavialines (e.g., *Gavialis*). Additional differences include the arrangement of the dentary toothrows in which the alveoli of the third and fifth dentary teeth are confluent with the fourth alveolus in *Astorgosuchus* (Martin et al., 2019:fig. 2), but are well separated in *Pelagosuchus* (Figs. 4E, F). *Astorgosuchus* also has an enlarged fourth dentary alveolus that is at least twice the size of the adjacent (third and fifth) teeth, however, the fourth alveolus in *Pelagosuchus* is of similar size to its neighboring teeth. A partial mandible associated with *Astorgosuchus* (Martin et al., 2019:fig. 4) shows an expanded symphysis at the level of the fifth dentary alveolus, which differs from the condition in *Pelagosuchus* in which the dentary alveoli 1-6 are anteroposteriorly aligned (Figs. 4E, F).

Additionally, there are notable differences and similarities between the skull of *Pelagosuchus pakistanensis* and the early gavialines, *Argochampsa* and *Eogavialis*, from Africa.

Among the differences, *Argochampsa* has a long, but narrow nasal bone that extends to most of the rostrum (Hua & Jouve, 2004:fig. 2), by contrast, *Pelagosuchus* has a comparatively wider nasal (Fig. 2A). Other anatomical differences include the position of the orbits, in which these are highly dorsalized in *Pelagosuchus* and *Argochampsa*, but more verticalized in *Eogavialis* (Andrews, 1906:plate XXIII). Although incomplete, *Pelagosuchus* has quadrangular orbits, whereas the orbits in *Argochampsa* and *Eogavialis* are circular in outline. Similarities between *Eogavialis* and *Pelagosuchus* include the arrangement of the first six dentary teeth, which are aligned anteroposteriorly, although in *Argochampsa* the first dentary tooth is positioned medially with respect to the posterior teeth (Jouve et al., 2006).

Although *Pelagosuchus pakistanensis* was retrieved as the basalmost within Gavialinae in our phylogenetic analysis (see below), the holotype shares two morphological characters associated with the lower jaw of the South American gavialine, *Gryposuchus pachakamue* (Salas-Gismondi et al., 2016). Both taxa possess a foramen situated on the posterolateral side of the surangular, near the articular fossa (Salas-Gismondi et al., 2016:fig. 2D). However, the same structure was described earlier by Wu et al. (2001: fig. 2) in *Leidyosuchus canadensis* (Lambe, 1907), but named it as "fossa on lateral surface of surangular." Whether the presence of this fossa in *G. pachakamue* and *Pelagosuchus* represents homology remains unknown, however, its absence in early and derived gavialines suggests that this condition could have appeared independently multiple times within Gavialinae. An additional similarity between *G. pachakamue* and *Pelagosuchus* is the extent of the posterior process of the dentary along the external mandibular fenestra. In both taxa, the dentary sends a posterior process that contributes to most of the dorsal margin of the mandibular fenestra but has a complex sutural contact with

the surangular, a condition that differs from that in any gavialines described thus far (Salas-Gismondi et al., 2016:fig. 6).

Phylogenetic Affinities

Phylogenetic analysis of *Pelagosuchus pakistanensis* recovered 6 most parsimonious trees (MPTs) of 984 steps (Consistency Index: 0.381, Retention Index: 0.762) after removing the uninformative characters (Supplementary File 2). The strict consensus retrieved several major nodes within Crocodylia as in previous studies, including Alligatoridae, Crocodylidae, Gavialidae, and some subgroups (Brochu & Rincón, 2004; Salas-Gismondi et al., 2019; 2022; Vélez-Juarbe et al., 2007). Crown-group gharials and their allies are recovered as a monophyletic group. *Tomistoma* and its morphologically similar taxa form a paraphyletic assemblage leading to Gavialinae with comparatively low supporting values (Fig. 6). Three subgroups within Gavialinae are recognized in the strict consensus: a group containing *Argochampsa* and *Aktiogavialis*; a group with *Eogavialis* and *Gavialis*; and Gryposuchinae (Fig. 3.6). Gryposuchinae is a subgroup within Gavialinae that includes seven species within four genera from the Americas (Salas-Gismondi et al., 2022). Not surprisingly, the exclusion of the gavialine taxa, *Dolichochampsa minima* and *Dagavialis gunai*, resulted in having Gryposuchinae highly resolved in the strict consensus. Crocodylidae appears as the immediate sister clade to Gavialoidea (Gavialinae + 'tomistomines'), and Alligatoridae is retrieved as the sister lineage to crocodylids and gavialoids. *Pelagosuchus pakistanensis* was recovered in the basalmost position within Gavialinae, with comparatively high nodal support values (Fig. 6).

Characters supporting the inclusion of *Pelagosuchus pakistanensis* within Gavialoidea are broadly cranial and mandibular features including: dorsal surface of rostrum mostly straight and curve dorsally before reaching the orbits (ch. 95[3]); a palatine process that sends two processes that converge anteriorly, forming a V-shaped suture with the maxilla, and a process extends beyond third maxillary alveolus that is anterior to suborbital fenestra (ch. 116[3]); mature skull table with nearly straight sides, posterolateral squamosal processes form long prongs (ch. 158[2]); a longirostrine rostrum with length greater than 70% of the total skull length (ch. 234[3]); projection of ventral margin of maxilla in dorsal view that has a convergent profile anteroposteriorly, at mid rostrum becoming subparallel (ch. 237[5]); a square-shaped to subrectangular supratemporal fossa (ch. 245[1]); a symphysis that flares anteriorly, with anterior region bearing teeth 1-2 at anterior margin and posterior region narrower (ch. 257[3]); and dentary teeth 3-4 set in tandem (ch. 258[2]). Characters that support the inclusion of *P. pakistanensis* within Gavialinae in our analysis include: a surangular-dentary suture that intersects the external mandibular fenestra at the posterodorsal corner (ch. 64[1]); quadrate with a detached, ventrally projected medial hemicondyle (ch. 181[4]); edge of maxillary tooth alveoli higher than the space between toothrow (ch. 182[1]); orbits wider than long (ch. 200[1]); frontal plate surface only little sculpted to smooth (ch. 202[1]); a supratemporal fossa larger than orbits (ch. 242[2]); and orbits with a strong dorsal component (ch. 250[2]).

After evaluating the character distribution and performance (Consistency Index) in the strict consensus, we found that *Pelagosuchus pakistanensis* shares three characters (181, 202, and 242) with some gryposuchine taxa. *Pelagosuchus* shares character 181 with *Siquisiquesuchus*, *Piscogavialis*, *Gryposuchus pachakamue*, and *G. croizati*; and characters 202 and 242 are shared with all species of the genus *Gryposuchus* (Fig. 6). Characters 181 (CI: 0.57)

and 202 (CI: 0.50) have high consistency indices, except for character 242 (CI: 0.40). The presence of these characters that were thought to be synapomorphies of Gryposuchinae now can be traced back to the Eocene (43–41 Ma) of the eastern Tethys Sea. The high consistency indices of these characters, along with similarities of the dentary process (see Comparisons), signal strong homology between gryposuchines and *Pelagosuchus*, suggesting a possible common ancestry of the American assemblage from Africa or Asia as has been previously suggested (Brochu & Rincón, 2004; Buffetaut, 1982; Langston, 1965; Langston & Gasparini, 1997; Vélez-Juarbe et al., 2007).

Paleoenvironmental Implications

Uncertainty remains over whether the last common ancestor of the extant gharial, *Gavialis gangeticus*, was a coastal to marine animal. Extinct forms from the Americas (*Siquisiquesuchus*, *Piscogavialis*) and the Caribbean (*Aktiogavialis*) have been found in coastal settings, possibly reflecting the actual environment in which they inhabited (Brochu & Rincón, 2004; Kraus, 1998; Vélez-Juarbe et al., 2007). Other forms from South America (*Gryposuchus*) occurred in fluvial settings, and the provenance of other forms (*Ikanogavialis*, *Eogavialis*) remains uncertain (Bown & Kraus, 1988; Gingerich, 1992; Gagnon, 1997; Linares, 2004; Salas-Gismondi et al., 2015; Sánchez-Villagra & Aguilera, 2006; Sill, 1970). Because there are several occurrences of Cenozoic taxa in Africa, Asia, and the Americas, an early marine phase has been hypothesized for the group, with restriction to freshwater as a comparatively recent event, as has been previously suggested (Vélez-Juarbe et al., 2007).

Pelagosuchus pakistanensis is the first known extinct gavialine derived from offshore, deep marine waters of the Tethys Sea (Gingerich et al., 1994; 1995; 2001). The holotype of *Pelagosuchus* was collected from the Upper Domanda Formation, which was deposited during the Eocene (43–41 Ma) in a passive continental marine margin (Clyde & Gingerich, 2003; Gingerich et al., 1995; 2001). Although it cannot be ruled out that the occurrence of *Pelagosuchus* may represent a washout from inland sources, such events are extremely rare in the fossil record. Taken together, the provenance of an early gavialine from marine deposits and the spatiotemporal distribution of other forms in Africa (*Argochampsa*, *Eogavialis*) and the Americas (Gryposuchinae) provide more evidence that early gavialines were capable of inhabiting oceanic waters.

Paleobiogeography of Gavialines

Today, Gavialinae is comprised of sixteen (fifteen extinct and one extant) species distributed within ten genera, all of which are found in Africa, Asia, and South America (Hua & Jouve, 2004; Jouve et al., 2006; Salas-Gismondi et al., 2016; 2019; 2022; Vélez-Juarbe et al., 2007). Half of the known taxa are predominantly Miocene–Pliocene forms from South America, namely the gryposuchines (Salas-Gismondi et al., 2016; 2019; 2022; Moraes-Santos et al., 2011; Vélez-Juarbe et al., 2007). Close affinities among these South American forms that distinguished them from other gavialines were first documented by Brochu & Rincón (2004), Kraus (1998), Langston (1965), and Langston & Gasparini (1997), and later formally recognized as a subgroup by Vélez-Juarbe et al. (2007) as the immediate sister clade to crown-group gharials. At that time, Gryposuchinae included one genus (*Aktiogavialis*) from the Oligocene of the Caribbean and four

genera (*Gryposuchus*, *Ikanogavialis*, *Piscogavialis*, *Siquisiquesuchus*) from the Miocene–Pliocene of South America (Brochu & Rincón, 2004; Hua & Jouve, 2004; Jouve et al., 2006; Vélez-Juarbe et al., 2007). Later, *Aktiogavialis* was placed outside Gryposuchinae as the sister taxon to the African species, *Argochampsa*, and interpreted to represent independent radiation (Salas-Gismondi et al., 2019; 2022), although some recent cladistic analyses have recovered *Aktiogavialis* + *Argochampsa* forming a polytomy within Gavialinae (unpubl. data). The distribution of Gryposuchinae and their evolutionary relationships to other African forms have suggested that the group bears an African, or less likely, Asian origin and later differentiated in the Miocene–Pliocene of South America (Brochu & Rincón, 2004; Hua & Jouve, 2004; Jouve et al., 2006; Salas-Gismondi et al., 2016; 2019; 2022; Vélez-Juarbe et al., 2007).

Although the spatiotemporal distribution of Gryposuchinae has become better established over the last three decades, the paleobiogeographical history of extinct gharials in Indo-Pakistan is comparatively poorly understood. All known fossil gharials from Indo-Pakistan are derived from Miocene strata, all of which are referred to *Gavialis* and *Rhamphosuchus* (Cautley, 1836; 1840; Cautley and Falconer, 1840; Martin, 2019). Based on the distribution of the extant and extinct gavialine populations and the tectonic setting of the Indo-Pakistan, gavialines most likely arrived in that landmass somewhere in the Paleogene before the final closure of the Tethys Sea and the collision of the Indian plate with Eurasia (Blakey, 2008; Clyde & Gingerich, 2003; Torfstein & Steinberg, 2020). *Pelagosuchus pakistanensis* provides evidence that gavialines arrived in the Eocene (c.a., 43–41 Ma) of Indo-Pakistan, and its discovery links important evolutionary and paleobiogeographic histories for Gavialinae.

The arrival of gavialines in the Eocene in the eastern parts of the Tethys Sea coincided with the Indian-Eurasian collision (Blakey, 2008; Torfstein & Steinberg, 2020). At the same

time, or later in the Oligocene, gavialines may have dispersed from Tethys to the Americas across the Atlantic Ocean, as evidenced by *Eogavialis*, an Eocene (39–33 Ma) taxon from Egypt (Salas-Gismondi et al., 2016; 2019; 2022; Vélez-Juarbe et al., 2007). Reconstruction of plate tectonics shows a tropical marine connection from India and Africa to the Americas and the Caribbean during the Paleogene, which could have served as a marine corridor for the dispersal of gavialines (Blakey, 2008). Strong affinities of the newly described taxon to gryposuchines and the occurrences of other early forms from Africa (*Argochampsa*, *Eogavialis*) suggest that Gryposuchinae bears a Tethyan signature, which is consistent with proposed paleobiogeographical hypotheses (Brochu & Rincón, 2004; Hua & Jouve, 2004; Jouve et al., 2006; Salas-Gismondi et al., 2016; 2019; 2022; Vélez-Juarbe et al., 2007). Subsequently, the closure of the Tethys Sea in the Oligocene–Miocene may have caused the separation of gavialine populations in the World. In Indo-Pakistan, the closure of the Tethys Sea in Eurasia and uplift of the Himalayas may have caused the isolation of gavialine populations from coastal marine to fluvial settings, leading to the differentiation of the two known genera (*Gavialis*, *Rhamphosuchus*) found in Miocene–Pliocene localities in the Siwaliks and Sindh (Martin; 2019; Martin et al., 2012; Cautley, 1836; 1840; Cautley and Falconer, 1840), whereas in the Americas, the group differentiated into six genera (*Aktiogavialis*, *Dadagavialis*, *Ikanogavialis*, *Gryposuchus*, *Piscogavialis*, *Siquisiquesuchus*) at similar times (Brochu & Rincón, 2004; Langston & Gasparini, 1997; Salas-Gismondi et al., 2016; 2019; 2022; Vélez-Juarbe et al., 2007). Fossil localities from the Paleogene, especially from Asia, will be crucial to better understanding of the complex history of Gavialinae and the role of geological processes in the evolution of the group.

Conclusions

New material of a large longirostrine crocodylian from the Eocene (43–41 Ma) Upper Domanda Formation in Pakistan brings evidence of the presence of gavialines in Asia before the final closure of the Tethys Sea during the collision of the Indian plate with Eurasia. Occurrence of the new taxon in offshore, deep marine sediments of the Tethys Sea provides more evidence of saltwater tolerance for early gavialines. Phylogenetic analysis resolves the new taxon as the basalmost member within Gavialinae with strong support values. Based on the distinct combination of morphological features exclusive to the holotype, we have established a new genus and species, *Pelagosuchus pakistanensis*. The new species bears strong affinities to the Miocene–Pliocene assemblage from South America (Gryposuchinae), which provides more evidence of a possible center of origin in Tethys for gryposuchines as previously suggested.

The occurrence of gavialines in the Eocene in Indo-Pakistan provides evidence that the group possibly arrived in that region before the closure of the Tethys Sea and during the collision of the Indian plate with Eurasia. After the closure of the Tethys Sea in the Oligocene–Miocene, gavialines possibly became geographically isolated in the World. In Indo-Pakistan, gavialines became restricted to fluvial habitats leading to the current distribution of the extant *Gavialis*, whereas in the Americas, gryposuchines rapidly diversified in the Miocene and declined in diversity in the Pliocene where they became extinct in the Pliocene.

Acknowledgments

We express gratitude to the Geological Survey of Pakistan for their collaboration in the field and for loaning the holotype specimen (GSP-UM 3332) to the University of Michigan Museum of Paleontology. We thank C. Sheehy III, the herpetology collection manager at the University of Florida, for providing access to specimens used in our analysis. We also thank Adam Rountrey, the vertebrate collection manager at UMMP, for access to specimens. Preparation of the holotype was carried out by William Sanders, the Chief Vertebrate Preparator at the UMMP. Special thanks go to Tariq Abdul Kareem and Kierstin Rosenbach for their valuable comments during the early stages of manuscript development. Funding support for this project was provided by the Department of Earth and Environmental Sciences Turner Diversity Grant 2021 at the University of Michigan. Additionally, we extend our appreciation to the reviewers for their constructive criticism that improved this manuscript.

References

Andrews, C. W. (1906). *A descriptive catalogue of the tertiary vertebrata of the Fayûm, Egypt*. British Museum (Natual History).

Benton, M. J., & Clark, J. M. (1988). Archosaur phylogeny and the relationships of the Crocodylia. In M. J. Benton (Eds.), The phylogeny and classification of the tetrapods. (pp. 295–338). *Clarendon Press*.

Berra, F., & Angiolini, L. (2014). The evolution of the Tethys region throughout the Phanerozoic: A brief tectonic reconstruction. In L. Marlow, C. Kendall, & L. Yose (Eds.), *Petroleum systems of the Tethyan region*. (pp. 1–27). *AAPG Memoir*.

Blakey, R. C. (2008). Gondwana paleogeography from assembly to breakup—A 500 m.y. odyssey. In C. R. Fielding, T. D. Frank, & J. L. Isbell (Eds.), *Resolving the Late Paleozoic Ice Age in time and space*. (pp. 1–28). *Geological Society of America Special Paper*.

Bown, T. M., & Kraus, M. J. (1988). Geology and paleoenvironment of the Oligocene Jebel Qatrani Formation and adjacent rocks, Fayum Depression, Egypt. *United States Geological Survey Professional Paper, 1452*, 1–60.

Brochu, C. A. (1997). Morphology, fossils, divergence timing, and the phylogenetic relationships of *Gavialis*. *Systematic Biology, 46*(3), 479–522.

Brochu, C. A. (1999). Phylogenetics, taxonomy, and historical biogeography of Alligatoroidea. *Journal of Vertebrate Paleontology, 19*(2), 9–100.

Brochu, C. A. (2003). Phylogenetic approaches toward crocodylian history. *Annual Review of Earth and Planetary Sciences, 31*, 357–397. https://doi.org/10.1146/annurev.earth.31.100901.141308

Brochu, C. A. (2004). A new Late Cretaceous gavialoid crocodylian from eastern North America and the phylogenetic relationships of thoracosaurs. *Journal of Vertebrate Paleontology, 24*(3), 610–633.

Brochu, C. A., & Rincón, A. D. (2004). A gavialoid crocodylian from the lower Miocene of Venezuela. *The Palaeontological Association, 71*, 61–79.

Brochu, C. A. (2006). Osteology and phylogenetic significance of *Eosuchus minor* (Marsh, 1870) new combination, a longirostrine crocodylian from the Late Paleocene of North America, Journal of Paleontology, 80(1), 162–186.

Brochu, C. A. (2007). Systematics and taxonomy of Eocene tomistomine crocodylians from Britain and northern Europe. *Palaeontology, 50*, 917–928.

Brochu, C. A. (2011). Phylogenetic relationships of *Necrosuchus ionensis* Simpson, 1937 and the early history of caimanines. *Zoological Journal of the Linnean Society, 163*, S228–S256.

Buffetaut, E. (1982). Systématiquec, origine et evolution des Gavialidae Sud-Américaines. *Geobios, 6*, 127–140.

Buscalioni, A. D., & Sanz, J. L. (1992). The small crocodile Bernissartia fagesii from the Lower Cretaceous of Galve (Teruel, Spain). *Bulletin de I'Institut royal des sciences naturelles de Belgique, 60*, 129–150.

Carpenter, K. (1983). *Thoracosaurus neocesariensis* (De Kay, 1842) (Crocodylia: Crocodylidae) from the Late Cretaceous Ripley Formation of Mississippi. *Mississippi geology, 4*(1), 1–10.

Cautley, P. T. (1936). Note on the fossil crocodile, of the Sivalik Hills. *Assiatic Researches, 19*, 25–38.

Cautley, P. T. (1936). On the structure of the Seválik Hills, and the organic remains found in them. *Transactions of the Geological Society of London, 5*, 267–278.

Cautley, P. T., & Falconer, H. (1840). Notice on the remains of a fossil monkey from the Tertiary strata of the Sewalik Hills in the north of Hindoostan. *Transactions of the Geological Society of London, 2*, 499–504.

Clark, J. M. (1994). Patterns of evolution in Mesozoic Crocodyliformes. In N. C. Fraser, & H.-D. Sues (Eds.). *The shadow of the dinosaurs*. (pp. 84–97). *Cambridge University Press*.

Clyde, W. C., Khan, I. H., & Gingerich, P. D. (2003). Stratigraphic response and mammalian dispersal during initial India-Asia collision: Evidence from the Ghazij Formation, Balochistan, Pakistan. *Geological Society of America, 31*(12), 1097–1100.

Delfino, M., Piras, P., & Smith, T. (2005). Anatomy and phylogeny of the gavialoid crocodylian *Eosuchus lerichei* from the Paleocene of Europe. *Acta Palaeontologica Polonica, 50*(3), 565–580.

Delfino, M., & de Vos, J. (2010). A revision of the Dubois crocodylians, *Gavialis bengawanicus* and *Crocodylus ossifragus*, from the Pleistocene *Homo erectus* beds of Java. *Journal of Vertebrate Paleontology, 30*(2), 427–441.

Drumheller, S. K., & Brochu, C. A. (2016). Phylogenetic taphonomy: A statistical and phylogenetic approach for exploring taphonomic patterns in the fossil record using crocodylians. *PALAIOS, 31*, 463–478.

Gagnon, M. (1997). Ecological diversity and community ecology in the Fayum sequence (Egypt). *Journal of Human Evolution, 32*, 133–160.

Gasparini, Z. B., & Buffetaut, E. (1980). *Dolichochampsa minima*, n. g. n. sp., a representative of a new family of eusuchian crocodiles from the Late Cretaceous of northern Argentina. *Neues Jahrbuch für Geologie und Paläontologie - Monatshefte, 1980*, 257–271.

Gingerich, P. D. (1992). Marine mammals (Cetacea and Sirenia) from the Eocene of Gebel Mokattam and Fayum, Egypt: stratigraphy, age, and paleoenvironments. *University of Michigan Papers in Paleontology, 30*, 1–84.

Gingerich, P. D., Raza, S. ., Arif, M., Anwar, M., & Zhou, X. (1994). New whale from the Eocene of Pakistan and the origin of cetacean swimming. *Nature, 368*, 884–847.

Gingerich, P. D., Arif, M., & Clyde, W. C. (1995). New archaeocetes (Mammalia, Cetacea) from the middle Eocene Domanda Formation of the Sulaiman Range, Punjab (Pakistan). *Contributions from the Musuem of Paleontology The University of Michigan, 29*(11), 291–330.

Gingerich, P. D., Ul-Haq, M., Khan, I. H., & Zalmout, I. (2001). Eocene stratigraphy and archaeocete whales (Mammalia, Cetacea) of Drug Lahar in the eastern Sulaiman Range, Balochistan (Pakistan). *Contributions from the Musuem of Paleontology The University of Michigan, 30*(11), 269–319.

Goloboff, P. A., & Catalano, S. A. (2023). TNT version 1.6, with a graphical interface for MacOS and Linux, including new routines in parallel. *Cladistics, 39*, 144–153.

Gürich, G. J. E. (1912). *Gryposuchus jessei*: ein neues schmalschnauziges Krokodil aus jüngeren ablagerungen des oberen Amazonas-Gebietes. *Jahrbuch der Hamburgischen Wissenschaftlichen Anstalten,* XXIX, 59–71.

Hua, S., & Jouve, S. (2004). A primitive marine gavialoid from the Paleocene of Morocco. *Journal of Vertebrate Paleontology, 24*(2), 341–350.

Iordansly, N. N. (1973). The skull of Crocodilia. In C. Gans, & T. Parsons (Eds.), *Biology of the reptilia*. (pp. 201–262), *London Academic Press*.

Iordansky, N. N. (1999). Jaw muscles of the crocodiles: structure, synonymy, and some implications on homology and functions. *Russian Journal of Herpetology, 7*(1), 41–50.

Jouve, S., Iarochene, M., Bouya, B., & Amaghzaz, M. (2005c). New material of *Argochampsa krebsi* (Crocodylia: Gavialoidea) from the Lower Paleocene of the Oulad Abdoun Basin (Morocco): phylogenetic implications. *Geobios, 39*, 817–832.

Jouve, S., Bardet, N., Jalil, N.-E., Suberbiola, X. P., Bouya, B. & Amaghzaz, M. (2008). The oldest African crocodylian: phylogeny, paleobiogeography, and differential survivorship of marine reptiles through the Cretaceous-Tertiary boundary. *Journal of Vertebrate Paleontology, 28*(2), 409–421.

Kraus, R. (1998). The cranium of Piscogavialis jugaliperforatus n. gen., n. sp. (Gavialidae, Crocodylia) from the Miocene of Peru. *Paläontologische Zeitschrift, 72*, 389–406.

Lambe, L. M. (1907). On a new crocodilian genus and species from the Judith River Formation of Alberta. *Transactions of the Royal Society of Canada, 4*, 219–244.

Langston, W. Jr. (1965). Fossil crocodilians from Colombia and the Cenozoic history of the Crocodilia in South America. *University of California Publications in Geological Sciences, 52*, 1–157.

Langston, W. Jr., & Gasparini, Z. (1997). Crocodilians, Gryposuchus, and the South American gavials. In R. F. Kay, R. H. Madden, R. C. Cifell, & J. Flynn (Eds.), *Vertebrate paleontology in the Neotropics: The Miocene fauna of La Venta, Colombia*. (pp. 113–154). *Smithsonian Institution Press, Washington*.

Linares, O. J. (2004). Bioestratigrafia de la fauna de mamiferos de las Formaciones Socorro, Urumaco y Codore (Mioceno Medio–Plioceno Temprano) de la region de Urumaco, Falcon, Venezuela. *Paleobiologia Neotropical, 1*, 1–26.

Lee, M. S. Y., & Yates, A. M. (2018). Tip-dating and homoplasy: reconciling the shallow molecular divergences of modern gharials with their long fossil record. *Proceedings of the Royal Society B: Biological Sciences, 285*, 20181071.

Mansharamani, D. K. (1965). Foramina-fossa and vacuities in the skull of *Crocodilus porosus* Schneider. *Proceedings Indian Academy of Sciences, 62*, 280–290.

Martin, J. E., Buffetaut, E., Naksri, W., Lauprasert, K., & Claude, J. (2012). *Gavialis* from the Pleistocene of Thailand and its relevance for drainage connections from India to Java. *PlosOne, 7*(9), 1–14.

Martin, J. E. (2019). The taxonomic content of the genus *Gavialis* from the Siwalik Hills of India and Pakistan. *Special Papers in Palaeontology, 5*, 483-497.

Martin, J. E., Antoine, P.-O., Perrier, V., Welcomme, J.-L., Metais, G., & Marivaux, L. (2019). A large crocodyloid from the Oligocene of the Bugti Hills, Pakistan. *Journal of Vertebrate Paleontology, 39*(4), 1–8.

Moraes-Santos, H., Bocquentin Villanueva, J., & Mann Toledo, P. (2012). New remains of a gavialoid crocodilian from the late Oligocene–early Miocene of the Pirabas Formation, Brazil. *Zoological Journal of the Linnean Society, 163*, S132–S139.

Norell, M. A. (1988). *Cladistic approaches to paleobiology as applied to the phylogeny of alligatorids* [Unpublished doctoral dissertation]. Yale University, New Haven.

Norell, M. A. (1989). The higher level relationship of extant Crocodylia. *Journal of Herpetology, 23*, 325–335.

Norell, M. A., & Clark, J. M. (1990). A reanalysis of Bernissartia fagesii, with comments on its phylogenetic position and its bearing on the origin and diagnosis of the Eusuchia. *Bulletin de I'Institut royal des sciences naturelles de Belgique, 60*, 115–128.

Nixon, K. C. (2002). Winclada (ver. 1.0000).

Nopcsa, F. (1923). Die Familien der Reptilien. *Fortschritte der Geologie und Palaentologie, 2*, 1–210.

Pilgrim, G. E. (1908). The Tertiary and post-Tertiary freshwater deposits of Baluchistan and Sind with notices of new vertebrates. *Records of the Geological Survey of India, 37*, 139–166.

Pilgrim, G. E. (1912). The vertebrate fauna of the Gaj series in the Bugti Hills and the Punjab. *Memoirs of the Geological Survey of India. Palaeontologica Indica New Series, 4*, 1–83.

Poe, S. (1996). Data set incongruence and the phylogeny of crocodilians. *Systematic Biology, 45*, 393–414.

Rehman, S. U., Riaz, . A., Ahmed, M., Ulhah, . F., Kashif, M., & Rehman, F. (2017). Sedimentology of Pir Koh Formation exposed at Dholi and Rakhi Gaj, Central Sulaiman Range, Pakistan. *Journal of Biodiversity and Environmental Sciences, 11*(6), 224–234.

Rio, J. P., & Mannion, P. D. (2021). Phylogenetic analysis of a new morphological dataset elucidates the evolutionary history of Crocodylia and resolves the long-standing gharial problem. *PeerJ, 9*, e12094.

Romer, A. S. (1956). *Osteology of the Reptiles*. University of Chicago Press.

Salas-Gismondi, R., Flynn, J. J., Baby, P., Tejada-Lara, J. V., Wesselingh, F. P., & Antoine, P.-O. (2015). A Miocene hyperdiverse crocodylian community reveals peculiar trophic dynamics in proto-Amazonian mega-wetlands. *Proceedings of Royal Society B, 282*, 1–10.

Salas-Gismondi, R., Flynn, J. J., Baby, P., Tejada-Lara, J. V., Claude, J., & Pierre-Olivier, A. (2016). A new 13 million year old gavialoid crocodylian from proto-Amazonian mega-wetlands reveals parallel evolutionary trends in skull shape linked to longirostry. *PLoS ONE, 11*(4), e0152453.

Salas-Gismondi, R., Moreno-Bernal, J., Scheyerc, T. M., Sánchez-Villagra, M. R., & Jaramillo, C. (2019). New Miocene Caribbean gavialoids and patterns of longirostry in crocodylians. *Journal of Systematic Palaeontology, 17*(12), 1049–1075.

Salas-Gismondi, R., Ochoa, D., Jouve, S., Romero, P. E., Cardich, J., Perez, A., DeVries, T., Baby, P., Urbina, M., & Carré, M. (2022). Miocene fossils from the southeastern Pacific shed light on the last radiation of marine crocodylians. *Proceedings of the Royal Society B: Biological Sciences, 289*, 20220380.

Sánches-Villagra, M. R., & Aguilera, O. A. (2006). Neogene vertebrates from Urumaco, Falcon State, Venezuela: diversity and significance. *Journal of Systematic Palaeontology, 4*, 213–220.

Shute, C. C. D., & Bellairs, A. D'A. (2010). The external ear in Crocodilia. *Proceedings of the Zoological Society of London*, 741–749.

Sill, W. D. (1970). Nota preliminar sobre un nuevo gavial del Plioceno de Venezuela y una discusion de los gaviales sudamericanos. *Ameghiniana, 7*, 151–159.

Smith-Paredes, D., & Bhullar, B.-A. S. (2019). The skull and head muscles of Archosauria. In J. M. Ziermann, R. E. Diaz Jr., & Diogo, R (Eds.)., Heads, jaws, and muscles: Anatomical, functional, and developmental diversity in chordate evolution (pp. 1–303). Springer.

Stevenson, C. J. (2015). Conservation of the Indian gharial *Gavialis gangeticus*: successes and failures. *International Zoo Yearbook, 49*, 150–161.

Torfstein, A., & Steinberg, J. (2020). The Oligo–Miocene closure of the Tethys Ocean and evolution of the proto-Mediterranean Sea. *Science Reports, 10*, 1–10.

Van Hinsbergen, D. J. J., Lippert, P. C., Li, S., Huang, W., Advokaat, E. L., & Spakman, W. (2019). Reconstructing Greater India: Paleogeographic, kinematic, and geodynamic perspectives. *Tectonophysics, 760*, 69–94.

Vélez-Juarbe, J., Brochu, C. A., & Santos, H. (2007). A gharial from the Oligocene of Puerto Rico: transoceanic dispersal in the history of a non-marine reptile. *Proceedings of the Royal Society B: Biological Sciences*, 274, 1245–1254. https://doi.org/10.1098/rspb.2006.0455

Vélez-Rosado, K. I., Wilson Mantilla, J. A., & Giingerich, P. D. (2024b). *A new basal gavialines (Crocodylia: Gavialinae) from the Eocene of Pakistan and its paleobiogeographical implications* [Manuscript in preparation]. Earth and Environmental Sciences, University of Michigan.

Wuc, X.-C., Russell, A. P., & Brinkman, D. B. (2001). A review of *Leidyosuchus Canadensis* Lambe, 1907 (Archosauria: Crocodylia) and an assessment of cranial variation based upon new material. *The Canadian Journal of Earth Science, 38*, 1665–1687.

Figures

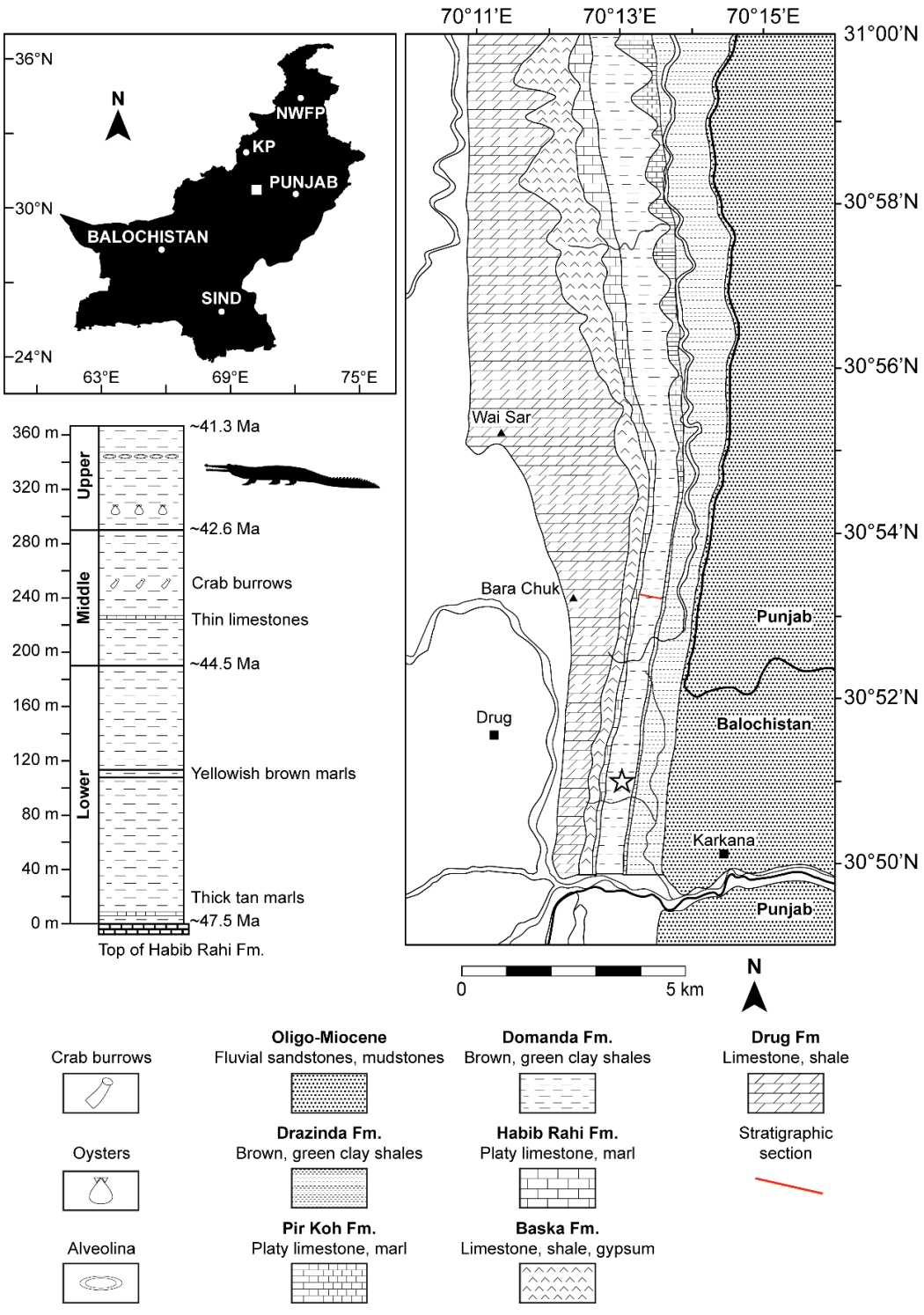

Figure 3.1. Geological map and stratigraphic section of Punjab and Balochistan showing the locality of the new crocodylian specimen (GSP-UM 3332), after Gingerich et al. (2001). The star represents where the holotype was collected.

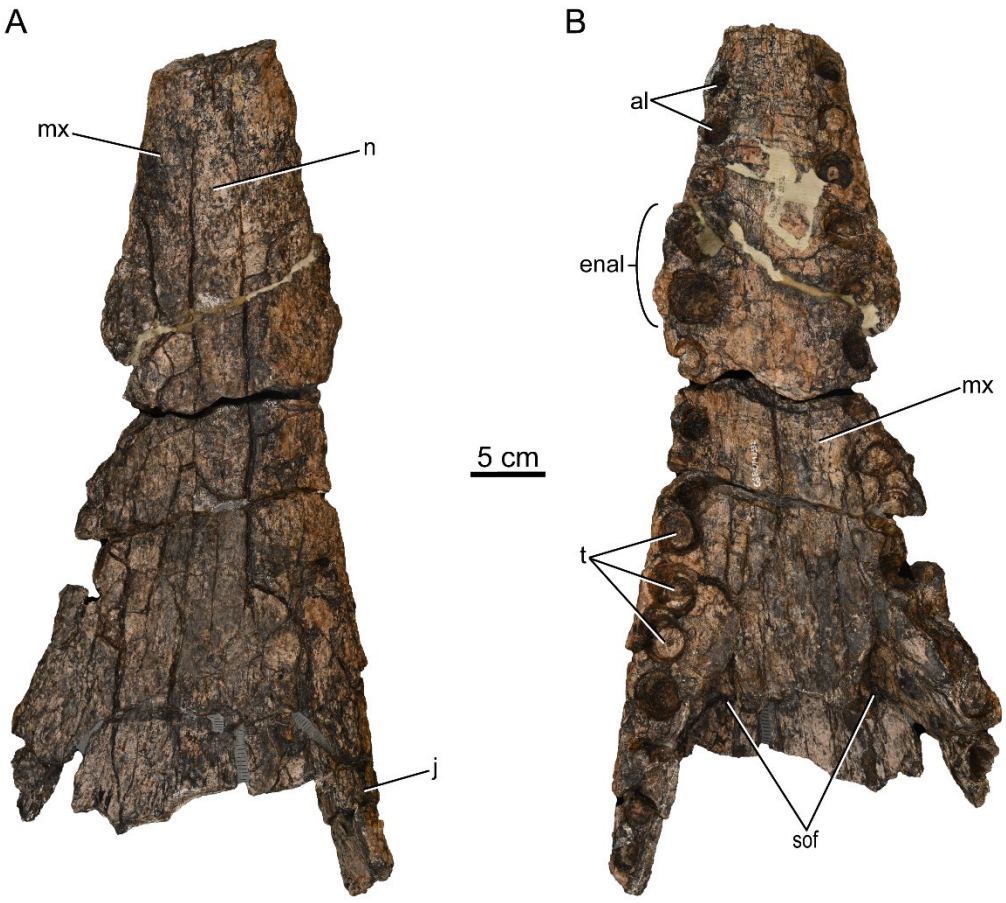

Figure 3.2. Rostrum of the holotype of *Pelagosuchus pakistanensis* in dorsal (**A**), and ventral (**B**) views. **Abbreviations: al**, alveoli; **enal**, enlarged alveoli; **j**, jugal; **mx**, maxilla; **n**, nasal; sof, suborbital fenestra; **t**, teeth.

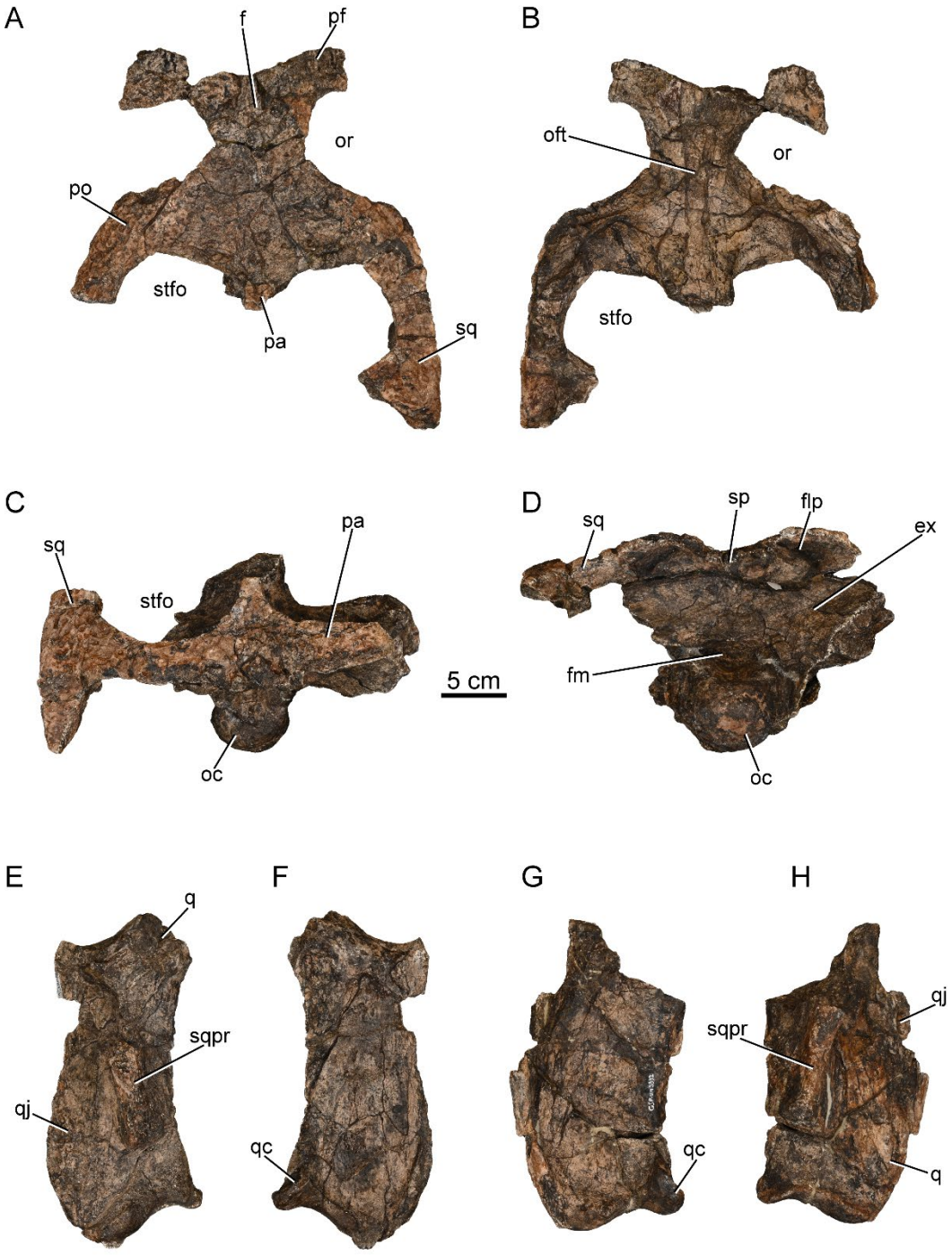

Figure 3.3. Elements of the skull table and braincase of *Pelagosuchus pakistanensis*. Dorsal (**A**) and ventral (**B**) views of the anterior portion of the skull table. Posterior portions of the skull table in dorsal (**C**) and posterior (**D**) views. Left and right quadrates in dorsal (**E**, **H**) and ventral (**F**, **G**) views. **Abbreviations: ex**, exoccipital; **f**, frontal; **flp**, foramen lacrum posterior; **fm**, foramen magnum; **oc**, occipital condyle; **oft**, olfactory tract; **or**, orbit; **pa**, parietal; **pf**, prefrontal; **po**, postorbital; **q**, quadrate; **qc**, quadrate condyle; **qj**, quadratojugal; **sp**, supraoccipital; **sq**; squamosal; **sqpr**, squamosal prong; **stfo**, supratemporal fossa.

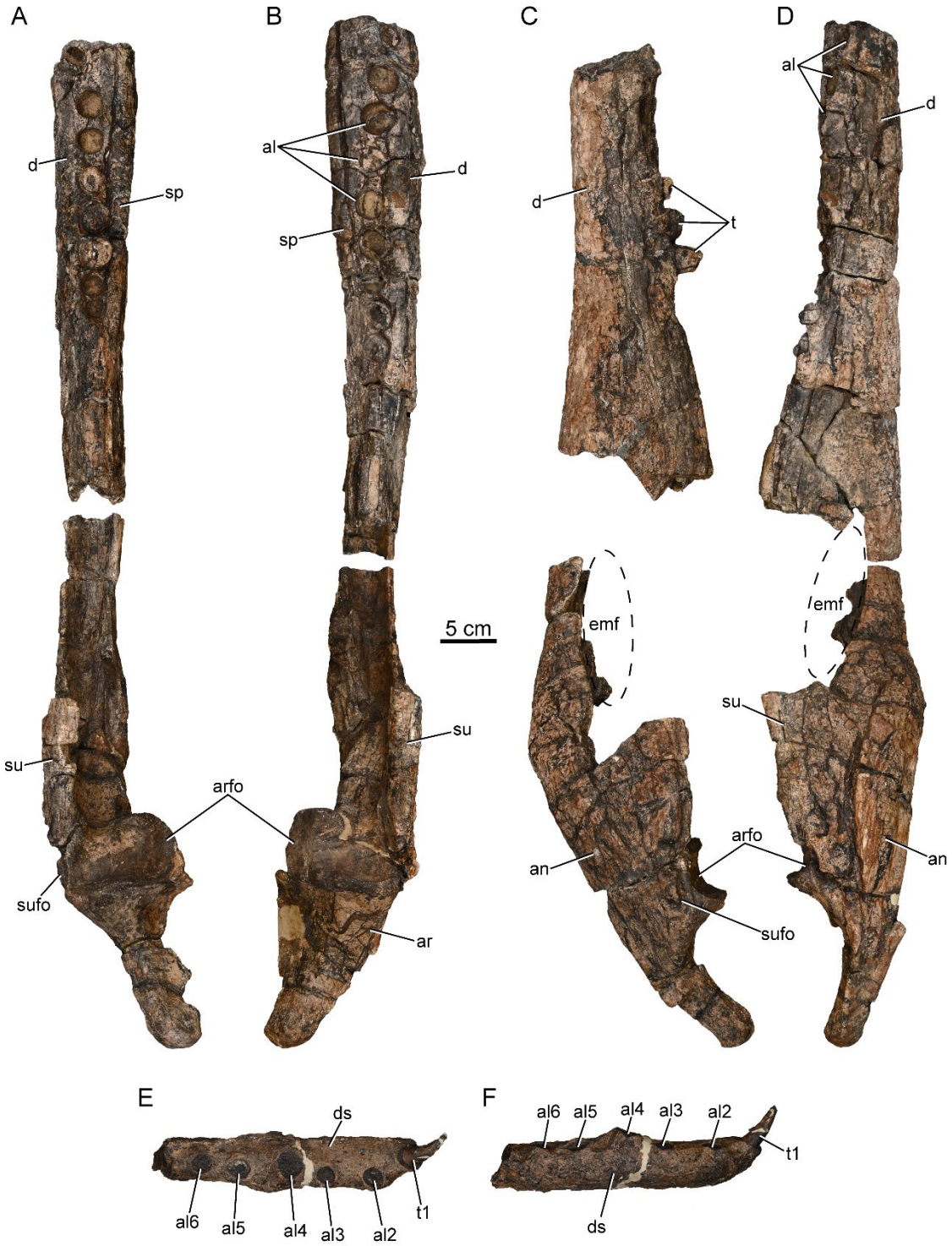

Figure 3.4. Mandibular rami of *Pelagosuchus pakistanensis* in dorsal (**A**, **B**) and lateral (**C**, **D**) views. Anterior portion of right dentary symphysis in dorsal (**E**) and lateral (**F**) views. **Abbreviations: al**, alveoli; **afro**, articular fossa; **an**, angular; **ar**, articular; **d**, dentary; **ds**, dentary symphysis; **emf**, external mandibular fenestra; **sp**, splenial; **su**, surangular; **sufo**, surangular fossa; **t**, teeth.

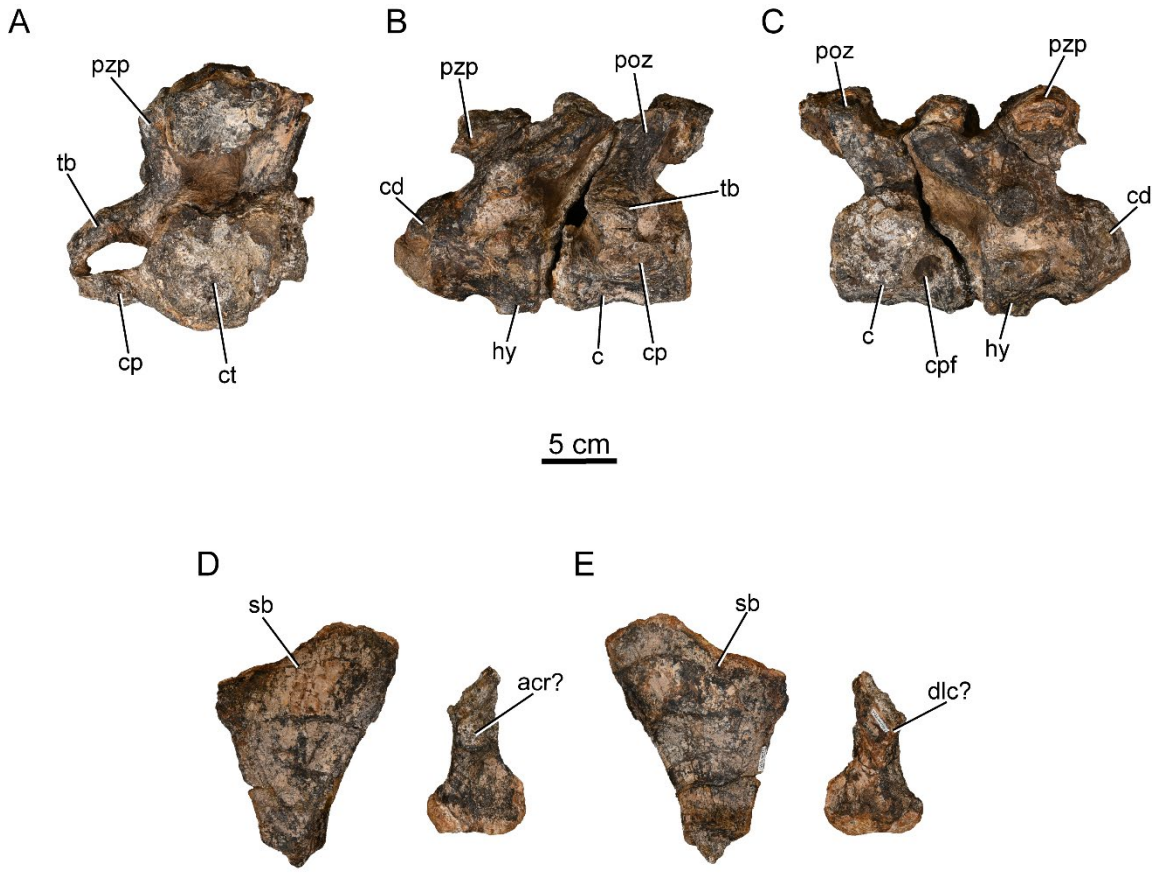

Figure 3.5. Associated postcrania of *Pelagosuchus pakistanensis*. Anterior (**A**), right lateral (**B**), and left lateral (**C**) views of dorsal vertebrae, and right scapula in lateral (**D**) and medial (**E**) views. **Abbreviations: acr?**, acromion process; **c**, centrum; **cd**, condyle; **cp**, capitulum; **cpf**, fossa of capitulum; **ct**, cotyle; **dlc?**, deltoid crest; **hy**, hypapophysis; poz, postzygapophysis; **pzp**, prezygapophysis; **sb**, scapular blade; **tb**, tuberculum.

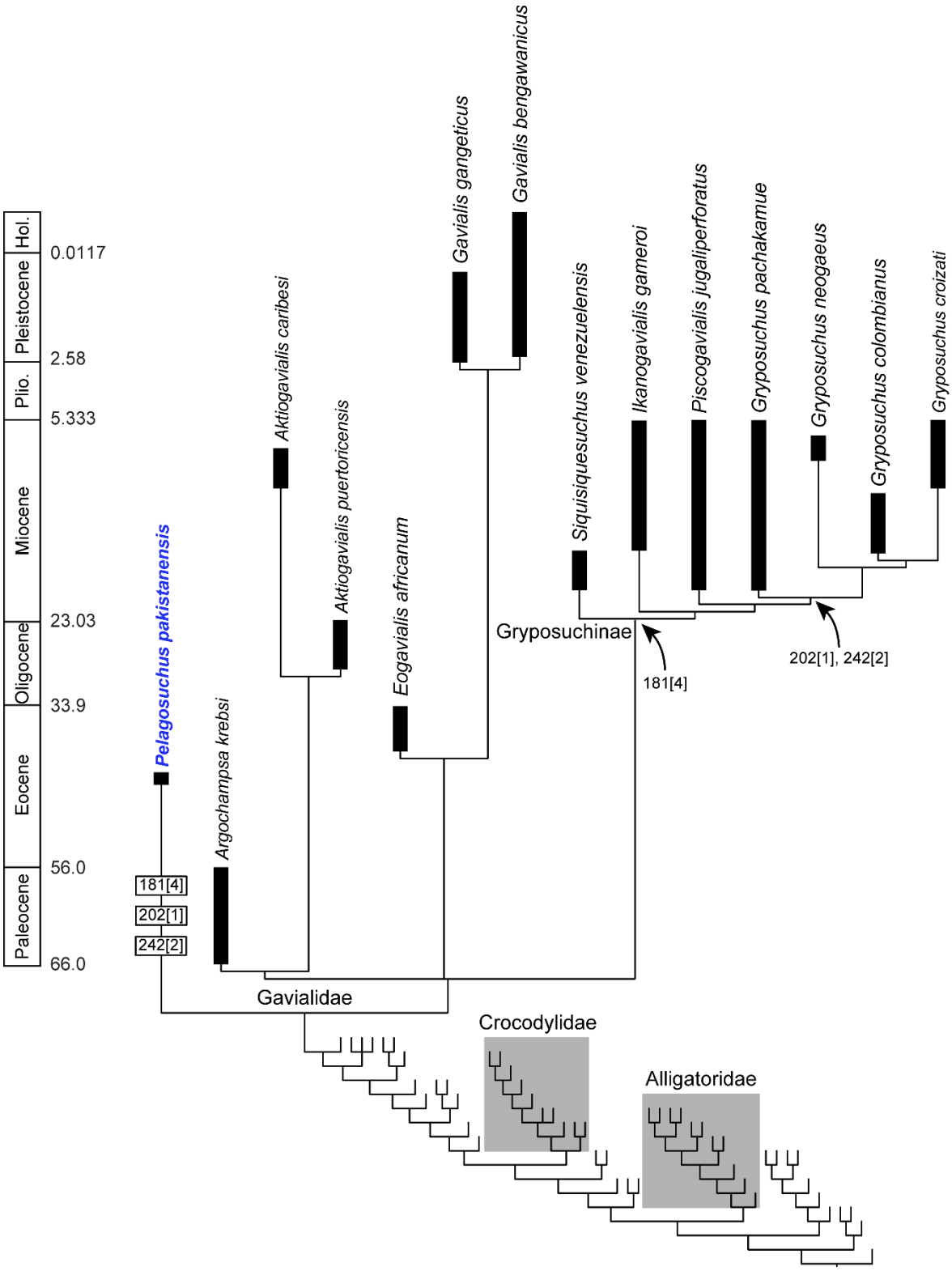

Figure 3.6. Time-calibrated strict consensus tree of 984 most parsimonious trees showing the position of *Pelagosuchus pakistanensis* within Gavialinae. Character states at nodes within Gryposuchinae are those shared with *Pelagosuchus*.

CHAPTER 4

A Biogeographic Model Provides Support for the Origin of Neotropical Gharials in South America

Abstract

Aim: The purpose of this study is to examine the origin and dispersal of gavialine crocodylians throughout space and time. We tested biogeographic hypotheses for the origins of fossil gharials in the New World and Old World, which included multiple trans-oceanic dispersals during the Cretaceous–Oligocene.

Location: Worldwide

Taxon: Crocodylia (Gavialidae)

Methods: We used an osteological character-taxon matrix of Crocodylia that includes the majority of extinct and extant crocodylians. We evaluate their evolutionary relationships under a tip-dated Bayesian framework and divergence events. We tested two biogeographical hypotheses using the R software BioGeoBEARS to reconstruct the ancestral ranges within Gavialinae to seek the most likely biogeographical scenario. Akaike Information Criterion was used to find the best-fitting biogeographic model given our dataset.

Results: Phylogenetic results show that the earliest gavialines resided in South America around the Cretaceous–Paleocene. Our analysis resolves three subgroups within Gavialidae: Gryposuchinae, *Gavialis*+*Eogavialis*, and *Aktiogavialis*. Divergence time estimates indicate that these three subgroups split in the Eocene at slightly different times. Comparisons of the historical

biogeographical reconstructions support the dispersal hypothesis as the best-fitting model over a vicariance model.

Main Conclusions: Our results support multiple dispersals starting during the Cretaceous–Paleocene from South America to Africa, Asia, and India. Two dispersal events occurred during the Eocene: the first from India to South America, and a second from Africa to the Caribbean, giving rise to *Aktiogavialis* and the gryposuchines, respectively. These dispersals were most likely facilitated by the connection of the New World to the Old World by the Tethys Sea. Our results also support the independent dispersal of *Aktiogavialis* from the Caribbean to South America during the Oligocene, coinciding with a drop in global drop in sea level and exposure of land due to regional uplift.

Introduction

Historical biogeography—the past distribution of species—has played a major role in the understanding of the evolutionary processes that have led to the current distribution of species. The inclusion of the paleontological record to understand the historical biogeography of species has also been fundamental for developing new hypotheses that explain the evolution of species across space and time. However, when biogeographical hypotheses rely on incomplete paleontological data, they can lead to dubious or weak interpretations that can later be replaced by new findings. Novel approaches in historical biogeographic studies have developed model-based analyses that can be used to test complex biogeographical hypotheses (Matzke, 2013; Ree & Smith, 2008). Still, these novel methods have been applied to paleontological data

comparatively recently, and provide an opportunity to test biogeographical hypotheses of major vertebrate groups.

Gavialine crocodylians (Gavialidae) present an opportunity to test historical biogeographical hypotheses under these new model-based approaches (Matzke, 2013). Gavialinae is a clade of long-snouted crocodylians represented today by a single taxon, the gharial *Gavialis gangeticus*, which is geographically restricted to the northern freshwater systems of India and Nepal (Stevenson, 2015). However, the gavialine fossil record shows a long evolutionary history that can be traced back to the Cretaceous, with members distributed in most landmasses and some known from coastal marine deposits (Brochu & Rincón, 2004; Buffetaut, 1987; Gasparini & Buffetaut, 1980; Kraus, 1988; Salas-Gismondi et al., 2016; 2019; 2022; Vélez-Juarbe et al., 2007). Thus, the current geographic and ecological distribution of the living gharial contrasts with what is found in the fossil record. Multiple dispersals among western (Africa, Asia, and India) and eastern (Americas) continents during the Cretaceous to Oligocene have been proposed as the most probable hypotheses to explain the distribution and divergence time of fossil gavialines (Brochu & Rincón, 2004; Kraus, 1988; Vélez-Juarbe et al., 2007). Still, these hypotheses remain to be tested under model-based approaches (Matzke, 2013; Ree & Smith, 2008). An ancestral range reconstruction under the dispersal vicariance (S-DIVA) model was recently incorporated into a phylogenetic tree of Crocodylia, the clade containing the living crocodylians (Alligatoridae, Crocodylidae, and Gavialidae) and their closest extinct relatives (Salas-Gismondi et al., 2022). Although the optimal biogeographic range reconstruction for most groups had high resolution, the ancestral ranges for some subgroups within Gavialidae were ambiguous (see Salas-Gismondi et al., 2022), especially for the node containing the South American gharials, the so-called gryposuchines. The incorporation of new fossil taxa from the

Cretaceous of South America and the Eocene of Pakistan in a phylogenetic context brings additional complexity to the divergence time and dispersal capabilities of gavialines that have never been considered before (Buffetaut, 1987; Gasparini & Buffetaut, 1980; Vélez-Rosado et al., 2024a; b). Thus, reconstructing the geographical ancestral range for Gavialidae is critical for understanding the divergence and relationships among the major clades within the group, when and where gavialines originate, and their dispersal capabilities.

In the present study, we test the dispersal hypotheses proposed by Brochu & Rincón (2004), Vélez-Juarbe et al. (2007), and Vélez-Rosado et al. (2024a; b) under a tip-dated Bayesian framework using a discrete morphological character dataset that includes the majority of extant and extinct crocodylians. We performed two independent biogeographical analyses: the first model without any dispersal probabilities, and an alternative model including the high dispersal probabilities among the western and eastern landmasses. We then use Akaike's Information Criterion to compare the best-fitting model for the dataset. The results of our study highlight the importance of incorporating biogeographic models in phylogenies to understand the complex geospatial distribution of species across millions of years, especially for extant groups that are geographically restricted and have low diversity in the present day.

Materials and Methods

Morphological data

The dataset used in this analysis consists of a discrete character state matrix of Vélez-Rosado et al. (2024a) that includes 69 operational taxonomic units and 248 morphological characters. This matrix is the result of previous phylogenetic studies (Brochu, 1997a; 1997b; 1999; 2000; 2003;

2004; Brochu & Rincón, 2004; Jouve et al., 2006; Salas-Gismondi et al., 2016; 2019; 2022; Vélez-Juarbe et al., 2007) and includes the majority of extinct (51 OTUs) and extant (18 OTUs) crocodylians. The OTUs in the dataset encompass a wide temporal range, including fossils from the Lower Cretaceous (145 Ma) to the present day and groups that are found worldwide (see Supporting Information S1).

Phylogenetic analysis

Phylogenetic analysis was performed under a tip-dated Bayesian framework using BEAST v.2.7.4 (Drummond & Rambaut, 2007). We chose this method in order to evaluate the evolutionary relationships of major groups—especially the unstable taxa—within Crocodylia when stratigraphic information is taken into account. Before building the model, all uninformative characters were removed from the matrix. We used the Mkv substitution model in the analysis, which is the only model for discrete morphological datasets available in Bayesian studies (Lewis, 2001). The tip dates panel was activated and we incorporated the last appearance datum of each OTU in the dataset: ages were taken from the published literature and the paleobiology database (https://paleobiodb.org). A site model with a gamma category count of 4 was set for each partition, with substitution rate and shape estimates in activated mode. An optimized relaxed clock with a mean rate of 1 and the fossilized birth-death model (Heath et al., 2014) was implemented. *Bernissartia fagesii* was chosen as the outgroup taxon and the clade origin was set to 145, which is the age of the first appearance datum of the outgroup. The Markov Chain Monte Carlo simulation was implemented with a chain of 40,000,000, sampling every 1,000 generations. We set a pre-burn-in of 25% and the remaining trees were used to compute a 50% maximum clade credibility tree with median heights (see Supporting Information

S2). Tree convergence and stability were achieved when the effective sample size reached values of >200 and detected in Tracer v.1.7.2 (Rambaut et al., 2018).

Biogeographic analysis

To investigate the historical biogeography of Gavialidae, ancestral ranges were estimated using the R package BioGeoBEARS (Matzke, 2013). We selected the Dispersal-Extinction-Cladogenesis (DEC) model to reconstruct the evolution of geographic ranges along the branches in a phylogenetic context (Ree & Smith, 2008). We did not utilize models with the DEC+J (J = jump dispersal) in our study because it has been proved that the J parameter is a poor model of founder-event speciation, thus statistical comparisons of its likelihood with the DEC model are inappropriate (Ree & Sanmartín, 2018). We defined nine geographic areas based on the distribution of the extinct and extant OTUs in the dataset, including Europe (E), South America (S), Caribbean (B), North America (N), Asia (A), Africa (F), Central America (C), Australia (U), and Greater India (I).

Two biogeographical hypotheses were tested in this study. The first model is the simplest, which has no dispersal probabilities and is used as the null hypothesis. The second biogeographical model was divided into time slices with different probability values: the first time slice represents the proposed hypothesis of dispersal from South America to Africa (Vélez-Rosado et al., 2024a) during the early Paleocene (62–55 Ma); and the second time slice representing the proposed dispersal in the Eocene (55–40 Ma) from Africa+Asia+Europe to the Americas (Brochu & Rincón, 2004; Salas-Gismondi et al., 2016; 2019; 2022; Vélez-Juarbe et al., 2007). The time slices were taken based on the last appearance datum of the oldest gavialines in the dataset, *Dolichochampsa minima* (64 Ma), *Argochampsa krebsi* (56 Ma), and *Pelagosuchus*

pakistanensis (41 Ma). The dispersal matrices include the following probability values: 1 = connected areas; 0.9 = connected but far; 0.75 = effective barrier (closed continents or islands); 0.1 = long distance barrier; and 0.001 = not yet emergent islands. Because the OTUs in the dataset are semi-aquatic tetrapods and it has been shown that large crocodylians can travel for long distances and periods (Read et al., 2007), we considered connected areas by water and not by land. Thus, any large landmass was taken as a possible geographic barrier when possible connections (i.e., rivers, and oceans) were unknown. We used Akaikes' Information Criterion (AIC) to compare the relative likelihood of the two models and the better model was used to estimate the biogeographical history of Gavialidae (see Supporting Information S3).

Results

Phylogenetic analysis

Our tip-dated Bayesian analysis recovered a fully-resolved topology with major groups and subgroups within Crocodylia as in previous studies (Brochu, 2004; Salas-Gismondi et al., 2016; 2019; 2022; Vélez-Juarbe et al., 2007). The three main crocodylian families (Alligatoridae, Crocodylidae, and Gavialidae) were retrieved as monophyletic. However, the interrelationships among some subgroups and individual OTUs differed from previous studies (Fig. 1). For instance, recent phylogenetic studies of morphological datasets have recovered *Tomistoma schlegelii* and its immediate relatives as a paraphyletic group at the stem of Gavialoidea (Lee & Yates, 2018; Salas-Gismondi et al., 2022). In our analysis, *Tomistoma* and its allies form a clade sister to crocodylids. Additionally, 'thoracosaurs,' a clade that includes long-snouted forms from North America and Europe were recovered at the stem of Gavialidae, which is similar to results

of earlier studies (Brochu, 2006; Salas-Gismondi et al., 2019). Surprisingly, the North American genus *Borealosuchus* was also recovered at the stem of Gavialidae in our analysis. Previous phylogenetic studies have consistently resolved *Borealosuchus* as a stem eusuchian forming a clade outside Crocodylia (Brochu, 2006; Delfino et al., 2005; Hua & Jouve, 2004; Salas-Gismondi et al., 2016; 2019; 2022; Vélez-Juarbe et al., 2007).

The South American gavialine, *Dolichochampsa minima*, which was recently evaluated in a phylogenetic context by Vélez-Rosado et al. (2024a) and recovered as an unstable OTU within Gavialidae, was recovered as the oldest gavialine in our phylogeny (Fig. 1). The South American assemblage, Gryposuchinae, forms a monophyletic assemblage (Bayesian Posterior Probability; BPP: 0.99) and subdivided into two main groups: one that includes *Dadagavialis* and *Gryposuchus*; and a second group containing *Ikanogavialis*, *Piscogavialis*, and *Siquisiquesuchus*. In our analysis, *Pelagosuchus pakistanensis*, a recently described taxon from the Eocene of Pakistan, was recovered as the immediate outgroup of Gryposuchinae (Vélez-Rosado et al., 2024b). *Gavialis* and *Eogavialis* form a subgroup and their close evolutionary relationships are highly supported (BPP: 0.95). Interestingly, the genus *Aktiogavialis*, which includes Caribbean and South American taxa, was recovered as the immediate outgroup to the other Neogene forms. *Aktiogavialis* was first considered as a gryposuchine by Vélez-Juarbe et al. (2007), but later analyses have recovered the genus forming a separate group within Gavialidae, although the evolutionary relationships between the three subgroups, *Aktiogavialis+Gavialis+Gryposuchinae*, were unresolved in recent cladistic studies (Salas-Gismondi et al., 2022; Vélez-Rosado et al., 2024a; b).

Divergence-time estimates show an origin for Gavialidae in the Paleocene (64 Ma), although the highest posterior density (HPD) of the divergence time is imprecise and it may

extend to the Cretaceous (73 Ma) based on the first appearance datum of *Dolichochampsa minima* (Vélez-Rosado et al., 2024a). The three gavialine subgroups (*Aktiogavialis*+*Gavialis*+Gryposuchinae) split in the Eocene at 55.5 Ma (HPD = 63.7–47.2 Ma). The Neotropical gharials, Gryposuchinae, diverged in the Eocene at 46.6 Ma (HPD = 53.8–41.7 Ma). The two main lineages within Gryposuchinae (*Gryposuchus*+*Dadagavialis* and *Ikanogavialis*+*Piscogavialis*+*Siquisiquesuhus*) split in the early Oligocene at 32.2 Ma (HPD = 42.6–22.9 Ma). The results of the phylogenetic analysis and divergence-time estimates with the biogeographic model are presented in Fig. 2.

Biogeographical analyses

Comparison of the AIC values supported the second hypothesis as the best-fitting model, being 32.2 units lower than the null model (Table 1). These results show that a model that includes the highest dispersal probabilities during Paleocene–Eocene explains the presence of *Aktiogavialis* and Gryposuchinae in the Americas, as opposed to being vicariant groups. Moreover, the best-fitting model shows two independent dispersals during the Eocene: one dispersal from Africa to the Caribbean at 50 Ma; and a second dispersal from India to South America at 46 Ma. Ancestral range reconstruction shows that the subgroups *Aktiogavialis* and *Eogavialis*+*Gavialis* originated in Africa, whereas Gryposuchinae originated from an Indian ancestor (Fig. 3).

Discussion

Below we discuss the uncertainties of two longirostrine clades and their impact on the gavialine diversity and biogeographic history. We then expand on the results of the best-fitting biogeographic model and provide an interpretation of the past distribution of gavialines.

Uncertainties within longirostrine crocodylians

This study presents a tip-dated phylogenetic tree of Crocodylia under a Bayesian framework that includes the majority of extinct (51) and living (18) taxa described thus far (Fig. 1). Although evolutionary relationships among higher-level groups are similar in our analysis to those of previous studies, uncertainties over the phylogenetic position of two longirostrine groups ("thoracosaurs" and Tomistominae) remain to be solved. "Thoracosaurs" is an extinct group of long-snouted forms that include taxa (*Eothoracosaurus*, *Eosuchus*, and *Thoracosaurus*) mainly from the Cretaceous–Paleocene of North America and Europe (Brochu, 2004; 2006; Carpenter, 1983; Delfino et al., 2005). Historically, "thoracosaurs" have been considered phylogenetically closer to gavialines primarily based on shared derived characters associated with the skull, and have been consistently retrieved as a basal group within Gavialidae in cladistic studies (Salas-Gismondi et al., 2019; Jouve et al., 2006; Vélez-Juarbe et al., 2007). It was not until recently that "thoracosaurs" were considered basal eusuchians, phylogenetically closer to the North American taxon *Borealosuchus*, which is more congruent with their temporal and geographical distribution (Lee & Yates, 2018; Salas-Gismondi et al., 2022). In the present study, "thoracosaurs" are retrieved as basal members within Gavialidae as in previous morphology-based studies, although with comparatively low support values (BPP: 0.6).

The other longirostrine group with an uncertain phylogenetic position is Tomistominae. Evolutionary relationships of tomistomines within Crocodylia have been a matter of controversy over the last three decades due to competing hypotheses between molecular and morphological-based studies. Molecular-based analyses have constantly retrieved a sister-group relationship between *Tomistoma* and *Gavialis* (Willis et al., 2007), whereas morphology-based studies

support *Tomistoma* and its fossil allies forming a clade sister to Crocodylidae (Brochu, 1997a; 2003; Salas-Gismondi et al., 2016; 2019; Vélez-Juarbe et al., 2007). It was not until recently that Salas-Gismondi et al. (2022) and Vélez-Rosado et al. (2024a) recovered tomistomines forming a paraphyletic group leading to crown-group gharials. Our analysis, which uses the dataset from previous studies (Salas-Gismondi et al., 2022; Vélez-Rosado et al., 2024a), suggests that Tomistominae might be a monophyletic group (BPP: 1) sister to Crocodylidae.

It thus seems that model selection (i.e., Bayesian, Likelihood, Parsimony) might play a critical role when inferring the evolutionary relationships of extinct and extant crocodylians in morphology-based analyses. Traditionally, morphologists have used parsimony to infer the evolutionary relationship among extinct and extant forms, whereas Bayesian models have been introduced to morphological data comparatively recently. Recent implementations of the Mk model in Bayesian analyses have been demonstrated to outperform parsimony in discrete morphological data and can accurately reconstruct the phylogenetic position of highly incomplete taxa (O'Reilly et al., 2023; Wiens & Moen, 2008), producing phylogenies with higher resolution. Thus, a Bayesian analysis that supports tomistomines closer to crocodylids under the same dataset that previously supported a closer position within Gavialidae in parsimony-based studies adds more complexity when inferring the evolutionary relationships of extinct and extant groups in morphology-based analyses (Brochu, 2006; Brochu & Rincón, 2004; Salas-Gismondi et al., 2016; 2019; Vélez-Juarbe et al., 2007). Reaching a consensus over the evolutionary relationships of tomistomines and "thoracosaurs" will be critical as their phylogenetic position could have an impact on the diversity and historical biogeography of Gavialidae.

Historical Biogeography of Gavialidae

The results of our analyses allow us to frame a complete biogeographic history of Gavialidae. The origin of Gavialidae can be traced back to the Cretaceous–Paleocene (72–64 Ma) of South America (Vélez-Rosado et al., 2024a). By the end of the Cretaceous or possibly in the early Paleocene, gavialines dispersed to the African continent (Figs. 3, 4) and later giving rise to *Argochampsa* and *Eogavialis* (Hua & Jouve, 2004; Jouve et al., 2006). Considering the proximity of South America and Africa and the paleocurrents during the end of the Cretaceous and early Paleocene, such intercontinental interchange might have occurred through the Guinean Gulf (Hay, 2009; Pucéatet al., 2005). After arriving in Africa, gavialines most likely continued to disperse eastward to mainland Asia and India throughout the Tethys Sea during the Eocene. Although there is an apparent gap in the stem between *Eogavialis* and *Gavialis*, the group most likely arrived at the Indian subcontinent before the closure of the Tethys Sea and the final collision of the Indian plate with Eurasia. Ancestral state reconstruction shows an African origin of *Gavialis* with high marginal probability (Table 2), and separation occurring by the end of Eocene (Figure 3).

Biogeographical hypotheses often proposed an African, Asian, or Indian origin of the South American gharials, Gryposuchinae, based on the close phylogenetic relationships of early forms in those continents (Hua & Jouve, 2004; Jouve et al., 2006; Vélez-Juarbe et al., 2007; Vélez-Rosado et al., 2024a). In our analysis, the ancestral range reconstruction of the best-fitting model shows that the most recent common ancestor of Gryposuchinae most likely resided in the Indian subcontinent (Fig. 4) with the highest ancestral range probability (Table 2). The most recent common ancestor of gryposuchines might have originated in the Eocene (46.6 Ma), based on their closest extinct relative and divergence-time estimates (Fig. 2). During the Eocene, the

Tethys Sea served as a marine corridor connecting India with the Americas (Berra & Angiolini, 2014). Certainly, some of the early forms from Africa (*Argochampsa*, *Eogavialis*, and *Pelagosuchus*) and South America (*Siquisiquesuchus*, *Piscogavialis*) have been retrieved from coastal marine deposits, indicating that they were probably well suited for these environments (Brochu & Rincón, 2004; Hua & Jouve, 2004; Jouve et al., 2006; Kraus, 1998; Vélez-Juarbe et al., 2007).

Recently it was proposed that the clade containing *Aktiogavialis* represents independent radiation from Africa (Salas-Gismondi et al., 2019; 2022). The ancestral state reconstruction of our analysis also supports an African origin for *Aktiogavialis*, which diverged in the early Eocene (55.5 Ma) (Fig. 2). Surprisingly, our biogeographic analysis strongly supports the Caribbean as the most likely ancestral range for the South American taxon *A. caribesi*, indicating that the clade dispersed southward later in the Oligocene (29.4 Ma). Interestingly, the high posterior density of the divergence time of the two *Aktiogavialis* taxa coincides with a global cooling event during the Eocene–Oligocene, which caused a sea level drop of up to 60 m (Haq et al., 1987; Miller et al., 2008). Together with regional tectonic uplift, this may have exposed sufficient land, allowing dispersals from the Caribbean to South America, the so-called GAARlandia hypothesis (Iturralde-Vinent, 2006; Iturralde-Vinent & MacPhee, 1999; MacPhee & Iturralde-Vinent, 1995). Controversies over GAARlandia are still debated (Ali, 2012; Ali & Hedges, 2021; Hedges, 2006), however, paleontological and geological evidence points to the emergence of land during the Eocene–Oligocene, which could have facilitated the dispersal of semi-aquatic organisms across these landmasses (Haq et al., 1987; Marivaux et al., 2020; Miller et al., 2008; Vélez-Juarbe et al., 2014).

Acknowledgments

We thank Adam Rountrey the collection manager of the University of Michigan Museum of Paleontology for providing access to collections used in this study. We also thank Coleman Sheehy III for access to the herpetology collection at the Florida Museum of Natural History. Permits were not required to obtain the data in this study. We are grateful to the reviewers for their comments that improved our manuscript.

Funding Information

This project was funded by the Scott Turner Award 2019 and 2021 provided by the Department of Earth and Environmental Sciences at the University of Michigan.

References

Ali, J. R. (2012). Colonizing the Caribbean: is the GAARlandia land-bridge hypothesis gaining a foothold? *Journal of Biogeography, 39*, 431–433.

Ali, J. R., & Hedges, S. B. (2021). Colonizing the Caribbean: New geological data and an updated land-vertebrate colonization record challenge the GAARlandia land-bridge hypothesis. *Journal of Biogeography, 48*, 2699–2707.

Berra, F., & Angiolini, L. (2014). The evolution of the Tethys region throughout the Phanerozoic: A brief tectonic reconstruction. In L. Malow, C. Kendall, & L. Yose (Eds.), *Petroleum systems of the Tethyan region* (pp. 1–27). AAPG Memoir.

Brochu, C. A. (1997a). Morphology, fossils, divergence timing, and the phylogenetic relationships of *Gavialis*. *Systematic Biology, 46*(3), 479–522. https://doi.org/10.1093/sysbio/46.3.479

Brochu, C. A. (1997b). A review of "*Leidyosuchus*" (Crocodyliformes, Eusuchia) from the Cretaceous through Eocene of North America. *Journal of Vertebrate Paleontology, 17*, 679–697.

Brochu, C. A. (1999). Phylogenetics, taxonomy, and historical biogeography of Alligatoroidea. *Journal of Vertebrate Paleontology, 19*(2), 9–100.

Brochu, C. A. (2000). Phylogenetic relationships and timing of *Crocodylus* based on morphology and fossil record, *Copeia, 46*, 657–673.

Brochu, C. A. (2003). Phylogenetic approaches toward crocodylian history. *Annual Review of Earth and Planetary Sciences, 31*, 357–397.

Brochu, C. A. (2004). A new Late Cretaceous gavialoid crocodylian from eastern North America and the phylogenetic relationships of thoracosaurs. *Journal of Vertebrate Paleontology, 24*(3), 610–633.

Brochu, C. A. (2006). Osteology and phylogenetic significance of *Eosuchus minor* (Marsh, 1870) new combination, a longirostrine crocodylian from the Late Paleocene of North America. *Journal of Paleontology, 80*(1), 162–186.

Brochu, C. A., & Rincón, A. D. (2004). A gavialoid crocodylian from the lower Miocene of Venezuela. *The Palaeontological Association, 71*, 61–79.

Buffetaut, E. (1987). Occurrence of the crocodilian *Dolichochampsa minima* (Eusuchia, Dolichochampsidae) in the El Molino Formation of Bolivia. *Bulletin van de Belgische Vereniging voor Geologie, 96*(2), 195–199.

Carpenter, K. (1983). *Thoracosaurus neocesariensis* (De Kay, 1842) (Crocodylia: Crocodylidae) from the Late Cretaceous Ripley Formation of Mississippi. *Mississippi geology, 4*(1), 1–10.

Delfino, M., Piras, P., & Smith, T. (2005). Anatomy and phylogeny of the gavialoid crocodylian *Eosuchus lerichei* from the Paleocene of Europe. *Acta Palaeontologica Polonica, 50*(3), 565–580.

Drummond, A. J., & Rambaut, A. (2007). BEAST: Bayesian evolutionary analysis by sampling trees. BMC Evolutionary Biology, 7, 1–8.

Gasparini, Z. B., & Buffetaut, E. (1980). *Dolichochampsa minima*, n. g. n. sp., a representative of a new family of eusuchian crocodiles from the Late Cretaceous of northern Argentina. *Neues Jahrbuch für Geologie und Paläontologie - Monatshefte, 1980*, 257–271.

Haq, B. U., Hardenbol, J. & Vail, P. R. (1987). Chronology of fluctuating sea levels since the Triassic. *Science*, *235*: 1156–1167.

Hay, W. (2009). Cretaceous oceans and ocean modelling. In X. Hu, C. Wang, R. W. Scott, M. Wagreich, & L. Jansa (Eds.), *Cretaceous ocean redbeds: stratigraphy, composition, origins, and paleoceanographic and paleoclimatic significance* (pp. 243–271). SEPM (Society for Sedimentary Geology) special publication.

Heath, T. A., Huelsenbeck, J. P., & Stadler, T. (2014). The fossilized birth-death process for coherent calibration of divergence-time estimates. *PNAS, 111*(29), E2957–E2966.

Hedges, S. B. (2006). Paleogeography of the Antilles and origin of west Indian terrestrial vertebrates. *Annals of the Missouri Botanical Garden, 93*(2), 231–244.

Hua, S., & Jouve, S. (2004). A primitive marine gavialoid from the Paleocene of Morocco. *Journal of Vertebrate Paleontology, 24*(2), 341–350. https://doi.org/doi: 10.1671/1104

Iturralde-Vinent, M. A. (2006). Meso-Cenozoic Caribbean paleogeography: implications for the historical biogeography of the region. *International Geology Review, 48*, 791–827.

Iturralde-Vinent, M. A., & MacPhee, R. D. E. (1999). Paleogeography of the Caribbean region: implications for Cenozoic biogeography. *Bulletin of the American Museum of Natural History, 238*, 1–95.

Jouve, S., Iarochene, M., Bouya, B., & Amaghzaz, M. (2006). New material of *Argochampsa krebsi* (Crocodylia: Gavialoidea) from the Lower Paleocene of the Oulad Abdoun Basin (Morocco): phylogenetic implications. *Geobios, 39*, 817–832.

Kraus, R. (1998). The cranium of Piscogavialis jugaliperforatus n. gen., n. sp. (Gavialidae, Crocodylia) from the Miocene of Peru. *Paläontologische Zeitschrift, 72*, 389–406.

Lee, M. S. Y., & Yates, A. M. (2018). Tip-dating and homoplasy: reconciling the shallow molecular divergences of modern gharials with their long fossil record. *Proceedings of the Royal Society B: Biological Sciences, 285*, 20181071.

Lewis, P. O. (2001). A likelihood approach to estimating phylogeny from discrete morphological character data. *Systematic Biology, 50*(6), 913–925.

MacPhee, R. D. E., & Iturralde-Vinent, M. A. (1995). Origin of the Greater Antillean land mammal fauna, 1: new Tertiary fossils from Cuba and Puerto Rico. *American Museum Novitatesz, 3141*, 1–31.

Marivaux, L., Vélez-Juarbe, J., Merzeraud, G., Pujos, F., Viñola López, L., Boivin, M., Santos-Mercado, H., Cruz, E. J., Grajales, A., Padilla, J., Vélez-Rosado, K. I., Philippon, M., Léticée, J.-L., Münch, P., & Antoine, P.-O. (2020). Early Oligocene chinchilloid caviomorphs from Puerto Rico and the initial rodent colonization of the West Indies. *Proceedings of Royal Society B, 287*, 1–10.

Matzke, N. J. (2013). *BioGeoBEARS: BioGeography with Bayesian (and likelihood) Evolutionary Analysis in R Scripts* [Rstudio].

Miller, K. G., Browning, J. V., Aubry, M. P., Wade, B. S., Katz, M. E., Kulpecz, A. A., & Wright, J. D. (2008). Eocene–Oligocene global climate and sea-level changes: St. Stephens Quarry, Alabama. *Geological Society of America Bulletin, 120*, 34–53.

O'Reilly, J. E., Puttick, M. N., Parry, L., Tanner, A. R., Tarver, J. E., Fleming, J., Pisani, D., & Donoghue, P. C. J. (2023). Bayesian methods outperform parsimony but at the expense of precision in the estimation of phylogeny from discrete morphological data. *Biology Letters, 12*, 1–5.

Pucéat, E., Lecuyer, C., & Reisberg, L. (2005). Neodymium isotope evolution of NW Tethyan upper ocean waters throughout the Cretaceous. *Earth and Planetary Science Letters, 236*, 705–720.

Rambaut, A., Drummond, A. J., Xie, D., Baele, G., & Suchard, M. A. (2018). Posterior summarization in Bayesian phylogenetics using Tracer 1.7. *Systematic Biology, 67*(5), 901–904.

Read, M. A., Grigg, G. C., Irwin, S. R., Shanahan, D. Franklin, C. E. (2007). Satellite tracking reveals long distance coastal travel and homing by translocated Estuarine Crocodiles, *Crocodylus porosus*. *Plos One, 2*(9), 1–5.

Ree, R. H., & Sanmartín, I. (2018). Conceptual and statistical problems with the DEC+J model founder-event speciation and its comparison with DEC via model selection. *Journal of Biogeography, 45*, 741–749.

Ree, R. H., & Smith, S. A. (2008). Maximum likelihood inference of geographic range evolution by dispersal, local extinction, and cladogenesis. *Systematic Biology, 57*, 4–14.

Salas-Gismondi, R., Flynn, J. J., Baby, P., Tejada-Lara, J. V., Claude, J., & Pierre-Olivier, A. (2016). A new 13 million year old gavialoid crocodylian from proto-Amazonian mega-wetlands reveals parallel evolutionary trends in skull shape linked to longirostry. *PLoS ONE, 11*(4), e0152453.

Salas-Gismondi, R., Moreno-Bernal, J., Scheyerc, T. M., Sánchez-Villagra, M. R., & Jaramillo, C. (2019). New Miocene Caribbean gavialoids and patterns of longirostry in crocodylians. *Journal of Systematic Palaeontology, 17*(12), 1049–1075.

Salas-Gismondi, R., Ochoa, D., Jouve, S., Romero, P. E., Cardich, J., Perez, A., DeVries, T., Baby, P., Urbina, M., & Carré, M. (2022). Miocene fossils from the southeastern Pacific shed light on the last radiation of marine crocodylians. *Proceedings of the Royal Society B: Biological Sciences, 289*, 20220380.

Stevenson, C. J. (2015). Conservation of the Indian gharial *Gavialis gangeticus*: successes and failures. *International Zoo Yearbook, 49*, 150–161.

Vélez-Juarbe, J., Brochu, C. A., & Santos, H. (2007). A gharial from the Oligocene of Puerto Rico: transoceanic dispersal in the history of a non-marine reptile. *Proceedings of the Royal Society B: Biological Sciences*, 274, 1245–1254.

Vélez-Juarbe, J., Martin, T., MacPhee, R. D. E., & Ortega-Ariza, D. (2014). The earliest Caribbean rodents: Oligocene caviomorphs from Puerto Rico. *Journal of Vertebrate Paleontology, 34*, 157–163.

Vélez-Rosado, K. I., Zalles-Grebetskaya, O. I., Wilson Mantilla, J. A., Schoene, B., Maloof, A., & Howes, B. (2024a). *New material of Dolichochampsa minima (Archosauria: Crocodylia) from the Cretaceous–Paleogene El Molino Formation of Bolivia sheds light on the early evolution of Gavialinae* [Manuscript submitted for publication]. Earth and Environmental Sciences, University of Michigan.

Vélez-Rosado, K. I., Wilson Mantilla, J. A., & Giingerich, P. D. (2024b). *A new basal gavialines (Crocodylia: Gavialinae) from the Eocene of Pakistan and its paleobiogeographical implications* [Manuscript in preparation]. Earth and Environmental Sciences, University of Michigan.

Wiens, J. J., & Moen, D. S. (2008). Missing data and the accuracy of Bayesian phylogenetics. *Journal of Systematic and Evolution, 46*(3), 307–314.

Willis, R. E., McAliley, L. R., Neeley, E. D., & Densmore, L. D. 2007. Evidence for placing the false gharial (*Tomistoma schlegelii*) into the family Gavialidae: inferences from nuclear gene sequences. *Molecular Phylogenetics and Evolution, 43*, 787–794.

Figures and Tables

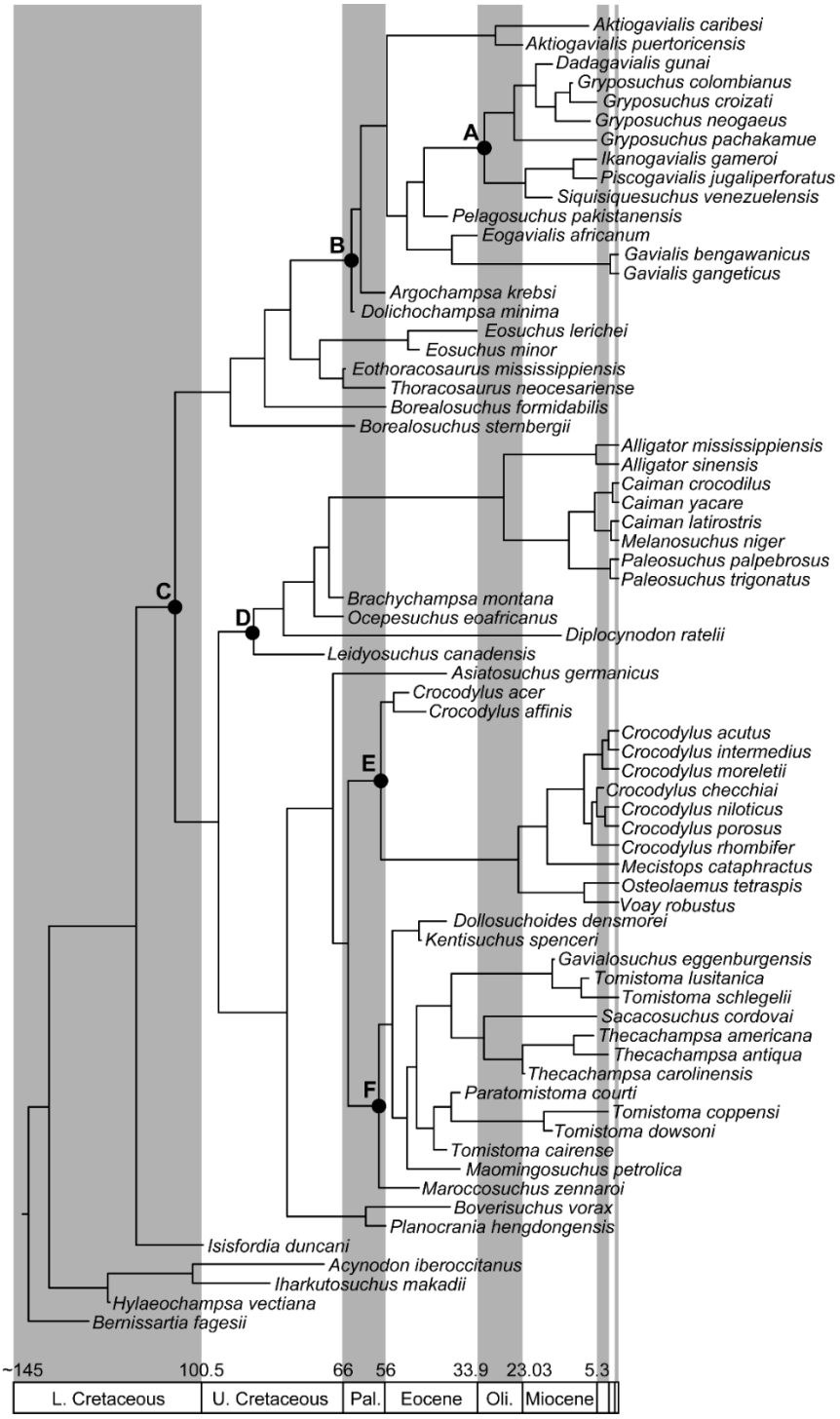

Figure 4.1. Time-calibrated phylogenetic tree after computing the maximum clade credibility tree (50%). Nodes represent the main groups within Crocodylia: A, Gryposuchinae; B, Gavialidae; C, Crocodylia; D, Alligatoridae; E, Crocodylidae; F, Tomistominae. The last three divisions in the geological time scale correspond to the Pliocene, Pleistocene, and Holocene.

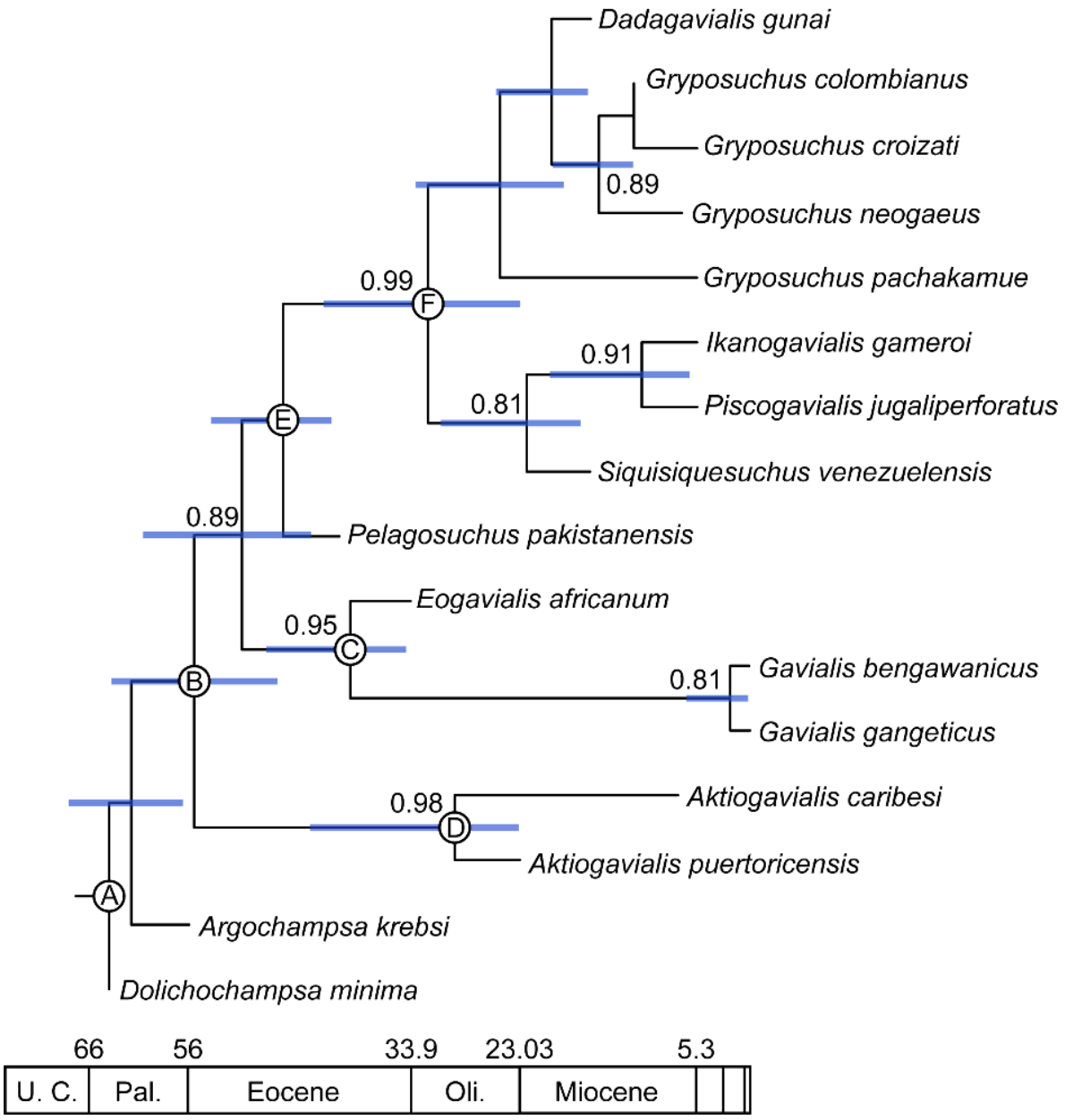

Figure 4.2. Maximum clade credibility showing the relationships of all OTUs within Gavialinae used in the analysis. Blue bars indicate the 95% highest posterior densities (HPD): **A**, 64; **B**, 55.5 Ma (63.6–47.2); **C**, 39.9 Ma (48.2–34.3); **D**, 29.4 Ma (43.9–23); **E**, 46.6 Ma (53.8–41.7); **F**, 32.1 Ma (42.6–22.9). These nodes represent major splitting events concordant with the dispersal of gavialines. Numbers at nodes represent the Bayesian Posterior Probabilities, BPP (>0.80). The last three divisions in the geological time scale correspond to the Pliocene, Pleistocene, and Holocene.

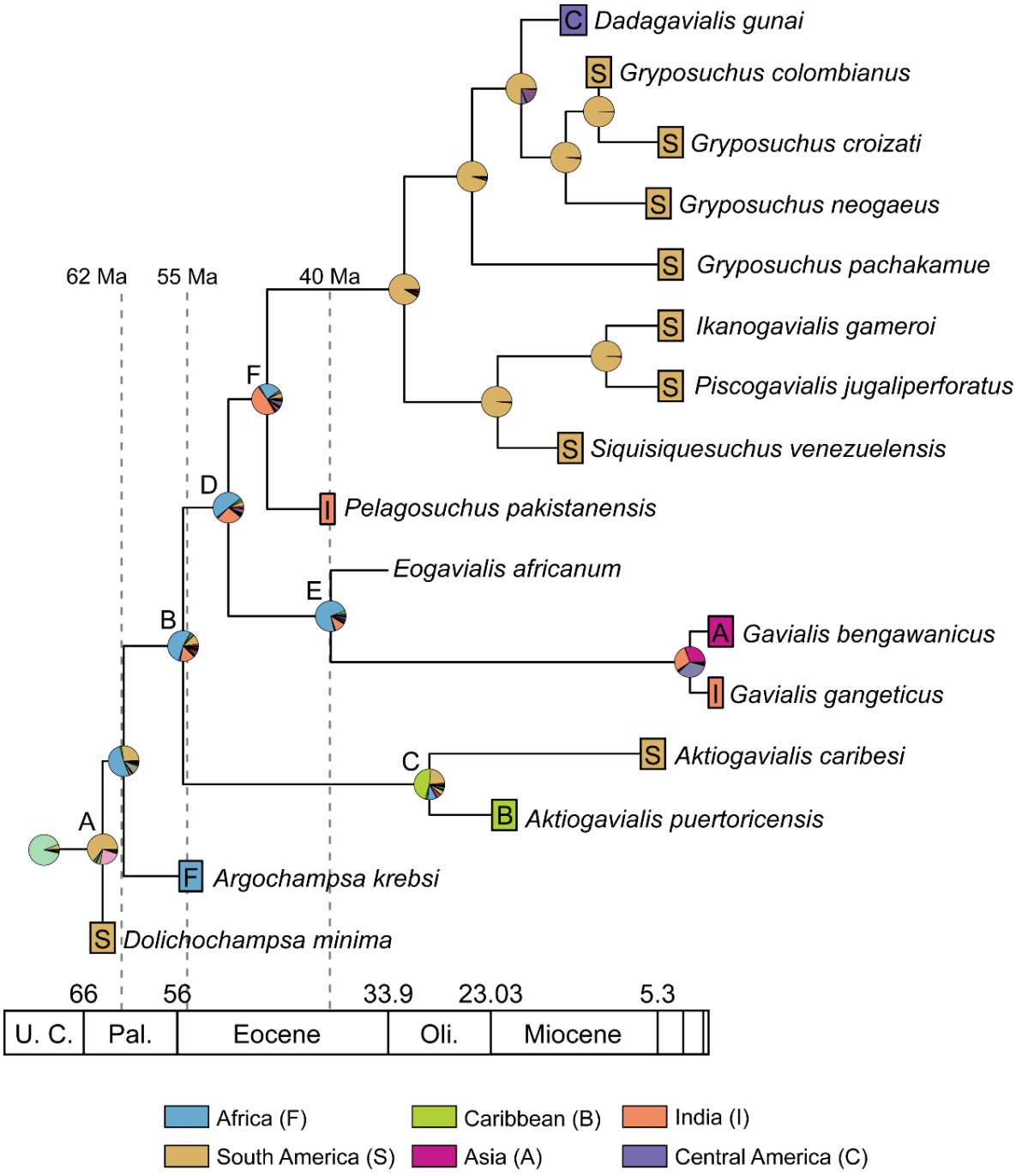

Figure 4.3. Maximum clade credibility tree showing the ancestral range reconstructions at nodes and tips of the best fitting biogeographical model. The three dashed lines represent the time slices. The letters at nodes correspond to the pie charts in Figure 4. The last three divisions in the geological time scale correspond to the Pliocene, Pleistocene, and Holocene.

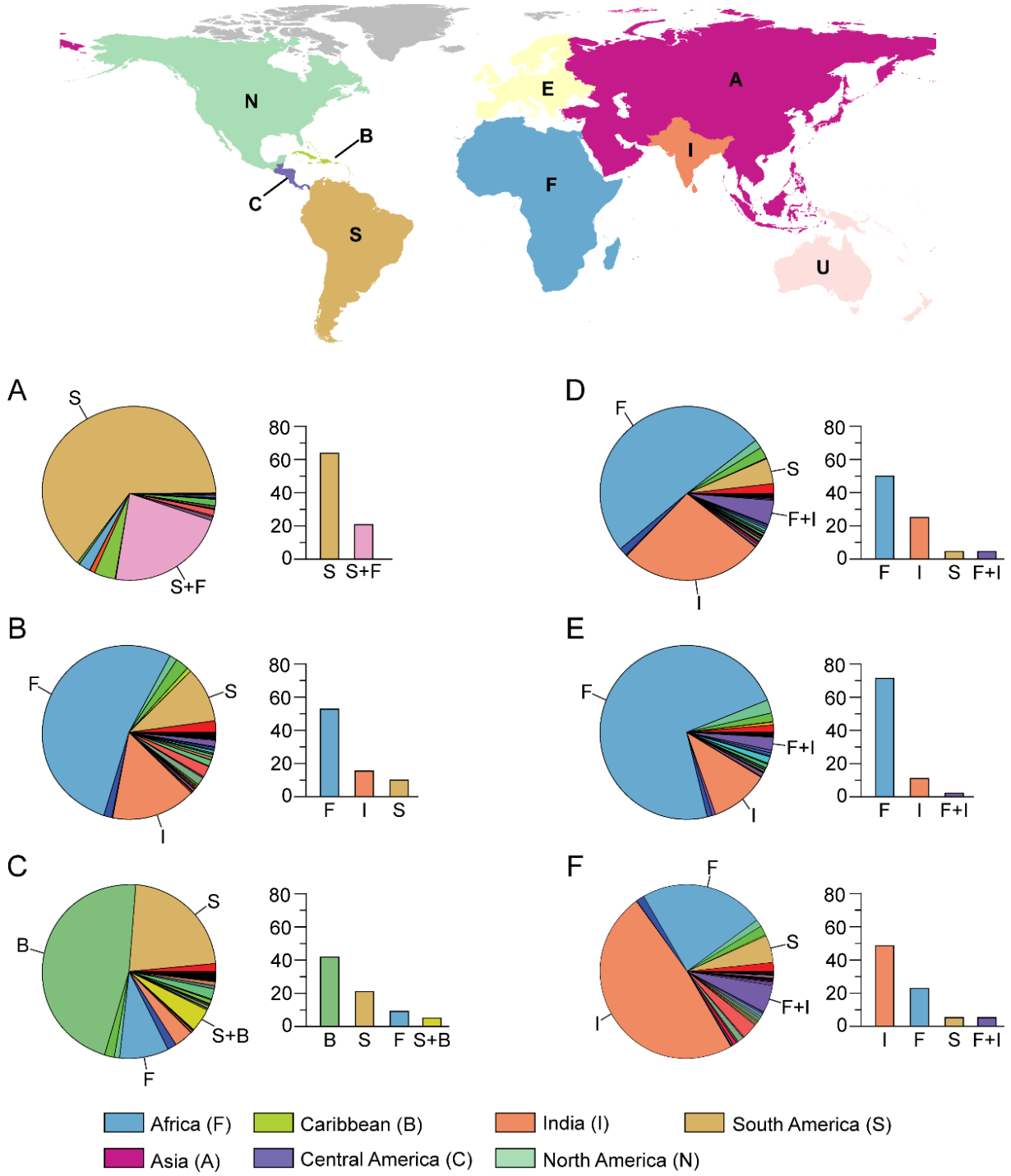

Figure 4.4. Global map showing the 9 geographic ranges used in our analysis and pie charts of major gavialines nodes. The letters of each pie chart correspond to the nodes of Figure 3. Bar plots show the ancestral ranges with the highest probability values (%) obtained in the biogeographic analysis.

Table 4.1. Comparison of the two analyses performed in BioGeoBEARS under the dispersal-extinction-cladogenesis (DEC) model. **Ln*L***, log-likelihood; **np**, number of parameters; ***d***, rate of dispersal; ***e***, rate of extinction; **AIC**, Akaike's Information Criterion; **Δ AIC**, AIC-min(AIC).

Models	**Ln*L***	**np**	***d***	***e***	**AIC**	**Δ AIC**	**AIC weight**
DEC – no dispersals	–146.9	2	0.005	0.079	297.9	32.2	$9.98e^{-8}$
DEC – dispersals	–130.8	2	0.012	0.491	265.7	0	0.99

Table 4.2. Most likely ancestral ranges at key nodes in the gavialine phylogeny under the best-fitting model (DEC – dispersals). Ancestral ranges: **C**, Caribbean, **F**, Africa, **I**, India.

DEC – dispersals	**Most likely ancestral range probabilities**
Aktiogavialis spp.	F (0.53)
Aktiogavialis caribesi	C (0.48)
Gavialis	F (0.72)
Gryposuchinae	I (0.48)

CHAPTER 5

Conclusions

This study combined fossil and extant morphological data and integrated phylogenetic and biogeographic methodologies to understand the evolutionary and biogeographic history of gavialids (Eusuchia: Crocodylia) across space and time. The results suggest that gavialids have an origin with a South American signal that can be traced back to the Cretaceous–Paleocene (73–64 Ma), followed by a complex biogeographic history with multiple dispersals during the Cenozoic among Western (the Americas) and Eastern (Africa, Asia, Europe, and India) landmasses. Thus, this study highlights the importance of incorporating fossils in phylogenies and biogeographic studies to understand patterns that are otherwise impossible when using data from extant organisms alone.

In Chapter 2, we describe new material of a small-bodied (~1 m), long-snouted crocodylian collected from the Cretaceous–Paleogene (c.a. 73–64 Ma) El Molino Formation referable to *Dolichochampsa minima*. We incorporated the new specimen into an expanded and modified osteological data matrix, along with other putative oldest gavialid crocodylians from North America ('thoracosaurs') and Africa (*Ocepesuchus eoafricanus*), to test their evolutionary relationships in a phylogenetic context. Our results reveal that *D. minima* is a gavialine, whereas 'thoracosaurs' are recovered outside of Crocodylia, and *O. eoafricanus* is recovered within alligatorids. The phylogenetic position of 'thoracosaurs' and differences in character states to gavialines imply that longirostry evolved independently in both clades. The age and provenance

of *D. minima* has important implications for gavialine origins and paleobiogeography. Its Late Cretaceous to early Paleogene age pulls down the origin of Gavialinae into the Mesozoic (73–64 Ma). Its South American provenance opens the possibility of an origin for Gavialinae on that landmass or elsewhere in Gondwana. Importantly, the occurrence of a Cretaceous–Paleogene gavialine in South America suggests a possible dispersal to Africa and Asia, lending support to the hypothesis that salinity tolerance appeared in early gavialine history, as previously proposed.

In Chapter 3, new material of a large longirostrine crocodylian from the Eocene (c.a., 43–41 Ma) Upper Domanda Formation in Pakistan suggests the presence of gavialines in Asia before the final closure of the Tethys Sea and collision of the Indian plate with Eurasia. Association of the new taxon to offshore, deep marine sediments of the Tethys Sea provides more evidence of saltwater tolerance for early gavialines. Phylogenetic analysis resolves the new taxon as the basalmost member within Gavialinae with strong support values. Based on the distinct combination of morphological features exclusive to the holotype, we have established a new genus and species, *Pelagosuchus pakistanensis*. The new species bears strong affinities to the Miocene–Pliocene assemblage from South America (Gryposuchinae), which provides more evidence of a possible center of origin in Tethys for gryposuchines as previously suggested. The occurrence of gavialines in the Eocene in Indo-Pakistan provides evidence that the group possibly arrived in that region before the closure of the Tethys Sea and the final collision of the Indian plate with Eurasia. After the closure of the Tethys Sea in the Oligocene–Miocene, gavialines possibly became geographically isolated in Western and Eastern landmasses. In Indo-Pakistan, gavialines transition to be restricted to fluvial habitats leading to the current distribution of the extant *Gavialis*, whereas in the Americas, gryposuchines rapidly diversified in the Miocene and declined in diversity in the Pliocene where they became extinct in the Pliocene.

Chapter 4 tested first, the evolutionary relationships of gavialids in a Bayesian framework, and two biogeographical hypotheses (vicariance vs. dispersal) for the distribution of the South American gryposuchines. The result of the Bayesian analysis supports the inclusion of *Dolichochampsa* and the new Pakistani crocodylian within Gavialidae, and 'thoracosaurs' and *Ocepesuchus* outside the group as in parsimony-based studies. Our biogeographic analyses support multiple dispersals starting at the Cretaceous–Paleocene from South America to Africa, Asia, and India. During the Eocene, two independent radiation events occurred: the first from India to South America, and a second from Africa to the Caribbean, giving rise to *Aktiogavialis* and the gryposuchines, respectively. These dispersals were most likely facilitated by the connection of the western and eastern landmasses by the Tethys Sea. Our results also support the independent dispersal of *Aktiogavialis* from the Caribbean to South America during the Oligocene, which coincides with a global sea drop and exposure of land due to regional uplift.

The next steps in understanding the evolutionary and biogeographic history of gavialids involve several key initiatives based on the findings of this study. Further exploration and excavation in South American and African sites, particularly in regions that date back to the Cretaceous–Paleocene, are crucial to uncovering more fossil evidence that can shed light on the early origins and diversification of gavialids. Expanding the osteological data matrix with new and existing fossil specimens from other continents will help refine the phylogenetic relationships within Gavialidae, particularly the position of early forms like *Dolichochampsa minima*, 'thoracosaurs,' and *Ocepesuchus eoafricanus*. Detailed comparisons of morphological features among these early forms and other crocodylian groups will be essential to understand convergent evolutionary traits, such as longirostry. Additionally, integrating molecular data from extant gavialids with fossil data in phylogenetic analyses can provide a more comprehensive

evolutionary timeline. Genetic studies on extant species may reveal evolutionary traits inherited from these ancient ancestors. Investigating the paleoenvironmental conditions that facilitated the early dispersals and radiation events, particularly the role of the Tethys Sea, can offer insights into the biogeographic patterns observed. Further research on the saltwater tolerance of early gavialines, supported by sedimentary analysis of fossil sites, and the application of geochemical studies (Oxygen and Carbon stable isotope analyses) will help clarify the ecological adaptations of these species. The introduction of biogeographic modeling using advanced computational methods can test hypotheses of vicariance versus dispersal in greater detail and will be key for understanding patterns of evolution across space and time.

APPENDIX A

Character Dataset Used in Chapters 2 and 3

Characters 1-46 correspond to Brochu (2011), characters 47-233 correspond to Salas-Gismondi et al. (2019), characters 234-259 correspond to Ristevski et al. (2018), and characters 260-264 are new. Characters or states in bold are new or modifications to the original characters. Characters 15, 20, 21, 30, 80, 83, 98, 99, 107, 110, 136, 170, 193, 191, 199, 209, and 214 were excluded from the parsimony analysis.

1. Ventral tubercle of proatlas: more than one-half the width of the dorsal crest (0); or no more than one-half the width of the dorsal crest (1).
2. Fused proatlas: boomerang-shaped (0); strap-shaped (1); massive and block-shaped (2).
3. Proatlas: with prominent anterior process (0); lacks anterior process (1).
4. Proatlas: has tall dorsal keel (0); lacks tall dorsal keel, dorsal side smooth (1).
5. Atlas intercentrum: wedge-shaped in lateral view, with insignificant parapophyseal processes (0); or plate-shaped in lateral view, with prominent parapophyseal processes at maturity (1).
6. Dorsal margin of atlantal rib: generally smooth with modest dorsal process (0); or with prominent process (1).
7. Atlantal ribs: without (0); or with very thin medial laminae at anterior end (1).
8. Atlantal ribs: lack (0); or possess large articular facets at anterior ends for each other (1).
9. Axial rib tuberculum: wide, with broad dorsal tip (0); or narrow, with acute dorsal tip (1).

10. Axial rib tuberculum: contacts diapophysis late in ontogeny, if at all (0); or early in ontogeny (1).
11. Anterior half of axis neural spine: orientated horizontally (0); or slopes anteriorly (1).
12. Axis neural spine: crested (0); or not crested (1).
13. Posterior half of axis neural spine: wide (0); or narrow (1).
14. Axis neural arch: lacks (0); or possesses a lateral process (diapophysis) (1).
15. Axial hypapophysis: located toward the center of centrum (0); or toward the anterior end of centrum (1).
16. Axial hypapophysis: without (0); or with deep fork (1).
17. Hypapophyseal keels: present on 11th vertebra behind atlas (0); 12th vertebra behind atlas (1); or tenth vertebra behind atlas (2).
18. Third cervical vertebra (first postaxial): with prominent hypapophysis (0); or lacks prominent hypapophysis (1).
19. Neural spine on third cervical long: dorsal tip at least half the length of the centrum without the cotyle (0); or short, dorsal tip acute and less than half the length of the centrum without the cotyle (1).
20. Cervical and anterior dorsal centra: lack (0); or bear deep pits on the ventral surface of the centrum (1).
21. Presacral centra: amphicoelous (0) or procoelous (1).
22. Anterior sacral rib: capitulum projects far anteriorly of tuberculum and is broadly visible in dorsal view (0); or anterior margins of tuberculum and capitulum nearly in same plane, and capitulum largely obscured dorsally (1).

23. Scapular blade: flares dorsally at maturity (0); or sides of scapular blade subparallel; minimal dorsal flare at maturity (1).
24. Deltoid crest of scapula: very thin at maturity, with sharp margin (0); or very wide at maturity, with broad margin (1).
25. Scapulocoracoid synchondrosis: closes very late in ontogeny (0); or relatively early in ontogeny (1).
26. Scapulocoracoid: facet anterior to glenoid fossa uniformly narrow (0); or broad immediately anterior to glenoid fossa, and tapering anteriorly (1).
27. Proximal edge of deltopectoral crest: emerges smoothly from proximal end of humerus and is not obviously concave (0); or emerges abruptly from proximal end of humerus and is obviously concave (1).
28. M. teres major and M. dorsalis scapulae: insert separately on humerus; scars can be distinguished dorsal to deltopectoral crest (0); or insert with common tendon; single insertion scar (1).
29. Olecranon process of ulna: narrow and subangular (0); or wide and rounded (1).
30. Distal extremity of ulna: expanded transversely with respect to long axis of bone; maximum width equivalent to that of proximal extremity (0); or proximal extremity considerably wider than distal extremity (1).
31. Interclavicle flat along length: without dorsoventral flexure (0); or with moderate dorsoventral flexure (1); or with severe dorsoventral flexure (2).
32. Anterior end of interclavicle: flat (0); or rod-like (1).
33. Iliac anterior process: prominent (0); or virtually absent (1).

34. Dorsal margin of iliac blade: rounded with smooth border (0); or rounded, with modest dorsal indentation (1); or rounded, with strong dorsal indentation (wasp-waisted; 2); or narrow, with dorsal indentation (3); or rounded with smooth border; posterior tip of blade very deep (4).
35. Supraacetabular crest: narrow (0); or broad (1).
36. Limb bones: relatively robust, and hindlimb much longer than forelimb at maturity (0); or limb bones very long and slender (1).
37. M. caudofemoralis: with single head (0); or with double head (1).
38. Dorsal osteoderms: not keeled (0); or keeled (1).
39. Dorsal midline osteoderms: rectangular (0); or nearly square (1).
40. Number of contiguous dorsal osteoderms per row at maturity: four (0); six (1); eight (2); or ten (3).
41. Nuchal shield: grades continuously into dorsal shield (0); or differentiated from dorsal shield, four nuchal osteoderms (1); or differentiated from dorsal shield, six nuchal osteoderms with four central and two lateral (2); or differentiated from dorsal shield, eight nuchal osteoderms in two parallel rows (3).
42. Ventral armour: absent (0); or single ventral osteoderms (1); or paired ventral ossifications that suture together (2).
43. Anterior margin of dorsal midline osteoderms: with anterior process (0); or smooth, without process (1).
44. Follicle gland pores on ventral scales: present (0); absent (1).
45. Ventral collar scales: not enlarged relative to other ventral scales (0); or in a single enlarged row (1); or in two parallel enlarged rows (2)

46. Median pelvic keel scales: form two parallel rows along most of tail length (0); or form single row along tail (1); or merge with lateral keel scales (2).

47. Dentary alveoli: alveoli for dentary teeth 3 and 4 nearly same size and confluent (0); **or third and fourth alveolus nearly same size, separated by thin space (1; [NEW]); or fourth alveolus larger than third, and both alveoli are close to each other and clearly apart from neighboring teeth (2; [NEW]);** or fourth alveolus larger than third, and alveoli are separated (**3**). [modified after Brochu, 1999, character 52]

48. Anterior dentary teeth: strongly procumbent (0); or project anterodorsally (1).

49. Mandibular symphysis: extends to fourth or fifth alveolus (0); or sixth to eighth alveolus (1); or ninth to twelfth alveolus (2); or thirteenth to eighteenth (3); or beyond eighteenth (4).

50. Dentary: gently curved between fourth and tenth alveoli (0); or **gently curved posterior to tenth alveolus** (1); or **strongly curved posterior to tenth alveolus (2: [NEW])**. [modified after Brochu, 1999, character 68]

51. Largest dentary alveolus immediately caudal to fourth: is 13 or 14 (0); 11 or 12 (1); no differentiation (2); or behind 14 (3).

52. Splenial: with anterior perforation for mandibular ramus of cranial nerve V (0); or lacks anterior perforation for mandibular ramus of cranial nerve V (1).

53. Mandibular ramus of cranial nerve V: exits splenial anteriorly only (0); or splenial has singular perforation for mandibular ramus of cranial nerve V posteriorly (1); or splenial has double perforation for mandibular ramus of cranial nerve V posteriorly (2).

54. Splenial in mandibular symphysis: present (0); absent (1).

55. Coronoid: bounds posterior half of foramen intermandibularis medius (0); or completely surrounds foramen intermandibularis medius at maturity (1); or obliterates foramen intermandibularis medius (2) at maturity.
56. Superior edge of coronoid: slopes strongly anteriorly (0); or almost horizontal (1).
57. Inferior process of coronoid: laps strongly over inner surface of Meckelian fossa (0); or remains largely on medial surface of mandible (1).
58. Coronoid: imperforate (0); or with perforation posterior to foramen intermandibularis medius (1).
59. Process of splenial: separates angular and coronoid (0); or no splenial process between angular and coronoid (1).
60. Angular–surangular suture: contacts external mandibular fenestra at posterodorsal margin at maturity (0); or passes broadly along ventral margin of external mandibular fenestra (long descending process of the surangular visible in lateral view) late in ontogeny (1).
61. Anterior processes of surangular: unequal, little or no ventral process (0); or subequal to equal, well development ventral process (1).
62. Surangular: with spur bordering the dentary tooth row lingually for at least one alveolus length (0); or lacking such spur (1).
63. External mandibular fenestra: absent (0); or present (1).
64. Surangular–dentary suture: intersects external mandibular fenestra anterior to posterodorsal corner (0), or at posterodorsal corner (1).
65. Angular: extends dorsally toward or beyond anterior end of foramen intermandibularis caudalis; anterior tip acute (0); or, does not extend dorsally beyond anterior end of foramen intermandibularis caudalis; anterior tip very blunt (1).

66. Surangular–angular suture lingually meets articular: at ventral tip (0); or dorsal to tip (1).
67. Surangular: continues to dorsal tip of lateral wall of glenoid fossa (0); or truncated and not continuing dorsally (1).
68. Articular–surangular suture: simple (0); or articular bears anterior lamina dorsal to lingual foramen (1); or articular bears anterior lamina ventral to lingual foramen (2); or bears laminae above and below foramen (3).
69. Lingual foramen for articular artery and alveolar nerve: perforates surangular entirely (0); or perforates surangular-articular suture (1).
70. Foramen aerum: at extreme lingual margin of retroarticular process (0); or set in from margin of retroarticular process (1).
71. Retroarticular process: projects posteriorly (0); projects posterodorsally (1).
72. Surangular: extends to posterior end of retroarticular process (0); or pinched off anterior to tip of retroarticular process (1).
73. Surangular–articular suture: orientated anteroposteriorly (0); or bowed strongly laterally within glenoid fossa (1).
74. Articular-surangular sulcus: sulcus between articular and surangular (0); or articular flush against surangular within the adductor fossa (1).
75. Dorsal projection of hyoid cornu: flat (0); or rod-like (1).
76. Dorsal projection of hyoid cornu: narrow, with parallel sides (0); or flared (1).
77. Lingual osmoregulatory pores: small (0); or large (1).
78. Tongue with keratinized surface: present (0); or absent (1).
79. Teeth and alveoli of maxilla and/or dentary: circular in cross-section (0); or posterior teeth laterally compressed (1); or all teeth compressed (2).

80. Maxillary and dentary teeth: with smooth carinae (0); or serrated (1); or with neither carinae nor serrations (2).
81. Naris: projects anterodorsally (0); or dorsally (1).
82. External naris: bisected by nasals (0); or nasals and nasal spine contact external naris and form posterior margin, but do not bisect it (1); or only nasal spine contacts external naris (2); or nasals excluded, at least externally, from naris; nasals and premaxillae still in contact (3); or nasals and premaxillae not in contact (4).
83. Naris: longer than wide (0); or wider than long (1).
84. External naris of reproductively mature males: remains similar to that of females (0); or develops bony excrescence (ghara) (1).
85. External naris: opens flush with dorsal surface of premaxillae (0); or circumscribed by a crest (1). [Brochu, 1999, character 85]
86. Premaxillary surface lateral to naris: smooth (0); or with deep notch lateral to naris (1).
87. Number of premaxillary teeth: five teeth (0); or four teeth early in posthatching ontogeny (1).
88. Major transversal diameter of the incisive foramen: smaller than or equal to the diameter of the first premaxillary alveolus (0); between one and two times the diameter (1); or equal to or more than 2 times the diameter of the first premaxillary alveolus (2).
89. Incisive foramen: completely situated far from premaxillary tooth row, at the level of the second or third alveolus (0); or abuts premaxillary tooth row (1); or projects between first premaxillary teeth (2).
90. Dorsal premaxillary processes: short, not extending beyond third maxillary alveolus (0); or long, extending beyond third maxillary alveolus (1).

91. Dentary tooth 4: occludes in notch between premaxilla and maxilla early in ontogeny (0); or occludes in a pit between premaxilla and maxilla, no notch early in ontogeny (1).
92. Dentary teeth (all): occlude lingual to maxillary teeth (0); or occlusion pit between seventh and eighth maxillary teeth; all other dentary teeth occlude lingually (1); or dentary teeth occlude in line with maxillary tooth row (2).
93. Largest maxillary alveolus: is no. 3 (0); or no. 5 (1); or no. 4 (2); or nos. 4 and 5 are same size (3); or no. 6 (4); or maxillary teeth homodont (5); or maxillary alveoli gradually increase in diameter posteriorly toward penultimate alveolus (6); or maxillary alveoli gradually increase in diameter posteriorly with two enlarged alveoli at mid/anterior of rostrum (7); **pseudo-homodont, some teeth variation (8; [NEW])**. [modified after Salas-Gismondi et al., 2022; character 93]
94. Maxillary toothrow posterior to first six maxillary alveoli: curved medially or linear (0); or curves laterally broadly (1).
95. Dorsal surface of rostrum: curves smoothly (0); or bears medial dorsal boss (1); **or it is generally straight, fitting the skull table (2: [NEW]); or it is mostly straight and curves dorsally before reaching the orbits (3; [NEW])**. [modified after Brochu, 1999; character 101]
96. Anterolaterally directed ridges (*sensu* Rio et al. 2021): absent (0); or present (1).
97. Preorbital ridges: absent or very modest (0); or very prominent at maturity (1).
98. Antorbital fenestra: present (0); or absent (1).
99. Vomer: entirely obscured by premaxilla and maxilla (0); or exposed on palate at premaxillary-maxillary suture (1).

100. Vomer: entirely obscured by maxillae and palatines (0); or exposed on palate between palatines (1).

101. Surface of maxilla within narial canal: imperforate (0); or with a linear array of pits (1).

102. Medial jugal foramen: small (0); or very large (1).

103. Maxillary foramen for palatine ramus of cranial nerve V: small or not present (0); or very large (1).

104. Ectopterygoid: abuts maxillary tooth row (0); or maxilla broadly separates ectopterygoid from maxillary tooth row (1).

105. Maxilla: terminates in palatal view anterior to lower temporal bar (0); or comprises part of the lower temporal bar (1).

106. Penultimate maxillary alveolus: less than twice the diameter of the last maxillary alveolus (0); or more than twice the diameter of the last maxillary alveolus (1).

107. Prefrontal dorsal surface: smooth adjacent to orbital rim (0); or bearing discrete knob-like processes (1).

108. Dorsal half of prefrontal pillar: narrow (0); or expanded anteroposteriorly (1).

109. Medial process of prefrontal pillar: expanded dorsoventrally (0); or expanded anteroposteriorly (1).

110. Prefrontal pillar: solid (0); or with large pneumatic recess (1).

111. Medial process of prefrontal pillar: wide (0); or constricted at base (1).

112. Maxilla: has linear medial margin adjacent to suborbital fenestra (0); or bears broad shelf extending into fenestra, making lateral margin concave (1).

113. Anterior face of palatine process: rounded or pointed anteriorly (0); or notched anteriorly (1).

114. Anterior ectopterygoid process: tapers to a point (0); or forked (1).

115. Palatine process: extends significantly beyond anterior end of suborbital fenestra (0); or does not extend beyond anterior end of suborbital fenestra (1).

116. Palatine process: generally broad anteriorly (0); **or palatines send two processes that are parallel to each other (1: [NEW]); or palatines send two processes that converged anteriorly, forming a V-shaped suture with the maxilla, process does not extend beyond third maxillary alveolus that is anterior to suborbital fenestra (2) [NEW]; palatine send two processes that converged anteriorly, forming a V-shaped suture with the maxilla, process extends beyond third maxillary alveolus that is anterior to suborbital fenestra (3) [NEW].** [modofied after Salas-Gismondi et al., 2022; character 116]

117. Lateral edges of palatines: smooth anteriorly (0); or with lateral process projecting from palatines into suborbital fenestrae (1).

118. Palatine–pterygoid suture: nearly at the posterior level of suborbital fenestrae (0); or far anteriorly from posterior angle of suborbital fenestra (1); or extends posterolaterally, behind the suborbital fenestra (2).

119. Pterygoid ramus of ectopterygoids: convex, posterolateral margin of suborbital fenestra with a concavity (0); or ramus roughly lineal, no concavity at the posterolateral margin of fenestra (1).

120. Lateral edges of palatines: parallel posteriorly (0); or flare posteriorly, producing shelf (1).

121. Anterior border of the choana: **situated anterior to middle part within the pterygoids (0: [NEW]); or choana extends to the anterior and posterior ends of the pterygoids (1: [NEW]); or choana is at the posteriormost side of the pterygoids (2: [NEW]).** [modified after Salas-Gismondi et al., 2022; character 121]

122. Projection of choana at maturity: projects posteroventrally (0); or anteroventrally (1).

123. Pterygoid surface surrounding internal choana: slightly depressed or flush with the choanal margins (0); or choanal margin completely surrounded by a neck (1); or choana surrounded posteriorly by a ridge (2).

124. Posterior rim of internal choana: not deeply notched (0); or deeply notched (1).

125. Internal choana: not septate (0); or with septum that remains recessed within choana (1); or with septum that projects out of choana (2).

126. Ectopterygoid–pterygoid flexure: disappears during ontogeny (0); or remains throughout ontogeny (1).

127. Ectopterygoid: extends to posterior tip of lateral pterygoid flange at maturity (0), or does not extend (1).

128. Posterior process of maxilla: no posterior process of maxilla within lacrimal or within lacrimal and prefrontal (0); or maxilla with posterior process within lacrimal (1); or maxilla with posterior process between lacrimal and prefrontal (2).

129. Prefrontals: separated by the frontal and nasals, anterior process of frontal extending far anterior to the anterior margin of the orbit equivalent or more than the length of the prefrontal in the orbit (0); or prefrontals separated by the frontal and nasals, anterior process of frontal around the same level or posterior to the anterior margin of the orbit (1); or prefrontals meet medially, anterior process of frontal around the same level or posterior to the anterior margin of the orbit (2).

130. Lacrimal: longer than prefrontal (0); or prefrontal longer than lacrimal (1); or lacrimal and prefrontal both elongate and nearly the same length (2).

131. Anterior tip of frontal: forms simple acute point (0); or forms broad, complex sutural contact either with the nasals or prefrontals (1).

132. Ectopterygoid: extends along medial face of postorbital bar (0); or stops abruptly ventral to postorbital bar (1).

133. Postorbital bar: massive (i.e. anteroposteriorly elongated) (0); or slender (i.e. circular in cross section) (1).

134. Postorbital bar: bears process that is prominent, dorsoventrally broad, and divisible into two spines (0); or bears process that is short and generally not prominent (1).

135. Ventral margin of postorbital bar: flush with lateral jugal surface (0); or inset from lateral jugal surface (1).

136. Postorbital bar: continuous with anterolateral edge of skull table (0), or inset (1).

137. Dorsal margin of orbit: flush with skull surface (0); or dorsal edges of orbits upturned (1); or dorsal and posterior edges upturned (2).

138. Ventral margin of the orbit: gently circular (0); or with a prominent notch (1).

139. Palpebral: forms from single ossification (0); or from multiple ossifications (1).

140. Quadratojugal spine: prominent at maturity (0) or greatly reduced **(1)**; or absent at maturity (**2**). [modified after Salas-Gismondi et al., 2022; character 140]

141. Quadratojugal spine: low, near posterior angle of infratemporal fenestra (0); or high, between posterior and superior angles of infratemporal fenestra (1).

142. Quadratojugal: forms posterior angle of infratemporal fenestra (0); jugal forms posterior angle of infratemporal fenestra (1); or quadratojugal–jugal suture lies at posterior angle of infratemporal fenestra (2).

143. Postorbital: neither contacts quadrate nor quadratojugal medially (0); or contacts quadratojugal, but not quadrate, medially (1); or contacts quadrate and quadratojugal at dorsal angle of infratemporal fenestra (2); or contacts quadratojugal with significant descending process (3).

144. Quadratojugal: bears long anterior process along lower temporal bar (0); or bears modest process, or none at all, along lower temporal bar (1).

145. Quadratojugal: extends to superior angle of infratemporal fenestra (0); or does not extend to superior angle of infratemporal fenestra; quadrate participates in fenestra (1).

146. Postorbital–squamosal suture: orientated ventrally (0); or passes medially ventral to skull table (1).

147. Dorsal and ventral rims of squamosal groove for external ear valve musculature: parallel (0); or squamosal groove flares anteriorly (1).

148. Squamosal–quadrate suture: extends dorsally along posterior margin of external auditory meatus (0); or extends only to posteroventral corner of external auditory meatus (1).

149. Posterior margin of otic aperture: smooth (0); or bowed (1).

150. Frontoparietal suture: deeply within supratemporal fenestra; frontal prevents broad contact between postorbital and parietal (0); or suture on skull table **U-shaped**, postorbital and parietal in broad contact (1); **or suture on skull table straight or complex, postorbital and parietal in broad contact (2; [NEW])**. [modified after Salas-Gismondi et al., 2022]

151. **Fronto-postorbital suture: is straight, posterior border of frontal being rectangular (0)**, **or suture diverge anteriorly (1); or convergent anteriorly (2)**. **[NEW character] Original character from Salas-Gismondi et al., (2022) was incorporated within character 150]**

152. Supratemporal fenestra with fossa: dermal bones of skull roof do not overhang rim at maturity (0); or dermal bones of skull roof overhang rim of supratemporal fenestra near maturity, small fenestrae (1); or supratemporal fenestra closes during ontogeny (2); or parietal is sharp-rimmed, overhanging anteriorly and medially the supratemporal fenestra, large fenestrae (3).

153. Shallow fossa anterior to the supratemporal fenestra: present (0); or no such fossa; skull table smooth anterior to supratemporal fenestra (1).

154. Medial parietal wall of supratemporal fenestra: imperforate (0); or bearing foramina (1).

155. Supratemporal fenestra, posterior wall: Parietal and squamosal widely separated by quadrate on posterior wall of supratemporal fenestra (0); or parietal and squamosal approach each other on posterior wall of supratemporal fenestra without actually making contact (1); parietal and squamosal meet along posterior wall of supratemporal fenestra (2).

156. Skull table surface: slopes ventrally in occipital view (0); or planar at maturity (1).

157. Squamosal on skull table late in ontogeny: horizontal or nearly so (0); or upturned to form a posterolateral discrete horn (1); or producing a high transversely oriented eminence at the posterior margin (2).

158. Mature skull table: with broad curvature; short posterolateral squamosal rami along paroccipital process (0); or with nearly straight sides; significant posterolateral squamosal rami along paroccipital process (1); or with nearly straight sides; posterolateral squamosal processes form long “prongs” (2).

159. Squamosal: does not extend to lateral extent of paroccipital process (0); or extends ventrolaterally to lateral extent of paraoccipital process (1).

160. Supraoccipital exposure on dorsal skull table: small (0); or points posteriorly to the caudal margin of the parietal (1); or absent (2); or large (but parietals still in posterior border) (3), or large such that parietal is excluded from posterior edge of table (4).

161. Anterior foramen for palatine ramus of cranial nerve VII: ventrolateral to basisphenoid rostrum (0); or ventral to basisphenoid rostrum (1).

162. Sulcus on anterior braincase wall lateral to basisphenoid rostrum: present (0); or braincase wall lateral to basisphenoid rostrum smooth, no sulcus (1).

163. Basisphenoid: not exposed extensively on braincase wall anterior to trigeminal foramen (0); or exposed extensively on braincase wall anterior to trigeminal foramen (1).

164. Exposure of prootic: extensive exposure of prootic on external braincase wall (0), or prootic largely obscured by quadrate and laterosphenoid externally (1).

165. Laterosphenoid bridge: comprised entirely of laterosphenoid (0); or with ascending process of palatine (1).

166. Capitate process of laterosphenoid: orientated laterally (0); or anteroposteriorly toward midline (1).

167. Parietal: with recess communicating with pneumatic system (0); or solid without recess (1).

168. Quadrate process: significant ventral quadrate process on lateral braincase wall (0); or quadrate–pterygoid suture linear from basisphenoid exposure to trigeminal foramen (1).

169. Lateral carotid foramen: opens lateral (0); or dorsal to basisphenoid at maturity (1).

170. Orientation of external surface of basioccipital ventral to occipital condyle at maturity: oriented posteroventrally (0); or posteriorly (1).

171. Posterior pterygoid processes: tall and prominent (0); or small and project posteroventrally (1); or small and project posteriorly (2).

172. Basisphenoid: thin (0); or anteroposteriorly wide ventral to basioccipital (1).

173. When basioccipital tuberae is higher than the pterygoid in front of it: basisphenoid and pterygoid not exposed ventral to basioccipital (0); or basisphenoid briefly exposed ventral to basioccipital at maturity; pterygoid short ventral to median eustachian opening (1); or basisphenoid exposed as broad sheet ventral to basioccipital at maturity; pterygoid tall ventral to median eustachian opening (2).

174. Exoccipital: with very prominent boss on paroccipital process; process lateral to cranioquadrate opening short (0); or exoccipital with small or no boss on paroccipital process; process lateral to cranioquadrate opening long (1).

175. Lateral eustachian canals: open dorsal (0); or lateral to medial eustachian canal (1).

176. Exoccipitals: terminate dorsal to basiccipital tubera (0); or send a process ventrally to the basioccipital tubera (1).

177. Quadrate foramen aerum: on mediodorsal angle (0); or on dorsal surface of quadrate (1).

178. Quadrate foramen aerum at maturity: small (0); or comparatively large (1); or absent (2).

179. Quadrate: lacks (0); or bears prominent, mediolaterally thin crest on dorsal surface of ramus (1).

180. Attachment scar for posterior mandibular adductor muscle on ventral surface of quadrate ramus: forms modest crests (0); or prominent knob (1).

181. Quadrate: with small ventrally reflected medial hemicondyle (0); or with small medial hemicondyle; dorsal notch for foramen aerum (1); or with prominent dorsal projection between hemicondyles (2); or with expanded medial hemicondyle (3); or more detached, ventromedially projected medial hemicondyle (4).

182. Edge of the maxillary tooth alveoli: lower or at the same level than the space between toothrow (0); or edge of maxillary tooth alveoli higher than the space between toothrow (toothrow underlined) (1).

183. Ventral border of exoccipital: convex and ventrally projected, hiding the posterior opening of the cranioquadrate passage from the occipital view (0); or straight, sharpen or smoothly convex and does not hide the posterior opening of the cranioquadrate passage from the occipital view (1).

184. Occipital surface: vertical or not visible in dorsal view (0); sloped, visible in dorsal view (1). [Character states were reversed]

185. Ventral premaxillary-maxillary suture: is mainly transversal to W-shaped (0); **or wide U-shaped (1; [NEW]); or wide V-shaped (2; [NEW]); or straight to transversal (3; [NEW]); or W-shaped and transversal at the midline (4; [NEW]);** or acute, posterior V-shaped suture **extending to the third maxillary alveolus (5); or acute, posterior V-shaped suture extending beyond the third maxillary alveolus (6; [NEW]); or W-shaped with long processes (see *Argochampsa krebsi*) (7; [NEW]); or short V-shaped suture not extending beyond the second maxillary alveolus (8; [NEW]); or complex suture (see *Maomingosuchus petrolica*) (9; [NEW]).** [modified after Salas-Gismondi et al., 2022; character 185]

186. Number of maxillary teeth: less than 18 teeth (0); 18 to 22 teeth (1); or more than 22 teeth (2).

187. Maximum lateral extension of skull table at maturity in dorsal view: situated around the same level (0); or medially to the lateral margin of the quadrate condyle (1).

188. Process of frontal: ends at the same level or posterior to the anterior extension of the prefrontal (0); or extends well anterior, **frontal process significantly long, more than the length of the frontal plate (1); or extends well anterior, frontal process is short (2) [NEW].** [modified after Salas-Gismondi et al., 2022; character 188]

189. Maxilla posterior process in ventral view: without tooth, short or absent (0); or long, longer to the distance between the three last teeth (1).

190. Interorbital bridge late in ontogeny: narrower to equivalent (0); or broader than the width of the orbit late in ontogeny (1).

191. Supratemporal fenestra at maturity: longer than wide, rounded (0); or quadrangular, wider than long (1).

192. Medial crest on the basioccipital: present (0); or absent (1).

193. Posterior dentary process between splenial and angular on the ventral side: absent (0); or present (1).

194. Dorsal margin of the surangular behind the postglenoid crest in lateral view: higher or equal (0), or lower than the surangular immediately anterior the postglenoid crest (1).

195. Orbit: posterior margin of the orbit anterior to the posterior margin of the suborbital fenestra (0); or posterior or at the same level than the posterior margin of the suborbital fenestra (1). [character measured at the level of the postorbital-frontal suture in the orbital margin]

196. Basioccipìtal-exoccipital process ventral to occipital condyle (basioccipital plate) in posterior view: with parallel or ventrally convergent sides (0); or ventrally divergent sides (1).

197. Smooth medial depression ventral to the basioccipital and posterior to the medial Eustachian foramen: absent (0); or present (1).

198. Dentary teeth series behind to alveoli 12-13: pointed to slightly blunt (0); or globular (1); or molariform multicusped (2).

199. First four alveoli in the dentary: are the same size or smaller than other dentary alveoli (0); or are the largest within the dentary (1).

200. Orbits late in ontogeny: longer than wide (0); or wider than long to rounded (1).

201. From the series composed by the three most posterior premaxillary alveoli: the intermediate alveolus is the biggest (0); or anterior and intermediate alveoli are bigger, similar in size (1); or the anterior alveolus is the biggest (2).

202. Frontal plate surface: well ornamented with deep pits and furrows (0); or surface only little sculpted to smooth (1).

203. Retroarticular longitudinal crest: absent (0); or present (1).

204. Infratemporal fenestra: bears an acute to straight dorsal angle, triangular shaped ITF (0); or its dorsal margin forms a gentle curve, not an angle, ovoid-shaped ITF (1).

205. Posterior bar of supratemporal fenestra (i.e., post-temporal bar): thick, equal or wider than the intertemporal bridge (0); thinner than the intertemporal bridge, flat dorsal surface (1); or thinner than the intertemporal bridge, convex dorsal surface (2).

206. Differentiated pterygoid bullae: absent (0); or presence (1).

207. Anterior diameter of skull table late in ontogeny: smaller than posterior diameter of skull table (0); or posterior skull table transversally constricted (1).

208. Orientation of the supratemporal fenestrae and post-temporal bar: Non-oblique (0); or oblique (1).

209. Choana: roughly circular in outline (0); or wider than long, straight transversal anterior margin (1).

210. Lateral jugal surface adjacent to the orbit: not perforated by multiple minute foramina (0); or perforated by one or two conspicuous, large foramina (2).

211. When splenial participates in mandibular symphysis: splenial constricted and forms narrow V within the symphysis, from its tip and along five alveoli (0); **or splenial forms a narrow V within the symphysis, from its tip and along less than five alveoli (1: [NEW]);** or splenial forms wide V **and extending beyond the sixth alveolus** (2); **or splenial constricted and forming a narrow V, extending beyond the sixth alveolus (3: [NEW])**. [modified after Salas-Gismondi et al., 2022; character 211]

212. Palatal surface of the maxillae in front of the suborbital fenestra: smooth or pierced by a posteriorly oriented foramen (0); or pierced by an oblique, anterolaterally oriented foramen (1) (possibly, a posterior palatal branch of the cranial nerve V).

213. Postoccipital processes: relatively close to each other (0); or widely separated (1).

214. When ventral premaxillary-maxillary suture acute V-shaped posteriorly: this suture does not exceed (0); or exceeds the second maxillary alveoli (1).

215. Palatine-maxillary suture: intersects suborbital fenestra at its anteromedial margin, maxilla sends a posterior process that exceeds the anterior margin of the suborbital fenestra (0); or intersects the suborbital fenestra nearly at its anteriormost limit, and no posterior maxillary process (1).

216. Number of teeth along the suborbital fenestrae: at least six teeth (0); or less (1).

217. Dentary, dorsoventral height at the level of alveoli 1-4 relative to alveoli 11-12: at the same level or higher (0); lower (1).

218. When splenial in symphysis: adjacent to no more than two dentary alveoli (0), between three and seven (1); or more than seven dentary alveoli (2).

219. When splenial excluded from symphysis: anterior tip of splenial passes ventral (0); or dorsal (1) to Meckelian groove.

220. Dentary, acute posterior process in the angular ventral to the external mandibular fenestra: present (0); absent (1).

221. Dentary, position of the acute posterior process in the angular ventral to the external mandibular fenestra: within the angular, no bordering the EMF (0); dorsal to angular, bordering the EMF (1).

222. Rostral ornamentation: canthi rostralii (*sensu* Rio & Manion, 2021; character 27): absent (0); present (1).

223. Rostral ornamentation: transverse ridge between the orbits (i.e. spectacle): absent (0); present (1).

224. Rostral ornamentation, anterior extent of the transverse ridge between the orbits (i.e. spectacle): posterior or level with the anterior orbital margin (0); anterior to anterior orbital margin (1).

225. Ratio of the intertemporal (parietal) bar width relative to the STF width: less than 0.3 (0); equal or more than 0.3 (1).

226. Long squamosal prongs (when these projections represent at least half of the length of the skull table): descend posteriorly from the skull table (0); at the same level as the skull table (1).

227. Medial posterior margin of the skull table (between STF) in dorsal view: roughly straight (0); or concave (1); or convex (2).

228. Naris: perimeter of roughly equivalent anterior and posterior shape (0); teardrop-shaped, more acute posteriorly (1).

229. Long ventral process of the exoccipitals: slender (0); anteroposteriorly wide (1).

230. Basioccipital tuberae: higher than the posterior border of the pterygoids (0); or lower than the posterior border of the pterygoids at the longitudinal axis (1).

231. When skull table surface slopes ventrally: dorsal profile lineal to roughly concave in occipital view, medial portion (i.e., supraoccipital) raised (0); skull table slopes ventrally from about the parietal-squamosal suture, roughly convex outline in occipital view, medial portion not raised (1).

232. When the EMF present: slit-like (0); large (1); or very large, most of foramen intermandibularis caudalis visible in lateral view (2).

233. Supratemporal fenestra, posterior wall: squamosal-parietal suture passes medially to the orbitotemporal foramen, little to no development of fossa medial to orbitotemporal foramen (0); squamosal-parietal suture intersects dorsal margin of orbitotemporal foramen or fossa, large medial fossa (1).

234. Rostrum, length relative to the total skull length: brevirostrine, rostrum length no more than **60%** of the total length (0); mesorostrine, rostrum length shorter than 67% of the total length (1); sublongirostrine, rostrum length longer than 67% of the total length, but not longer than 70% (2); longirostrine, rostrum length longer than 70% of the total length (3); **hyper-longirostrine, rostrum length equal or longer than 80% of the total skull length (4: [NEW])**. [modified after Ristevski et al., 2018; character 5]

235. Rostrum, relation with the skull at maturity, in dorsal view: rostrum well defined, broadening abruptly at orbits (0); rostrum poorly defined, smoothly broadening and fitting the skull at orbits (1). [modified after Ristevski et al., 2018; character 8]

236. Maxilla, projection of ventral margin in lateral view: ventral maxillary margin is straight (0); ventral maxillary margin festooned, being convex and concave at locations, assuming a sinusoidal profile (1); ventral maxillary margin is overall convex, from contact with premaxilla to contact with jugal (2). [Ristevski et al., 2018; character 80]

237. **Maxilla, projection of ventral margin in dorsal view: maxilla expands laterally in locations (coincident with festooning waves, when present), with maxilla sinusoidal (0); maxilla has a concave profile, expanded posterolaterally to fit the jugal and maxilla retain a subparallel orientation across most of its rostrum (1); maxilla is subparallel, fitting the premaxilla and jugal (2); maxilla has a convergent profile posteriorly, at mid rostrum it becomes subparallel (3); maxilla expands laterally in locations (coincident with festooning waves, when present), with maxilla gently sinusoidal (4); maxilla has a convergent profile anteroposteriorly, at mid rostrum it becomes subparallel (5); maxilla is mostly parallel, expanding laterally just anterior to orbits (6).** [modified after Ristevski et al., 2018; character 81]

238. Maxilla, number of waves, when festooning is present: a single clearly identifiable wave is present, at the anterior section of the maxilla, with ventral maxillary margin poorly sinusoidal (0); two major waves clearly identifiable, separated by an evident concave area, with ventral maxillary margin strongly sinusoidal and a corresponding dorsally directed wave on the dorsal edge of the dentary (1). [Ristevski et al., 2018; character 82]

239. Maxilla, lateral exposure of occlusal pit for the 11^{th} dentary tooth, at maturity: not exposed laterally, dentitions may overbite or interlock, but lateral wall of occlusal pit is closed (0); laterally open, with occlusal surface exposed as a shallow notch (1). [Ristevski et al., 2018; character 83]

240. Maxilla, presence of multiple cecal recesses at the surface within narial canal: absent, surface imperforate (0); present (1). [Ristevski et al., 2018; character 85]

241. Supratemporal fenestra, size proportional to the orbit at maturity: clearly smaller than the orbit (0); fenestra subequal to the orbit (1); supratemporal fenestra larger than orbit (2). [Ristevski et al., 2018; character 106]

242. Supratemporal fossa, size proportional to the orbit at maturity: clearly smaller than the orbit, or fossa closed by skull table elements (0); fossa subequal to the orbit (1); supratemporal fossa larger than orbit (2). [Ristevski et al., 2018; character 107]

243. Supratemporal fossa, presence of main axis: main axis indistinct, or poorly distinct (0); main axis evident and much longer than secondary axis (1). [Ristevski et al., 2018; character 109]

244. Supratemporal fossa, orientation of main axis late in ontogeny: both axes diverge anteriorly (0); both axes parallel (1); both axes converge anteriorly (2). [Ristevski et al., 2018; character 110]

245. Supratemporal fossa, overall shape: elliptic (0); square-shaped to subrectangular (1); **triangle-shaped (2: [NEW])**; circular (3); **pentagonal-shaped (4: [NEW])**; **teardrop-shaped, mostly elliptical (5: [NEW]); teardrop-shaped, mostly circular (6: [NEW])**. [Ristevski et al., 2018; character 111]

246. Skull roof, alignment of parietal, frontal, and nasals in a teep angle: absent (0); present (1). [Ristevski et al., 2018; character 116]

247. Frontal, proportional width of main body (between orbits) relative to width of the supratemporal skull roof at maturity: narrow, usually 20-30% of the width of the skull roof

(0); wide, usually 40-50% of the width of the skull roof (1). [Ristevski et al., 2018; character 134]

248. Parietal, morphology of the medial surface at maturity: broad throughout, with a wide sculpted region separating fossae (**width similar to temporal bar, squamosal-postorbital**) (0); narrow, **less the width of temporal bar** (1). [modified after Ristevski et al., 2018; character 145]

249. Upper temporal bars, orientation in dorsal view: temporal bars mostly parallel, giving the skull roof a rectangular outline (0); temporal bars oblique and anteriorly convergent, giving the skull roof a trapezoidal outline in dorsal view (1); **temporal bars oblique and anteriorly diverging (2: [NEW]); temporal bars sinusoidal (3: [NEW]); posterior temporal bars parallel or oblique (squamosal), but anterior temporal bar (postorbital) expand laterally (4: [NEW]).** [modified after Ristevski et al., 2018; character 148]

250. Orbits, orientation in dorsal view (not considering palpebrals): orbits fully lateral (0); orbits face dorsolaterally (1); orbits with a strong dorsal component (2). [Ristevski et al., 2018; character 157]

251. Choana, shape in palatal view: subcircular, elliptic or lanceolated (0); triangle-shaped (1); rectangular (slit-like) (2); V-shaped or reversed triangle (3); butterfly-shpaed (4); **square-shaped (5: [NEW])**. [modified after Ristevski et al., 2018; character 239]

252. Choana, general morphology: choana wider than long (0); length and width subequal (1); choana longer than wide (2). [Ristevski et al., 2018; character 240]

253. Pterygoid ventral rami (wings), orientation in lateral view: poorly to mildly inclined, no more than 45 degrees (0); strongly verticalized, 50 degrees or more relative to the horizontal. plane (1). [Ristevski et al., 2018; character 264]

254. Basioccipital, presence of basal tubera: absent (0); tubera present, large and pendulous (1). [Ristevski et al., 2018; character 288]

255. Mandible, overall morphology in dorsal view: mandible is narrow, hemimandibles are confluent, with left and right alveolar margins running alongside each other (0); mandible is broad, hemimandibles are mostly parallel, but alveolar margins meet medially at first alveolus forming a wide arched line, giving the mandible a broad-U shape (1). [Ristevski et al., 2018; character 319]

256. Mandible, orientation of hemimandibles at their medial contact: Hemimandibles meet at approximately 45 degrees of each other, **hemimandibles strongly diverged** (0); **Evidently acute angle, hemimandibles meet at an angle less than 45 degrees and gradually meet at the symphysis (1: [NEW])**; broad angle, hemimandibles meet at approximately 70 degrees of each other, or more (2). [Ristevski et al., 2018; character 320]

257. Symphysis, morphology of anterior end: symphysis tapers anteriorly, with no constriction at mid-posterior sections (0); symphysis clearly constricted at fifth-sixth alveoli (1); symphysis flares anteriorly, with anterior region bearing teeth 1-4 at anterior margin and posterior region narrower (but constriction poorly defined) (2); symphysis flares anteriorly, with anterior region bearing teeth 1-2 at anterior margin and posterior region narrower (but constriction poorly defined) (3). [Ristevski et al., 2018; character 333]

258. Symphyseal alveoli 3-4, relative position: tooth 3 medial to tooth 4 (0); tooth 3 anteromedial to tooth 4 (1); teeth 3-4 set in tandem (2); tooth 4 lateral to tooth 3 (3); **tooth 3 lateral to tooth 4 (4: [NEW])**. [modified after Ristevski et al., 2018; character 405]

259. Symphyseal alveolus 2, relative position: not in line with alveoli 3-4 and closer to the medial line (0); in line with alveoli 3-4, as close as these to the medial line (1); not in line with alveoli 3-4, at a more lateral position (2). [Ristevski et al., 2018; character 407]

260. Medial margin of orbit with respect to supratemporal fenestra: medial margin of orbit at the same level of medial margin of supratemporal fenestra (0); medial margin of orbit near the level of the center of the supratemporal fenestra (1); medial margin of orbit near the level of the lateral margin of the supratemporal fenestra (2). [new character]

261. Arrangement of dentary alveoli along toothrow: spaced between alveoli is relatively constant, and space is less than the diameter of the teeth, with posterior teeth being closer than anterior teeth (0); most alveoli are in tight contact across the toothrow (1); Space between alveoli is inconsistent (2); alveoli arranged in couplets, space between alveoli not constant across the dentary (3); space between alveoli is similar in length of alveolar diameter and space decreased posteriorly (4); space between alveoli is similar in length of alveolar diameter and constant across the dentary, but the third and fourth alveoli are well-separated from the neighboring teeth by a diastema and nearly confluent (sensu Brochu, 2004) (5); space between alveoli is similar in length of alveolar diameter and mostly constant across the dentary (6). [new character]

262. Nasals, relative width: Nasals truncated at the middle but retaining similar width anterior and posterior (0); Nasals constricted anteriorly, being thinner than the posterior end (1); Nasals retained most of their width anteroposteriorly, gradually decreasing in width anteriorly (2). [new character]

263. Length of dentary symphysis relative to the total length of lower jaw: Symphysis is small (0); Symphysis closer to one-third of the total length (1); Symphysis is subequal to the half of the total length (2); Symphysis forms more than half of the total length (3). [new character]

264. Absence of presence of a prefrontal step (*sensu* Delfino et al., 2005): absent (0); present (1). [new character]

265. Width of palatines compared to the width of suborbital fenestra: palatines width is thin or subequal to the width of suborbital fenestra, and lateral margins are parallel or subparallel (0); or palatines is thin or subequal to the width of the suborbital fenestra, and anterior lateral walls expand laterally (1); or palatines width is thicker than the width of the suborbital fenestra, lateral side of palatine expands anteriorly (2); palatines width is thicker than the width of the suborbital fenestra, lateral side of palatines are subparallel to parallel (3); palatines are subequal to the suborbital fenestra, and constricted at the midline (4); palatines width is subequal to suborbital fenestra, lateral margins of palatines are sinusoidal (5). [new character]

APPENDIX B

List of Specimens Observed

List of additional specimens observed in this dissertation. Abbreviations: UF, University of Florida, UMMZ, University of Michigan Museum of Zoology.

1. *Alligator mississippiensis* – UF 43151
2. *Alligator sinensis* – UF 105540, 67829
3. *Acherontisuchus guajiraensis* – UF/IGM 34 (holotype), UF/IGM 35
4. *Caiman crocodilus* – UF 80934
5. *Caiman yacare* – UF 121263
6. *Crocodylus acutus* – UF 151167
7. *Crocodylus novaeguineae* – UF 71780
8. *Crocodylus porosus* – UF 71779
9. *Crocodylus siamensis* – UF 71182
10. *Dadagavialis gunai* (Holotype) – UF 312850
11. cf. *Dadagavialis gunai* – UF 280096
12. *Gavialis gangeticus* UF – 118998, UMMZ 155302
13. *Dyrosaurus* sp. – UF 227200
14. *Mecistops cataphractus* – UF 145926
15. *Paleosuchus palpebrosus* – UF 75023, UF 87980
16. *Tomistoma schlegelii* – UMMZ 129397, UMMZ 174416, UMMZ 128552

APPENDIX C

R Scripts Used in Chapter 4

List of packages to be installed before running the analysis

```
install.packages("optimx", dependencies=TRUE, repos="http://cran.rstudio.com")
install.packages("snow")
install.packages("phylobase", dependencies=TRUE, repos="http://cran.rstudio.com")
install.packages("rexpokit")
install.packages("cladoRcpp")
install.packages("rlang")
install.packages("usethis")

install.packages("devtools")
install.packages("stringr")
install.packages("installr")
install.packages("permute")
install.packages("htmltab")
devtools::install_github("Rdatatable/data.table")
install.packages("SparseM")
install.packages(file.choose(), repos=NULL)
install.packages("devtools")
library(devtools)

devtools::install_github(repo="nmatzke/BioGeoBEARS", dependencies=TRUE)   ## choose 3
##

install.packages("Rcpp", dependencies=TRUE)
install.packages("RcppArmadillo", dependencies=TRUE)
install.packages("gdata", dependencies=TRUE)
install.packages("gtools", dependencies=TRUE)
install.packages("xtable", dependencies=TRUE)
install.packages("plotrix", dependencies=TRUE)
install.packages("vegan", dependencies=TRUE)
install.packages("FD", dependencies=TRUE)
install.packages("SparseM", dependencies=TRUE)
install.packages("ape", dependencies=TRUE)
install.packages("phylobase", dependencies=TRUE)
install.packages("rexpokit", dependencies=TRUE)
install.packages("cladoRcpp", dependencies=TRUE)
```

```
install.packages("lattice")
```

Load the packages in R studio

```
library(optimx)
library(snow)
library(phylobase)
library(rexpokit)
library(cladoRcpp)
library(rlang)
library(usethis)
library(devtools)
library(stringr)
library(installr)
library(permute)
library(SparseM)
library(htmltab)
library(kexpmv)     #click on 2#
library(BioGeoBEARS)
library(geometry)
library(ade4)
library(ape)
library(lattice)
library(Rcpp)
library(RcppArmadillo)
library(gdata)
library(gtools)
library(xtable)
library(plotrix)
library(vegan)
library(FD)
library(SparseM)
library(ape)
library(rexpokit)
library(parallel)
library (gridExtra)
```

Load the Phylogeny [".newick" file]

```
trfn=np(paste("Croc_tree.newick", sep=""))
tr=read.tree(trfn)
plot(tr, cex = 0.4, label.offset = 4, x.lim = 200, y.lim = 70, align.tip.label = TRUE)
axisPhylo()
```

Load the geography data

```
geogfn=np(paste("Croc_geography.data", sep=""))
moref(geogfn)
tipranges=getranges_from_LagrangePHYLIP(lgdata_fn=geogfn)
tipranges
```

Maximum range size observed = 3 for this dataset #

```
max(rowSums(dfnums_to_numeric(tipranges@df)))
```

 # number of areas the species can occupy #

```
max_range_size = 3
numstates_from_numareas(numareas=9, maxareas=3, include_null_range=TRUE)
memory.limit(size=80000)
```

 # Run DEC model 1 #

```
BioGeoBEARS_run_object = define_BioGeoBEARS_run()
```

 # read the timeperiods and multipliers files #

```
BioGeoBEARS_run_object$timesfn = "timeperiods_1.txt"
BioGeoBEARS_run_object$dispersal_multipliers_fn = "multipliers_1.txt"
BioGeoBEARS_run_object = readfiles_BioGeoBEARS_run(BioGeoBEARS_run_object)
```

 # Give BioGeoBEARS the location of the phylogeny Newick file #

```
BioGeoBEARS_run_object$trfn = trfn
```

 # Give BioGeoBEARS the location of the geography text file #

```
BioGeoBEARS_run_object$geogfn = geogfn
BioGeoBEARS_run_object = section_the_tree(inputs=BioGeoBEARS_run_object,
make_master_table=TRUE, plot_pieces=FALSE, cut_fossils=FALSE)
```

 # Input the maximum range size #

```
BioGeoBEARS_run_object$max_range_size = max_range_size
BioGeoBEARS_run_object$min_branchlength = 0.000001
BioGeoBEARS_run_object$include_null_range = FALSE  # set FALSE for DEC model #
```

 # Good default settings to get ancestral states #

```
BioGeoBEARS_run_object$return_condlikes_table = TRUE
BioGeoBEARS_run_object$calc_TTL_loglike_from_condlikes_table = TRUE
```

```
BioGeoBEARS_run_object$calc_ancprobs = TRUE    # get ancestral states from optim run #

# Look at the BioGeoBEARS_run_object; it's just a list of settings etc. #

BioGeoBEARS_run_object

# This contains the model object #

BioGeoBEARS_run_object$BioGeoBEARS_model_object

# This table contains the parameters of the model #

BioGeoBEARS_run_object$BioGeoBEARS_model_object@params_table

# Number of cores to use #

BioGeoBEARS_run_object$num_cores_to_use = 6

# RUn DEC model #

resfn = "Croc_model_1.Rdata"
res = bears_optim_run(BioGeoBEARS_run_object)
save(res, file=resfn)
resDEC = res
resDEC

## Plot the DEC model ##

pdffn = "model_1.pdf"
pdf(pdffn, width=8.5, height=11)

analysis_titletxt = "DEC model"
results_object = resDEC
scriptdir = np(system.file("extdata/a_scripts", package="BioGeoBEARS"))

res2 = plot_BioGeoBEARS_results(results_object, analysis_titletxt, plotwhat="text",
label.offset=0.45, tipcex=0.6, statecex=0.4, splitcex=0.5, titlecex=2, plotsplits=TRUE,
cornercoords_loc=scriptdir, include_null_range=FALSE, tr=tr, tipranges=tipranges,
plotlegend=TRUE, legend_ncol=NULL,legend_cex = 0.5)
res2

dev.off()
cmdstr = paste("open", pdffn, sep="")
system(cmdstr)
```

```
pdffn_4 = "model_1_2.pdf"
pdf(pdffn_4, width=8.5, height=11)

plot_BioGeoBEARS_results(results_object, analysis_titletxt, plotwhat="pie", label.offset=0.40,
tipcex=0.6, statecex=0.25, splitcex=0.2, titlecex=1, plotsplits=TRUE,
cornercoords_loc=scriptdir, include_null_range=FALSE, tr=tr, tipranges=tipranges,
plotlegend=TRUE, legend_ncol=NULL,legend_cex = 0.5)

dev.off()
cmdstr = paste("open", pdffn_4, sep="")
system(cmdstr)

# Probabilities of states  Analysis 1 #

res$ML_marginal_prob_each_state_at_branch_top_AT_node

trtable = prt(tr, printflag=FALSE)
head(trtable)
tail(trtable)

# You can plot APE node labels with #

pdffn_2 = "APE_nodes.pdf"
pdf(pdffn_2, width=8.5, height=11)

plot(tr, label.offset=3, cex=0.5)
axisPhylo()
nodelabels(cex=0.5)
tiplabels(1:length(tr$tip.label), cex=0.5)

dev.off()
cmdstr = paste("open", pdffn_2, sep="")
system(cmdstr)

# Get your states list (assuming, say, 9-area analysis, with max. rangesize=3) #

max_range_size = 3
areas = getareas_from_tipranges_object(tipranges)

# This is the list of states/ranges, where each state/range is a list of areas, counting from 0 #

states_list_0based = rcpp_areas_list_to_states_list(areas=areas, maxareas=max_range_size,
include_null_range=FALSE)

# Make the list of ranges #
```

```
ranges_list = NULL
for (i in 1:length(states_list_0based))
{
 if ( (length(states_list_0based[[i]]) == 1) && (is.na(states_list_0based[[i]])) )
 {
  tmprange = "_"
 } else {
  tmprange = paste(areas[states_list_0based[[i]]+1], collapse="")
 }
 ranges_list = c(ranges_list, tmprange)
}

# Look at the ranges list #

ranges_list
```

 # Make the node numbers the row names #
 # Make the range_list the column names #

```
range_probabilities =
as.data.frame(res$ML_marginal_prob_each_state_at_branch_top_AT_node)
range_probabilities
row.names(range_probabilities) = trtable$node
row.names(range_probabilities)
names(range_probabilities) = ranges_list
```

 # Look at the table (first six rows)

```
head(range_probabilities)
```

 # Write the table to a tab-delimited text file (for Excel etc.) #

```
write.table(range_probabilities, file="range_probabilities_COPY.txt", quote=FALSE, sep="\t")
```

 # Look at the file #

```
moref("range_probabilities_COPY.txt")

prt(tr)
```

 # Plot legend for ALL states/ranges (there may be a ton, and getting them all to display is hard) #

```
pdffn = "colors_legend_all.pdf"
pdf(pdffn, width=8.5, height=12)
```

```
areanames = names(tipranges@df)
areanames

include_null_range = TRUE

states_list_0based_index = rcpp_areas_list_to_states_list(areas=areanames,
maxareas=max_range_size, include_null_range=include_null_range)

statenames = areas_list_to_states_list_new(areas=areanames, maxareas=max_range_size,
include_null_range=include_null_range, split_ABC=FALSE)
statenames

relprobs_matrix = resDEC$ML_marginal_prob_each_state_at_branch_top_AT_node
MLprobs = get_ML_probs(relprobs_matrix)
MLstates = get_ML_states_from_relprobs(relprobs_matrix, statenames, returnwhat="states",
if_ties="takefirst")

colors_matrix = get_colors_for_numareas(length(areanames))
colors_list_for_states = mix_colors_for_states(colors_matrix, states_list_0based_index,
plot_null_range=include_null_range)
colors_list_for_states

possible_ranges_list_txt = areas_list_to_states_list_new(areas=areanames,
maxareas=max_range_size, split_ABC=FALSE, include_null_range=include_null_range)
cols_byNode = rangestxt_to_colors(possible_ranges_list_txt, colors_list_for_states, MLstates)

legend_ncol=NULL
legend_cex=0.5
colors_legend(possible_ranges_list_txt, colors_list_for_states, legend_ncol=legend_ncol,
legend_cex=legend_cex)

dev.off()
cmdstr = paste("open ", pdffn, sep="")
system(cmdstr)
```

 # Run DEC model 2 #

```
BioGeoBEARS_run_object = define_BioGeoBEARS_run()
```

 # read the timeperiods and multipliers files #

```
BioGeoBEARS_run_object$timesfn = "timeperiods_2.txt"
BioGeoBEARS_run_object$dispersal_multipliers_fn = "multipliers_2.txt"
BioGeoBEARS_run_object = readfiles_BioGeoBEARS_run(BioGeoBEARS_run_object)
```

 # Give BioGeoBEARS the location of the geography text file #

```
BioGeoBEARS_run_object$geogfn = geogfn
BioGeoBEARS_run_object$trfn = trfn
BioGeoBEARS_run_object = section_the_tree(inputs=BioGeoBEARS_run_object,
make_master_table=TRUE, plot_pieces=FALSE, cut_fossils=FALSE)

# Input the maximum range size #

BioGeoBEARS_run_object$max_range_size = max_range_size

BioGeoBEARS_run_object$min_branchlength = 0.000001
BioGeoBEARS_run_object$include_null_range = FALSE  # set FALSE for DEC model #

# Good default settings to get ancestral states #

BioGeoBEARS_run_object$return_condlikes_table = TRUE
BioGeoBEARS_run_object$calc_TTL_loglike_from_condlikes_table = TRUE
BioGeoBEARS_run_object$calc_ancprobs = TRUE    # get ancestral states from optim run #

# Look at the BioGeoBEARS_run_object; it's just a list of settings etc. #

BioGeoBEARS_run_object

# This contains the model object #

BioGeoBEARS_run_object$BioGeoBEARS_model_object

# This table contains the parameters of the model #

BioGeoBEARS_run_object$BioGeoBEARS_model_object@params_table

# Number of cores to use #

BioGeoBEARS_run_object$num_cores_to_use = 6

# RUn DEC model #

resfn_5 = "Croc_model_2.Rdata"

res_5 = bears_optim_run(BioGeoBEARS_run_object)
save(res_5, file=resfn_5)
resDEC_5 = res_5
resDEC_5

# Plot the DEC model #
```

```
pdffn_5 = "model_2_1.pdf"
pdf(pdffn_5, width=8.5, height=11)

analysis_titletxt = "DEC model"
results_object = resDEC_5
scriptdir = np(system.file("extdata/a_scripts", package="BioGeoBEARS"))

res6 = plot_BioGeoBEARS_results(results_object, analysis_titletxt, plotwhat="text",
label.offset=0.45, tipcex=0.6, statecex=0.4, splitcex=0.5, titlecex=2, plotsplits=TRUE,
cornercoords_loc=scriptdir, include_null_range=FALSE, tr=tr, tipranges=tipranges,
plotlegend=TRUE, legend_ncol=NULL,legend_cex = 0.5)
res6

dev.off()
cmdstr = paste("open", pdffn_5, sep="")
system(cmdstr)


pdffn_4 = "model_2_2.pdf"
pdf(pdffn_4, width=8.5, height=11)

plot_BioGeoBEARS_results(results_object, analysis_titletxt, plotwhat="pie", label.offset=0.40,
tipcex=0.6, statecex=0.25, splitcex=0.2, plotsplits=TRUE, titlecex=0.5, show.tip.label = TRUE,
tipboxes_TF=TRUE, pie_tip_statecex=0.7, cornercoords_loc=scriptdir,
include_null_range=FALSE, tr=tr, tipranges=tipranges, plotlegend=TRUE,
legend_ncol=NULL,legend_cex = 0.5)

dev.off()
cmdstr = paste("open", pdffn_4, sep="")
system(cmdstr)
```

 # Probabilities of states Analysis 2 #

```
res_5$ML_marginal_prob_each_state_at_branch_top_AT_node

trtable = prt(tr, printflag=FALSE)
head(trtable)
tail(trtable)
```

 # You can plot APE node labels with #

```
pdffn_2 = "APE_nodes_2.pdf"
pdf(pdffn_2, width=8.5, height=11)

plot(tr, label.offset=3, cex=0.5)
axisPhylo()
```

```
nodelabels(cex=0.5)
tiplabels(1:length(tr$tip.label), cex=0.5)

dev.off()
cmdstr = paste("open", pdffn_2, sep="")
system(cmdstr)
```

 # Get your states list (assuming, say, 9-area analysis, with max. rangesize=3) #

```
max_range_size = 3
areas = getareas_from_tipranges_object(tipranges)
```

 # This is the list of states/ranges, where each state/range is a list of areas, counting from 0 #

```
states_list_0based = rcpp_areas_list_to_states_list(areas=areas, maxareas=max_range_size,
include_null_range=FALSE)
```

 # Make the list of ranges #

```
ranges_list = NULL
for (i in 1:length(states_list_0based))
{
 if ( (length(states_list_0based[[i]]) == 1) && (is.na(states_list_0based[[i]])) )
 {
  tmprange = "_"
 } else {
  tmprange = paste(areas[states_list_0based[[i]]+1], collapse="")
 }
 ranges_list = c(ranges_list, tmprange)
}
```

 # Look at the ranges list #

```
ranges_list
```

 # Make the node numbers the row names #
 # Make the range_list the column names #

```
range_probabilities =
as.data.frame(res_5$ML_marginal_prob_each_state_at_branch_top_AT_node)
range_probabilities
row.names(range_probabilities) = trtable$node
row.names(range_probabilities)
names(range_probabilities) = ranges_list
```

 # Look at the table (first six rows)

```
head(range_probabilities)

# Write the table to a tab-delimited text file (for Excel etc.) #

write.table(range_probabilities, file="range_probabilities_2.txt", quote=FALSE, sep="\t")

# Look at the file #

moref("range_probabilities_2.txt")

prt(tr)

# Model testing  DEC Models #
# Set up empty tables to hold the statistical results

restable = NULL
teststable = NULL

LnL_1 = get_LnL_from_BioGeoBEARS_results_object(resDEC) # 2 parameters
LnL_1
LnL_2 = get_LnL_from_BioGeoBEARS_results_object(resDEC_5)  # 2 parameters
LnL_2

numparams1 = 2
numparams2 = 2

stats = AICstats_2models(LnL_1, LnL_2, numparams1, numparams2)
stats
stats$AIC1
stats$AIC2
stats$pval

res1 = extract_params_from_BioGeoBEARS_results_object(results_object=resDEC,
returnwhat="table", paramsstr_digits=3)
res2 = extract_params_from_BioGeoBEARS_results_object(results_object=resDEC_5,
returnwhat="table", paramsstr_digits=3)

rbind(res1, res2)
tmp_tests = conditional_format_table(stats)
tmp_tests

restable = rbind(restable, resDEC, resDEC_5)
teststable = rbind(teststable, tmp_tests)
restable
teststable
```

APPENDIX D

Geographic Data Used in Chapter 4

69 9 (E S B N A F C U I)
Acynodon_iberoccitanus_70.6 100000000
Aktiogavialis_caribesi_7.2 010000000
Aktiogavialis_puertoricensis_23 001000000
Alligator_mississippiensis_0 000100000
Alligator_sinensis_0 000010000
Argochampsa_krebsi_56 000001000
Asiatosuchus_germanicus_41.3 100000000
Bernissartia_fagesii_127 100000000
Borealosuchus_formidabilis_55.8 000100000
Borealosuchus_sternbergii_63.3 000100000
Boverisuchus_vorax_40.4 000100000
Brachychampsa_montana_66 000100000
Caiman_crocodilus_0 010000000
Caiman_latirostris_0 010000000
Caiman_yacare_0 010000000
Crocodylus_acer_50.3 000100000
Crocodylus_acutus_0 001100100
Crocodylus_affinis_46.2 000100000
Crocodylus_checchiai_3.6 000001000
Crocodylus_intermedius_0 010000000
Crocodylus_moreletii_0 000000100
Crocodylus_niloticus_0 000001000
Crocodylus_porosus_0 000000010
Crocodylus_rhombifer_0 001000000
Dadagavialis_gunai_15.9 000000100
Diplocynodon_ratelii_13.8 100000000
Dolichochampsa_minima_64 010000000
Dollosuchoides_densmorei_41.3 100000000
Eogavialis_africanum_33.9 000001000
Eosuchus_lerichei_33.9 100000000
Eosuchus_minor_47.8000100000
Eothoracosaurus_mississippiensis_66 000100000
Gavialis_bengawanicus_0.1 000010000
Gavialis_gangeticus_0 000000001
Gavialosuchus_eggenburgensis_15.9 100000000
Gryposuchus_colombianus_11.6 010000000
Gryposuchus_croizati_5.3 010000000
Gryposuchus_neogaeus_6.8 010000000
Gryposuchus_pachakamue_5.3 010000000

Hylaeochampsa_vectiana_122.4 100000000
Iharkutosuchus_makadii_83.6 100000000
Ikanogavialis_gameroi_5.3 010000000
Isisfordia_duncani_99.6 000000010
Kentisuchus_spenceri_47.8 100000000
Leidyosuchus_canadensis_70.6 000100000
Maomingosuchus_petrolica_38 000010000
Maroccosuchus_zennaroi_47.8 000001000
Mecistops_cataphractus_0 000001000
Melanosuchus_niger_0 010000000
Ocepesuchus_eoafricanus_66 000001000
Osteolaemus_tetraspis_0 000001000
Paleosuchus_palpebrosus_0 010000000
Paleosuchus_trigonatus_0 010000000
Paratomistoma_courti_38 000001000
Pelagosuchus_pakistanensis_41 000000001
Piscogavialis_jugaliperforatus_5.3 010000000
Planocrania_hengdongensis_55.8 000010000
Sacacosuchus_cordovai_5.3 010000000
Siquisiquesuchus_venezuelensis_15.97 010000000
Thecachampsa_americana_6 000100000
Thecachampsa_antiqua_2.5 000100000
Thecachampsa_carolinensis_23 000100000
Thoracosaurus_neocesariense_56 000100000
Tomistoma_cairense_41.2 000001000
Tomistoma_coppensi_2.5 000001000
Tomistoma_dowsoni_15.9 000001000
Tomistoma_lusitanica_7.2 100001000
Tomistoma_schlegelii_0 000010000
Voay_robustus_0 000001000

APPENDIX E

Multipliers and Timeperiods Used in Chapter 4

Multipliers

E	S	B	N	A	F	C	U	I
1	0.9	0.9	0.9	1	1	0.75	0.1	1
0.1	1	1	1	0.1	0.1	1	0.1	0.1
0.1	1	1	1	0.1	0.1	1	0.1	0.1
0.9	1	1	1	0.75	0.9	1	0.1	0.75
1	0.75	0.75	0.75	1	1	0.1	1	1
1	0.9	0.9	0.9	1	1	0.9	0.75	0.9
0.75	1	1	1	0.1	0.75	1	0.1	0.75
0.1	0.1	0.1	0.1	0.75	0.75	0.1	1	0.75
1	0.9	0.9	0.9	1	0.9	0.75	0.75	1

E	S	B	N	A	F	C	U	I
1	0.9	0.9	0.9	1	1	0.75	0.1	1
0.1	1	1	1	0.1	0.1	1	0.1	0.1
0.1	1	1	1	0.1	0.1	1	0.1	0.1
0.9	1	1	1	0.75	0.9	1	0.1	0.75
1	0.75	0.75	0.75	1	1	0.1	1	1

1	0.9	0.9	0.9	1	1	0.9	0.75	0.9
0.75	1	1	1	0.1	0.75	1	0.1	0.75
0.1	0.1	0.1	0.1	0.75	0.75	0.1	1	0.75
1	0.9	0.9	0.9	1	0.9	0.75	0.75	1

E	S	B	N	A	F	C	U	I
1	0.9	0.9	0.9	1	1	0.75	0.1	1
0.9	1	1	1	0.75	0.9	1	0.1	0.75
0.9	1	1	1	0.75	0.9	1	0.1	0.75
0.9	1	1	1	0.75	0.9	1	0.1	0.75
1	0.75	0.75	0.75	1	1	0.75	1	1
1	0.9	0.9	0.9	1	1	0.75	0.75	0.9
0.75	1	1	1	0.75	0.75	1	0.1	0.75
0.1	0.1	0.1	0.1	0.75	0.75	0.1	1	0.75
1	0.75	0.75	0.75	1	0.9	0.75	0.75	1

E	S	B	N	A	F	C	U	I
1	1	0.001	1	1	0.9	0.1	0.1	0.1
1	1	0.001	1	0.1	0.75	1	0.75	0.75
0.001	0.001	0.001	0.001	0.001	0.001	0.001	0.001	0.001
1	1	0.001	1	0.75	0.9	1	0.1	0.1
1	0.1	0.001	0.75	1	0.9	0.1	0.1	0.1
0.9	1	0.001	0.09	0.9	1	0.9	0.9	0.9

0.1	1	0.001	1	0.1	0.9	1	0.1	0.1
0.1	0.75	0.001	0.1	0.1	0.9	0.1	1	1
0.1	0.75	0.001	0.1	0.1	0.9	0.1	1	1

END

Timeperiods

40

55

62

142

APPENDIX F

Morphological Character-Taxon Matrix

Bernissartia fagesii

??????0???0111102100?00?0?000???0000?100010???00003000??????010??000?00?01????001
10?10010010600001?????1010????101000?000??00000001100110?0?0??0?0?00?010?00002?
????????000?000000000000?010000??100?10000000000?00???0000???00?1?00???-
?111010?0{0 1}1{0 1}0000010{1 2}1000000000000

Iharkutosuchus makadii

??10113??1??????110???00??10?1????0001??0
0020110610001?0???0110????000000010010000120110 01?100?2-
0?00?0???02???000?3?????1???1000000??1100?010000000?01?02000000000000-
0??110????00???20?0???0101-0000---0001{1 2}011002000-1?000

Hylaeochampsa vectiana

??0?????0????????
??0?0?10001?00??0110?0?000000001000000?0?2211000011 0????1?0?000000100000000?????1?
001001000?0110000??100000??000??0?0?000?0??-
?1?1??????00?1?1??01??01??0??000000100001 10?????0??003

Isisfordia duncani

?0110?????10?01??10??0000???01??0001?1?0110??????02???????????1??????????????20110
?100201105100?1?????0000??0?000001100 10001?100010???10??100??000000001000000???
???????0111000???001001?00?0??????000?0?000?00?-???00?????????????????11220-
000100010005010???0?012001

Borealosuchus sternbergii

000000000011001 0?10010000001010000 01?00???0???011010000000?10010000000100000??0
0030?000200018120010001000001?0?000001100?000101000101111 00?100100?000000100?0
100?000?1?001001100000000010011?000000?00000?00000000?101??010?0000?1??0?0?1?111
0010001100000 1??100002105?001

Borealosuchus formidabilis

000?000?0?1100100100100000010100000 1?000?20???0120200000?001?0100000001000 01??0 0030?000100028120010 0?000001000000 02?1?000001010021 01?1100010 0?00?00000010000 1000??????00100110000000010011100 00?000000100000000 0?01?0001-
0000?1?00?0?1?3113?100002300001021 00??21052000

Osteolaemus tetraspis

??1100001000101010001110011111201110111111110003100110101000001100001101011101 0 1010001011100210001100010000011011001011102010101000101111 1?00101010012111000 0110111101011110110000003010201000000010000000000000000-
01?000?0?000?1?00?0?1111101100010000000001000010022004

Voay robustus

??????0????????0???011?????111??1110??????1???3110210101000001100011111011????0012 0?1002?0021000110001000001101000101100201010100000111110?0010111001111100011111 ??1101?1111011000000301030100000?01000000000000000-
01?000?00000?1?00?0?1111101100012000 0?0101000001112 00?

Brachychampsa montana

1010110010110 0???0001??00011110 0?000?103111???3100010 1????01110?00001110100??00 110?1002111010000100?0010001?0?0100002112 1?0101210111111100?110200?011200101001 03?00101?0010011001000101 0?0100000011001000000000000-
01?000??0?00?1?01?0?1?1114100001200000101101 20?0112002

Diplocynodon ratelii

??????0??????000???010?00?1111001400?10??21???0100110 1????0111000001??101????001 30?100?1012300001000101000??0?00000010120?0101000101111 00??1010010000001010010 0100001?1010011001000101 0?01000000?1000000000000000-
01?001?0010101?00?0?11111?1000010000001?11000010?2200?

Alligator mississippiensis

1011110011010010000010110111111001100111210111031000111010010111000101111010001 0010001102101020000100000100011100000000112120201111111111002-
0200101111010200102100111100100210010001010001000000110000000000000000-
01?010?1000001?00?0?2111141000010000001311012010022002

Alligator sinensis

1011111011110010100010110111111001100111211111231000011 0?0010111000001 1?101??01 0010001101101020000100000100011001000000012120201111111111002-

02001011110102001021001111001002100100010103010000?11000000000000000-
01?010?1000001?00?0?2101141000010000001021012010022003

Caiman yacare

10111100111000100000101011111100110011112211103100111110101010101102011001010100120010012011200001000001000110010000021121211111201111111002-
02011001111112001041001011001002101100010104010000001100000000000010-
01?000?1010111?0000?110114100000-000001301012010022002

Caiman crocodilus

10111100111000100000101011111100110011112211103100111110101010101102011001010100120010012011200001000001000110010000021121211111101111111002-
02011001111112001041001011001002101100010100010000001100000000000010-
01?000?1010111?0000?111114100000-000001301012010022002

Caiman latirostris

10111000111000100000101?1111100110011112211203100111110101111101102011001??01
00120010022010200101000001000110010000021121211111101111111002-
02011001111112001041001011001002101100010103010000001100000000000010-
11?010?1010111?0000?111114100000-000001301012010022004

Melanosuchus niger

10111100?1?00100000101011111100110011112211203100111110101011101102011001??01
00120010022010200101100001000110010000021121211111101111111002-
02011001211112001041001011001002101100010103010000001100000000000010-
11?010?1010111?1000?111114100000-000041301012010022004

Paleosuchus trigonatus

10011111110100101000100011111121130011113211123100112121111011101102011001010110120010111010200001000001000110001000111121211110101111111012-
02011001202?200103100101100100210110001010301000000110000000000010-
01?000?10100???0000?1?111410000---000013110l2?1?-22005

Paleosuchus palpebrosus

10011111110100101010100011111121130011113211123100112121111011101102011001?0101
10120010111010200001000001000110001000111121211110101111111012-
02011001202l?200103100101100100210110001010401000000110000000000010-
01?000?10111???0000?1?011410000---000010110l2?1?-22005

Eothoracosaurus mississippiensis

??????0????????????01??000????????00?01???0????1312??0??????1?1???00?010?0????00130?
0002?00280200l0??000000????000020100200????001?0??100?2-
01???10000010?001?0?????????100110?000000005111?010?0?0000100?00000000l?0001-
??00?1?00?010?31?3-101102400001??1001221051200

Thoracosaurus neocesariense

??????0??????111???010?????011?????0?01???0???2131???0????????10?000?01?0?????00130
?0002?10280200100??000000?0?0000201?020000?00000000100?2-
010??1?000010000l0??00000?00100?100000000005??1?010?00?00?0????0?00000?????01-
??00?1?00??1003103-101102400001??1001221051200

Eosuchus minor

??????0???0??111???01?00?0101????200?010??0???2131??000??0000?10?000001000????0013
0?0001?10280?00100?000000??000000111l0?0000?1000100??100?1?0100?10?110100001?0?
00??1???101110101000000000?00000??000000000?0?00?0?01?0101-
0?00?0?2?1011021?3??0000-300101??1001???031210

Eosuchus lerichei

???????????01011???01???????11???????11???1???21310??0????????????????????????00130?
100?010280?00100?0010000???0000111100000?0100010?10100?100?0?010?12010?0010?????
?????10??10101000000000100000??00000000??0000?0001?0101-??00?0??0?01??3103-
1000000001010110012?21031210

Dolichochampsa minima

??????????????????????0??????????????????????31??2??0????????????????????????00??????
?????2500??1????????????????????0?020001?1??2?
?????????1???1????????????0??0??????1????????????????????????????-
1??????00???00010?322?6????

Acynodon iberoccitanus

??3010310l????????0????????0?0?????00010?1
00100106000010??00100????000000002?00???200101?0100?110?0000??000100000?2?????
????1???0????0100001012000??100100000000000?0???10????0101?20?????0?04--
?00120010010010?????112002

Leidyosuchus canadensis

????0?0????????1????010000011?1??10?0?11??11???0110?00000?0?01?110000011101????000
20?100200003000010000010001000100001000200010100010111100?110100100100010000l0

0?00001?00100110010001010011000?1100000000000000101?0010?000101?00?0?1?11100
0?00120001012110?0?100?2001

Paratomistoma courti

??1??1??00001010?????0??????
?????2??3?0??????????01?0????????????????????0000??11?1?????1??01??11310?00?000?1000?10
1?0?100?????0?0???0??0????00????00?0?00????1??????0100?1?2???111?1?????000130010?1??
10?????0?2?0?

MUSM 1513

??10?11?00??000?0????00??????
?????????001?0?1?0??0????0?00?10102000001?000?011100?000?100100??01000020??????0?
??12001?00000?11???10?0100?010??1?00101000?00??1???0100?002?00011?????????????????
??????????????0?

Asiatosuchus germanicus

001?0?0?1?001010?0101?000?1111??1??0??????1???3110100?????00110000??0101?00??000
20?1000?000100001?0???10000??0?00010???020?00010000?111100???0100?001??0100001?0?
???????1100?10000030?03010?00?0?1????0000?0??0?0-
?1???00?0?00?1?00???1?11101?0?????0???1?????????????00

Planocrania hengdongensis

??????????????????1?????????????????????????3110???0????????1????0?0??0?????20020?1
?????01300??1????0?000????0????01?02????????0?0?1?1100????????0?0??0100?0100?????1??
?1???10?10001????????0????????0?0000?0??0??-
?1?00?0??010?1?1????1?11????0?????????????????1??????0?

Boverisuchus vorax

????0?0???0100100?01?00000111??0100?10???1???3110?000?????0??100000?1??0?????210
20?1002?00030001100?000000??0?000000110200010100000111110???0100001001010000100
????01??1100210000002010301000??1000?000000?0000-
?1?0?00?0010?1?10?0?1?11121?000115011010110001??122100

Gavialis gangeticus

020000000000111101101000000011100000?000000031422000000000001000000011000100
0014011000010250300100000000000000000300102000001200000001210000100010020010000
0101000000000121?10100000100621211111101100110001100102001110 2-
1?00?1?21110113006-10011210110200010032216 2303

Gavialis bengawanicus

?????????????111?????????????????????1????????3?422000?????10010000000110??????4??
???0?10250300100?000??00???01?030?1?2??0???2?0?0000?21?00?100010020010??101???0?
0?00??1?1010???0100611?111?1011001?0001100102??11102-1?00?1?211101?3006-
10011210110200010032216230?

Eogavialis africanum

????????1?????11???010??????????0?????????0???31422000?????10?110000??1100????00130
?10000102503001??0000000000000030?10200000?0000001110?000100?1002?010000201?
0?000??0121?10100000110601010100101100110010100012001010?-
1?00?00211101130?06?10?????0??????0?0032??6230?

Gryposuchus colombianus

????0?0???001??????01??000?????????????????0???31422?000100000011000?01100????0013
111010?10250300100?0?0000??0?000031010200000110000000121?000100?1001?010010201?
00100?00121010100?111?1020111?10110012111210?1300?1102-0?00?0121000113106-
10?????0??????0?003??062303

Gryposuchus pachakamue

??314220?0?????00011?000?01110????00130?
10100102503001??000000????000031010200?0110000001110?00000001?020010??0201???
??0???1?101?10004110?10210110101100121112100?130011102-0100?0121000113106-
10221210011??0100322062300

Gryposuchus neogaeus

??11?????????????00130?10
100102??3?0?0????0?????????????????????????????12????????01????01??102?1?????????1?
?0??1????0111??0??111???110012????2?00????01?????0100???21?00113106-
10221010012??0100???06230?

Gryposuchus croizati

??31422??0????????????????????????00140?10
1?0102503001??000000????000031?102?????1?000?000121?00??0?01??2001??102?1???????
??1210101??0041?1?10?1111??01100121?2?01?13?011?02-??00?0121??01?3106-
10121010111?1200100322162303

Aktiogavialis caribesi

??3142????????????????????????????0????????
????2503001?0????000????00?0300?020?????0000?0?1110???????01??1000??102?1?????0???

1?101?1??0001?1?1121001??011?00????0?10???0???1?????00?110???0??3006-
1001101001220??100322062300

Aktiogavialis puertoricensis

??
???????3??????????????????????????0?0????????????2??????????00200000l0??1?00??0???121
0??1???????1?????001???1?????0??0?10????0???????????1?0?0?0?????????0??01?0022???100
???0?2?0?

Argochampsa krebsi

?????0?00?0?11?1??????????0???????????0???????31?2????????????????????????????0?130?1
0010102503001O0??1??0?1???00?030???2000???00010111110???00000?0020010?10201?0???
0???????1???00001117210?001??011?0010??0?000??00?00?????00?1100??1??3006-
100110100102000100320062300

Dadagavialis gunai

??4????0??????????????????????00?3?????
??1?2503001???0000001?0?000031??0????????00000001?1???????0???1001??1?????????0???
????????????1?162?210????0??????0???1???130??11?????00???????????006-
10?????00112????00???062302

Ikanogavialis gameroi

??31422O?0??????001????0?01?00????00?30??
0?0?10250300100?000000????0000310?02000001?000?000110?000?0?01??20010000201?????
0??01210?010?00?1?06212101l??01?00?10??21000100011102-??00?012?0?0114106-
100112100101????00???06230?

Siquisiquesuchus venezuelensis

??????????????????1?????????????????????????31422??0?0?????0???????0????????00130?1
0?00102503001O???000?01???000030??02???????00??001?1????0????1?0?0010?002?1???????
?0?2101010??041?0621?101??10?0?00201?2100??3?01??02-??00?11???001?4106-
101112100011???100322062302

Piscogavialis jugaliperforatus

????????????????????????????????1??????0??????31422?0001?011001?00??101?00????00130?
10100102503001O0?000000??0?0000310102O?0001?0000001110?0000010100200100102O1?0?
1?0?0?12??1?1000041116212101?0101?00010112?000130011102-0100?0121000114106-
100112100131O1?000322062300

Maroccosuchus zennaroi

???????1?????????????????????????1100?1????????31201??0?????10110??001??011????00120?
1001?10210300100??1??001???0100300?020100?110000111111??00001100??210100?0202????
?0???11?11?000?030?0?010?00001100000?000000000101???00?0000?00?1?0?1121101100002
20010101100?21122203

Dollosuchoides densmorei

0010??????111010?00?1??000111???1?000??????????31201??0?????100100?0??0101?????001?
0?10?10102103001 00??00?00????0100300102010101 1000?111110???0?0??1??21010?0020001
???????10?110000??30108010001 0?0?00000100?01000?101?0100?0100?0001?0?1?31?5010?1
00100101011000321062200

Kentisuchus spenceri

??????0?????????????1?????????????????????????????120???0????????1000?1101?11????00120?1
00??10210300100???0000??0?0100301102 01?0011000?111110??????0?0??21010?00200?????
1?111?0?100?0?030?080?0?000??100??0100?0?00?01?10010????00?0001?0?1131?501010020
00101???000???0?220?

Gavialosuchus eggenburgensis

??????????????????????1???00130?10
0??10210300100??00?00????00?030??020?0?01?000???1110?0???0??1?????1??00200????????
11???100??0030?0?010?010???00?0010??0?00?0??1?01?????00?000???????1???10?????????1?
??000?????220?

Maomingosuchus petrolica

??312011000??00100101000101010????00130
?1001?10210300101?010000????0100301002010001 0000?111100?002?10000?2101??00200??
???????1?01100000030109010000?0100000100101000010 0?0101-
0000?0001?0?113115010000000010102100 03?1162200

Sacacosuchus cordovai

??3122100000????001?????????????????00130?1
00111021030010??0000001?0?000??0?1020000???000?111100??0?00?010?20310?00?02?????
1??11?01100??00301080100010??10000010?00000000101?0101-0?00?0?01?011?3103-
10000210010102?000???062300

Tomistoma dowsoni

??00130?10
???102?0300100??00?00????000030??????????0000???1110???????01??1?310?002?0?????0??

?1?0?1?0???0?0?000?2000????0????10??0?00?0?00?11?????00?0021?01???1?????????????1?
??0???????220?

Tomistoma schlegelii

021100001000101000101100011111101100110130100031320100000001001000000010100010
001300100011021030010101000001101000130000201000110000111110000011000012101000
020001100101111011000000301000100000011000001000000000101?0101?0000?0001?0?113
1?501000100001110110003210622 00

Tomistoma coppensi

??0????????1???????1???????001?0?10
01010?1030010????0000????0?????????????????000??11110???????01????310?00200?????????
1???1??0000301 0?01?0000??100?0010?00000?0??0??10??0?00?0021??11??1?????????????1?
??0????????2?0?

Tomistoma lusitanica

??????0????????????01?????????????????10???1???3122???0?????10?10000??0101?????00130?
100??10210300101?10000011 0?0000300?02010?01?0000111110?0001???101??010000200011
001??11101100000030109010000 0??10000010 0?000001011?101?0?00?0001?0?1??1????????
??????1???0????????2?0?

Tomistoma cairense

??3??2???0????????1000001?1010????00?30?1
?????025?3??1?0????000??0?0000301102000?0?0100?011110???01??010???01000020001??0?
??11?001??0000311000 10?000???00000?0??0000001 0??1101???00?102??011??1????????????
??1???0????????2?0?

Thecachampsa carolinensis

????0000?????010?01?110?01??????1?00?000??1???3120??00?????10010?0031?1010????0013
0?10011102103001 0???00000????0010301102?10?01?000???1100???0?0?????2001??002?????
??????11?11????????0?080120010?1?0??0010??00000?1?1101?????00?000????1?31151100012
100111001000321042200

Thecachampsa_americana

0??0??????????1????01?000?1111??1100?000??1???312010?0?????1001?00031?1010?1??0013
0?10011102103001 00?100000????0010301102010?0?1000?011110?000?010101??0100002 02?
??0?0??1110110 0?2003010801200 10?0?0000010010000001?110101-
0000?0001?0?1??1?????????????1???0????????220?

Thecachampsa antiqua

02000000??001010?0001101011?1??11?0?00???1???3122???0?100?1??1000031?101?0???00
130?10011102103001 00?100000??0?0000301?02000101100000111 10???0101010 1??01000020
00??00???1110?100?2003?1080120010??0000001000000000?0110101-
??00?000??0?1??1??????????????1???0???????2?0?

Crocodylus falconensis

??00?????????1??1?????????????????????100???02101001??1???000????0???0???????????0000?111110????????0????01??00?0??????????????????????0?0?010000??????00000?00?00?0???????????00?1??0???11?1????1?????????1???0???????200?

Crocodylus niloticus

10110000101010100010111001111120120011112010103100110101000101100011101011101000120010011002100001001100000110100100010020011010000011111000010110001 1?01000100111010111100110000030100010010000100000000000000000-01?010?00000?1?20?0?11211011100020111010110001101220 01

Crocodylus porosus

11110000100010101010111000111120120011112010103100110101000101100011101011101000120010011002100011001100000110100100000020 00?0100000111110000101100012101000010011110101111001100000301000100000001000000000000010-01?000?00000?1?01?0?11211011100026111010110001101220 03

Crocodylus acutus

00110000101010110010111001111120120011102010103100110101000101100011101011101000120010011002101001001100000110100100010020001010000011111000010110001210100001001111010111011100000301000100000001000000000000000-01?010?00000?1?21?0?11111011100026101110110001101220 00

Crocodylus rhombifer

00110000101010100 01?11100111 1?2011001111201010310011010100010110001110101110100012001001100210100100110000011010010001002000101000001111100001011000111010001100111101?11110111000003010001000000010000000000000000-01?010?00000?1?20?0?11211011100002111311110001102220 00

Crocodylus intermedius

001?0000101010100 01?11100111 1?2012001111201010311011010100000110001110101110100012001001100210100100110000011010010001002000101000001111100001011000 12?01000

0100111101011110111000003010001000000010000000000000000-
01?000?00000?1?20?0?11?1101110 0?261???1??1000110{1 2}22000

Crocodylus moreletii

001?000010101010001?111001111?2012001111201010310011010100010110001110101110100012001001100210100100110000011010010001002000101000001111100001011000120010001000111010111101110000030100010000000100000000000000-
0??000?00000?1?20?0?1111101110002010101??1000110122000

Crocodylus checchiai

??00120?10011002101001 00?1000001101001000100 2000?0?000001111 10?001011000121010000100?111010111?00110000030100010000 0?01000?000?00000?0-
01?01??????0?1?20?0?1?11101110012?11111???000110122001

Crocodylus acer

??00120?1001?10210000100??000001???000100?1020?000100010111100?002?01?00?20010000100?1??0??11100?10000003 0?000100000??100??00?000000?0-???00?????00?1?00?0??11110111000-
010101011000?10022000

Crocodylus affinis

001101001?100010000111000011110011 00?10???1???3110110101000001100000001011 00??0120?100?100110000100?010000??0?000100110201000100000111100?0?010??001200100 0010?1??0???1100110000003 0?0001000000?100??00??00000?0-
0??0010?0000?1?01?0?1?111?111000001010101100 0?10022000

Mecistops cataphractus

10??0100100000100000111001111120120011111010003110210101000100100011101 01?1010013001001100210000100010000011010000201102000101000001111100001011000121010000100111101011110110000003010001010000010000000000000000-
01?110?00000?1?01?0?113100111001000010100100012206 2000

Ocepesuchus eoafricanus

??500?0??????????????????????????????1???1????????0????????2?010?0?101???????????????01????1?0???0?0??????????????0??????????????????0??????????????????????3????????????????????